Neuroprotective Effects of Ketone Bodies during Hypoglycemia

by

Peter W. Schutz
B.A. (Hons.), University of Cambridge, 1993
M.Phil., University of Cambridge, 1995
M.D., Medical University of Vienna, 2004

A THESIS SUBMITTED IN PARTIAL FULFILLMENT OF
THE REQUIREMENTS FOR THE DEGREE OF
Doctor of Philosophy
in
THE FACULTY OF GRADUATE STUDIES
(Pathology and Laboratory Medicine)

THE UNIVERSITY OF BRITISH COLUMBIA
(Vancouver)

April, 2011

Abstract

The ketone body D-3-hydroxybutyrate (3OHB) is an alternative energy substrate for the brain during hypoglycemia. The capacity and limitations of 3OHB to compensate for cerebral glucose depletion in developing brain is insufficiently understood.

We studied the effect of 3OHB treatment in a newly developed infant rat model of insulin induced, sustained, and EEG-controlled hypoglycemia. Continuous treatment with 3OHB during hypoglycemia resulted in increased 3OHB plasma levels in hypoglycemic animals and delayed the onset of clinical coma and of EEG burst-suppression (burst-suppression coma). 3OHB treated animals did not survive after resuscitation with glucose, compared to 80% survival of untreated hypoglycemic pups. Cleaved-caspase-3 immunohistochemistry and double labelling studies demonstrated a 20-fold increase of apoptotic mature oligodendrocytes in white matter of 3OHB treated animals, indicating a limited protective effect of 3OHB treatment.

In contrast to glucose, D-3-hydroxybutyrate is not an anaplerotic substrate. Anaplerosis plays in important role in cerebral glutamate glutamine metabolism. Combination of D-3-hydroxybutyrate with the anaplerotic substrate propionate could enhance its protective effect during hypoglycemia.

We compared the effectiveness of treatment with a single dose D-3-hydroxybutyrate alone or combined with propionate at the time of EEG burst-suppression coma. Both treatments resulted in a reversion of EEG activity from burst suppression to continuity, but only combined treatment resulted in clincal improvement of the comatose state. 3OHB alone largely corrected pathometabolic changes of glutamate metabolism but not of glycolytic and pentose phosphate pathway intermediates or of long chain acylcarnitines. Combined treatment was not associated with biochemical corrections over and above those achieved by 3OHB alone for the metabolites measured.

3OHB treatment has a limited effectiveness on clinical and neuropathology outcome after hypoglycemia in infant rats. The limited effectiveness of 3OHB treatment may be related to its inability to support glycolysis with associated pentose phosphate pathway and anaplerotic activity. Combined treatment with propionate enhances 3OHB's protective effect during hypoglycemic coma. Future protective treatment should be based on complementary metabolic substrates.

Preface

The research presented in this thesis resulted in two manuscripts for publication (chapters 3 and 4). Chapter 3 has been published in *Experimental Neurology* (Schutz, et al., 2011b), chapter 4 has been published in a revised version in *Molecular Genetics and Metabolism* (Schutz, et al., 2011a). The contents of chapter 3 has been presented in part at the European Metabolic Group Meeting in Amsterdam in 2009, chapter 4 has been presented in part as a poster and abstract at the Annual Symposium of the Society for the Study of Inborn Errors of Metabolism (SSIEM) in 2008.

The model development part of this project was designed by me in consultation with Dr. Sylvia Stockler, organized (logistics, animal ethics), and performed by me with the exception of the preparation of the high fat diet and GC-MS analyses of rat milk samples, which were performed in the lab of Dr. Sheila Innis. Data analysis was done by me and Dr. Sylvia Stockler. Interpretation of milk analysis data was done by me and Dr. Sheila Innis. Development of the non-invasive EEG method was in consultation with Dr. Peter Wong.

The study in chapter 3 was devised and designed by me in consultation with Dr. Sylvia Stockler, it was performed by me. Histological analysis was done with technical help from Narinda Dhat of the CFRI Histology Core Facility. Immunohistochemical methods were set up and adapted under my supervision and in consultation with Dr. John O'Kusky. Analysis of EEG data was in consultation with Dr. Peter Wong. Overall data analysis, interpretation, and drafting of the manuscript was done by me. Manuscript revisions were done by me and Dr. Sylvia Stockler.

The study in chapter 4 was devised and designed by me in consultation with Dr. Sylvia Stockler, it was performed by me. Laboratory measurement of amino acids, serum propionate, and pentose phosphate pathway intermediates in tissue homogenates and serum was done by me and Dr. Eduard Struys, measurement of acyl-carnitine species was done by Dr. Graham Sinclair. Analysis of EEG data was in consultation with Dr. Peter Wong. Overall data analysis, interpretation, and drafting of the manuscript was done by me. Manuscript revisions were done by me and Dr. Sylvia Stockler.

The research carried out for this thesis has been approved by the University of British Columbia Animal Care Committee. The study for the validation of blood metabolite measurements (section 2.4) was approved under the Animal Care Certificate number A06-0287, the development of the non-invasive EEG recording method (section 2.3.1) under Animal Care Certificate number A06-0314, and the other experiments done for model development and studies in chapters 3 and 4 under Animal Care Certificate number A06-1556.

Table of Contents

List of Tables

List of Figures

Acknowledgements

The research presented in this thesis would not have been possible without the thoughts, criticisms, and endeavours of many. First and foremost I would like to thank my supervisors Sylvia Stockler and Sheila Innis. Sylvia for the opportunity to work on a challenging project in an atmosphere of free exploration and scientific creativity. Her ability to step back, see through, and condense as well as her commitment to clinical and scientific investigations as basis for the improvement of patient care are an inspiration. Sheila for her passion for research, her generous support, and her patience with me, when I was lost in the world of metabolic pathways. Both for their guidance in the multifaceted world of pathology research. My gratitude is also due to my supervisory committee who supported me from the start.

During the project I have profited from the expertise of many colleagues. I would like to thank John O'Kusky for starting me on histological technique and for teaching me about the pathohistology of the developing brain, Peter Wong for showing me how to read EEG traces, and Eduard Struys for introducing me to tandem mass spectrometry.

Staff at the CFRI animal facility and at the CFRI histology core facility, in particular Narinda Dhatt, were extremely helpful with technical advice and practical support. None of the research would have been possible without their help.

Last but not least I would like to thank my wife Judith for her support and flexibility, and for living with me through the uncertainties that appear to invariably accompany a PhD project.

PETER W. SCHUTZ

Innsbruck
October 2010

1. Introduction, Literature Review, and Research Aims

1.1 Hypoglycemia in infancy and alternative substrates

Hypoglycemia, or low blood glucose levels, in human neonates and infants has long been recognised as a medical condition and carries the risk of permanent neurological damage. The precise nature of determinants for permanent damage are not exactly known. The concentration of glucose in plasma and the duration of pathologically low values are important parameters, but insufficient to predict the actual consequences in neonates and infants. Another factor contributing to the susceptibility for brain injury is the infant's ability to mount a protective metabolic response during hypoglycemia. Evidence suggests that the developing brain in particular is capable of utilizing ketone bodies (acetoacetate and D-3-hydroxybutyrate) as alternative substrates beside its main substrate glucose (Cremer, 1982, Kraus, et al., 1974, Persson, et al., 1972). In addition, glucose consumption in the brain increases during postnatal development (Kinnala, et al., 1996), suggesting that an additional contribution from alternative substrates may have a proportionately larger effect during the early postnatal period.

Neonates and infants differ in their ability to produce ketone bodies in response to hypoglycemia according to their health state. Healthy, appropriate-for-gestational-age babies born at term have typically high ketone levels during hypoglycemia (ketotic hypoglycemia), which may occur for instance during the first days of life during the adaptation to extra uterine conditions. High ketone levels are probably protective for their brains (Hawdon, et al., 1992). On the other hand, babies and infants born preterm, suffering from intrauterine growth restriction (Hawdon and Ward Platt, 1993), presenting with hypersecretion of insulin (hyperinsulinism) or certain inborn errors of energy metabolism, fail to increase circulating ketone bodies during hypoglycemia (hypoketotic hypoglycemia). These infants are perceived to be at increased risk for neurological sequelae.

Outcome studies in children affected by recurrent hypoketotic hypoglycemia caused by hypersecretion of insulin due to Persistent Hyperinsulinemic Hypoglycemia of Infancy showed that 20-40% of these children incur considerable psychomotor or mental retardation despite state of the art treatment, which includes medication to block insulin secretion or surgical removal of a large part of

the pancreas (Meissner, et al., 2003, Menni, et al., 2001). Patients affected with disorders of fatty acid oxidation, a genetically caused impairment of fat metabolism, are at risk of hypoglycemic episodes without compensatory ketone production, and this undoubtedly contributes to long term morbidity in this disease group.

The exogenous provision of ketone bodies in cases such as these has been advocated as an additional treatment strategy (Olpin, 2004) and clinical case studies of oral administration of D,L-3-hydroxybutyrate have been undertaken with promising results (Plecko, et al., 2002, Van Hove, et al., 2003). The key advantage of using ketone bodies as additional supplements is that ketone plasma levels may be more stable than glucose levels in a setting of impaired glucose homeostasis, which underlies most conditions predisposing to recurrent hypoglycemias. They might thus represent a valuable adjunct to the therapeutic management of children at risk of recurrent hypoketotic hypoglycemia.

There is, however, only scarce experimental evidence on the effectiveness and limitations of ketone bodies to protect the developing brain during hypoglycemia, apart from general clinical experience. It has been demonstrated that D-3-hydroxybutyrate prevents degenerative neuronal changes in brain slices from rats at various ages during aglycemic incubation (Izumi, et al., 1998), that the injection of D,L-3-hydroxybutyrate reverses cerebral hypoglycemic symptoms in weanling mice (Thurston, et al., 1986), that mice on a ketogenic diet (a high fat diet that causes increased circulating ketone bodies) have less cerebral hypoglycemic symptoms after low and medium insulin doses (Johnson and Weiner, 1978), and that 21 day old rats which have been weaned on to a ketogenic diet show less neurodegeneration during a 2 hour episode of moderate hypoglycemia than animals on a normal diet (Yamada, et al., 2005). Overall these results show that ketone bodies influence the effect of hypoglycemia on brain function and neuronal survival. However, these results are of limited value only as a basis for future neuroprotective strategies based on ketone therapy for the following reasons. Firstly, results from brain slice studies on hypoglycemic neurodegeneration cannot be extrapolated to the brain in vivo because energy metabolism in brain slices differs with respect to the intact brain in two fundamental respects. A) Substrate supply to the brain in vivo is regulated by the blood brain barrier formed by endothelial cells of the brain capillaries. This barrier is not functional in brain slice experiments. B) The major determinant of energy requirements in the brain is the intensity of neurophysiologic activity (conduction and transmission of electrical signals)(Erecinska, et al., 2004). The density of signal transmission in isolated brain slices is naturally much reduced compared to the intact brain. Pathological energy shortage is always the result of a mismatch between supply and demand. The pathological consequences of hypoglycemia in brain

slices may thus differ from those in vivo, and protective effects in brain slice experiments can only serve as an indication of what to expect in the intact animal.

Second, in vivo experiments involving the ketogenic diet do not differentiate between effects due to elevated plasma D-3-hydroxybutyrate levels and effects due to other changes induced by the diet. These include changes in lipid metabolism (Dell, et al., 2001), changed endocrine patterns (Schwartz, et al., 1989), and changes in protein expression patterns (Sullivan, et al., 2004). Moreover, these experiments did not control for the actual levels of ketone bodies in circulation during the hypoglycemic episode. Since insulin was used to induce hypoglycemia in these experiments and since insulin curbs production rates of ketone bodies, it may be expected that levels were inconstant.

Third, clinical experience and brain slice experiments on the capacity of ketone bodies to sustain neurotransmission (Arakawa, et al., 1991, Wada, et al., 1997) indicate that there are limitations to their effectiveness. The nature of these limitations has not been explored so far. Knowledge of these limitations will be essential for the development of ketone based neuroprotective strategies.

Given the therapeutic promise of alternative energy substrates in paediatric medicine and the insufficient knowledge about their actual effectiveness and limitations, we perceive a need for research directed at closing this gap.

1.2 Research rationale

Our research aims at improving the experimental basis for the use of D-3-hydroxybutyrate supplementation alone, or in combination with other substrates, as protective strategy in conditions with a risk of recurrent hypoglycemia, or of cerebral glucose depletion of other causes, in newborns and infants. Since brain slice or cell culture models suggest a certain effectiveness but have limited applicability, an *in vivo* model of the effects of hypoglycemia on the brain in infancy should be used for further studies. The animal model must be designed so that high rates of cerebral ketone metabolism can be achieved.

1.3 Animal models of hypoglycemic neurodegeneration

The first systematic animal studies of hypoglycemia were based on insulin injection in adult rats under halothane anaesthesia with electrographic monitoring of cerebral activity (EEG), and control of blood gases and circulatory parameters during the hypoglycemic episode. After the hypoglycemic episode, animals survived for 1 week to allow brain injury to evolve (Auer, et al.,

1984b). During hypoglycemia, the EEG shows a progression from normal cortical background activity via slowing and burst suppression patterns to an isoelectric recording (flat line). In this model, brain injury manifests as selective neurodegeneration and is caused only during isoelectric EEG tracings. Moreover, the density of neuronal death in the brain is proportional to the length of the isoelectric stage. Recent investigations of the mechanisms of hypoglycemia induced neuronal death and neuroprotective strategies against it were based on this model (Ferrand-Drake, et al., 2003, Suh, et al., 2003).

During the last few years concern about moderate hypoglycemic episodes in paediatric diabetes patients has led to some studies of moderate hypoglycemia in infancy. Results from suckling mice and pigs suggest that clinically asymptomatic episodes of moderate hypoglycemia may cause neurodegeneration in the infant brain (Kim, et al., 2005, McGowan, et al., 2005). In these studies, animals were injected with insulin and remained under observation over 2 hrs (piglets) or 4 hrs (mice). During this time their behaviour remained unaltered, but neurodegeneration was found upon subsequent analysis. These studies did not monitor cerebral activity by EEG. In an early investigation repeatedly induced severe hypoglycemia in 6-10 day old rats with subsequent motionless episodes resulted in histological signs of irreversible neurodegeneration 4 days after the last insult (Jones and Thomas Smith, 1971). The functional state of the brain during these episodes was not reported.

A more recent study in young adult animals has looked at the neuropathological outcome from repeat moderate hypoglycemia in 21 to 26 day old rats post weaning (Yamada, et al., 2004). Animals were not anesthetised and remained moderately hypoglycemic over 2.5hrs. The investigators found that some animals became symptomatic (loss of posture, clonic limb jerks), but apparently none developed isoelectric EEG tracings. Upon neuropathological analysis, selective neurodegeneration was found in the cortex.

This study by Yamada et al. (2004) suggests that a period of isoelectric EEG may not be necessary for neurodegeneration to evolve in rats. This contrasts with previous studies using the adult rat model reported by Auer et al. (1984b). The contrast might be due to the effect of anaesthesia. Volatile anaesthetics are used in the adult rat model whereas Yamada et al. (2004) did not use anaesthesia. Volatile anaesthetics are now known to have a neuroprotective effect, probably by reducing the damaging influence of excitotxicity (Kawaguchi, et al., 2005). Excitotoxicity is one of the causes of neuronal death during hypoglycemia (Auer and Siesjo, 1993). Considering also the recent reports from mice and piglets it appears that the association of hypoglycemic brain damage with an isoelectric EEG may not always hold, but general conclusions are made difficult by interspecies differences, age differences, and the scarcity of data. We will, therefore, assume that the

state of cortical activity is a major determinant of neurodegeneration during severe hypoglycemia, being aware that isoelectricity may not be the only such state in an unanaesthetized animal.

In summary, animal models to date have shown that severe hypoglycemia inducing isoelectric EEG recordings causes neurodegeneration in the adult rat brain. The EEG is a central technique to monitor the severity of the effect of hypoglycemia on the brain. Moderate hypoglycemia over a longer time causes less well-defined neurodegeneration in the developing brain of mice and pigs. When this thesis research was commenced, we were aware of no EEG controlled models of the effects of severe hypoglycemia on the developing brain. The development of such a model was prerequisite for this project (Project Objective A).

1.4 Hypoglycemia: Pathobiochemistry and pathogenesis of brain injury

The brain reacts to insufficient plasma glucose levels with a progressive reduction in the state of consciousness (from awake, via lethargic and stuporous, to comatose), sometimes with seizure activity. Underlying these signs of dysfunction in the central nervous system is an altered cerebral metabolism accompanied by changes in electrophysiological activity. Hypoglycemia also causes the selective degeneration of neurons in animal models, especially in the cortex and hippocampus. The correlation between cerebral symptoms (clinical, EEG), metabolic aberrations, and neurodegeneration are not entirely understood and may depend to some extent on the model used.

Studies with existing animal models have shown that hypoglycemic animals progress gradually from a state of full alertness to deep coma and EEG suppression. The progression can stretch over a period of 1-2 hours. The gradual nature of this progression is explained by the utilization of endogenous cerebral energy substrates. Major endogenous substrate reserves are astroglial glycogen and cerebral amino acids. Once these reserves are used up, depletion of cerebral ATP levels (bioenergetic failure) may result and trigger neuronal cell death pathways. In the adult rat model, bioenergetic failure occurs at the onset of EEG suppression (Behar, et al., 1985, Lewis, et al., 1974b).

Cerebral glycogen as reserve substrate during hypoglycemia has recently been reviewed (Brown and Ransom, 2007, Gruetter, 2003). Under hypoglycemic conditions total brain glycogen is gradually used up supporting brain function in the absence of an external glucose supply in adult rat and human brain (Choi, et al., 2003, Oz, et al., 2009). EEG suppression in the rat model indicates glycogen depletion. Degradation of glycogen generates glycosyl-units that are metabolically equivalent to glucose. Glycogen reserves are one determinant of the time span between onset of hypoglycemia and the development of cerebral symptoms, in particular of EEG suppression. An 80%

increase of cerebral glycogen reserves results in a delay of coma by about 90 minutes in adult rats (Suh, et al., 2007a).

Cerebral amino acids can play a role as substrates for oxidative energy metabolism during hypoglycemia (Agardh, et al., 1981, Honegger, et al., 2002, Lewis, et al., 1974a). In particular glutamate can be channelled into the citric acid cycle (CAC) for partial or complete degradation (Hertz and Hertz, 2003, Sutherland, et al., 2008). Utilization of glutamate as substrate for the CAC requires prior removal of the amino group, which may either occur as transamination by exchange or as deamination producing free ammonia. Overall the result of ongoing large scale oxidative glutamate utilization in the absence of glucose as source of acetyl-CoA results in the accumulation of aspartate and ammonia, and a depletion of glutamate and glutamine (Figure 1.1). Accumulation of ammonia may eventually limit the oxidative utilization of cerebral glutamate during hypoglycemia, especially because the normal pathway for ammonia detoxification in the brain via formation of glutamine is impossible during hypoglycemia because glutamine is synthesized from glucose.

Once endogenous glycogen and glutamate reserves are exhausted during the gradual progression to the loss of cerebral function (EEG suppression), glucose deprivation results in a reduced supply of glycolytic intermediates and acetyl-CoA. The insufficient supply of acetyl-CoA may eventually cause depletion of ATP and phosphocreatine (bioenergetic failure) (Behar, et al., 1985, Gorell, et al., 1976, Lewis, et al., 1974b).

Hypoglycemic brain injury evolves as a result of metabolic changes and is mediated by several cellular mechanisms. The best understood type of hypoglycemic injury is selective neuronal death, which has been studied in the adult rat model. Evidence for hypoglycemic white matter injury is beginning to emerge only now from MRI studies in human patients, with few experimental studies published to date.

Hypoglycemic neuronal death is not a direct consequence of ATP depletion but it is mediated by several mechanisms (Suh, et al., 2007d). These include an increase in extracellular excitotoxic amino acids combined with a compromised bioenergetic state of cells, NMDA-receptor activation, the effect of reactive oxygen species, and activation of poly(ADP-ribose)polymerase 1 and caspase 3, ultimately resulting in neuronal apoptosis. More recent studies have demonstrated a role of zinc release from presynaptic terminals during hypoglycemia, glucose reperfusion and subsequent NADPH oxidase activation in the pathogenesis of neuronal death (Haces, et al., 2009, Suh, et al., 2003, Suh, et al., 2007c). ROS production and PARP activation take place to a significant extent during glucose reperfusion. This may have important therapeutic implications. In developing brain, A1 adenosine receptor activation may contribute to neuronal death (Kim, et al., 2005). Little other evidence has been published on hypoglycemic neuronal injury in immature brain and its mechanisms.

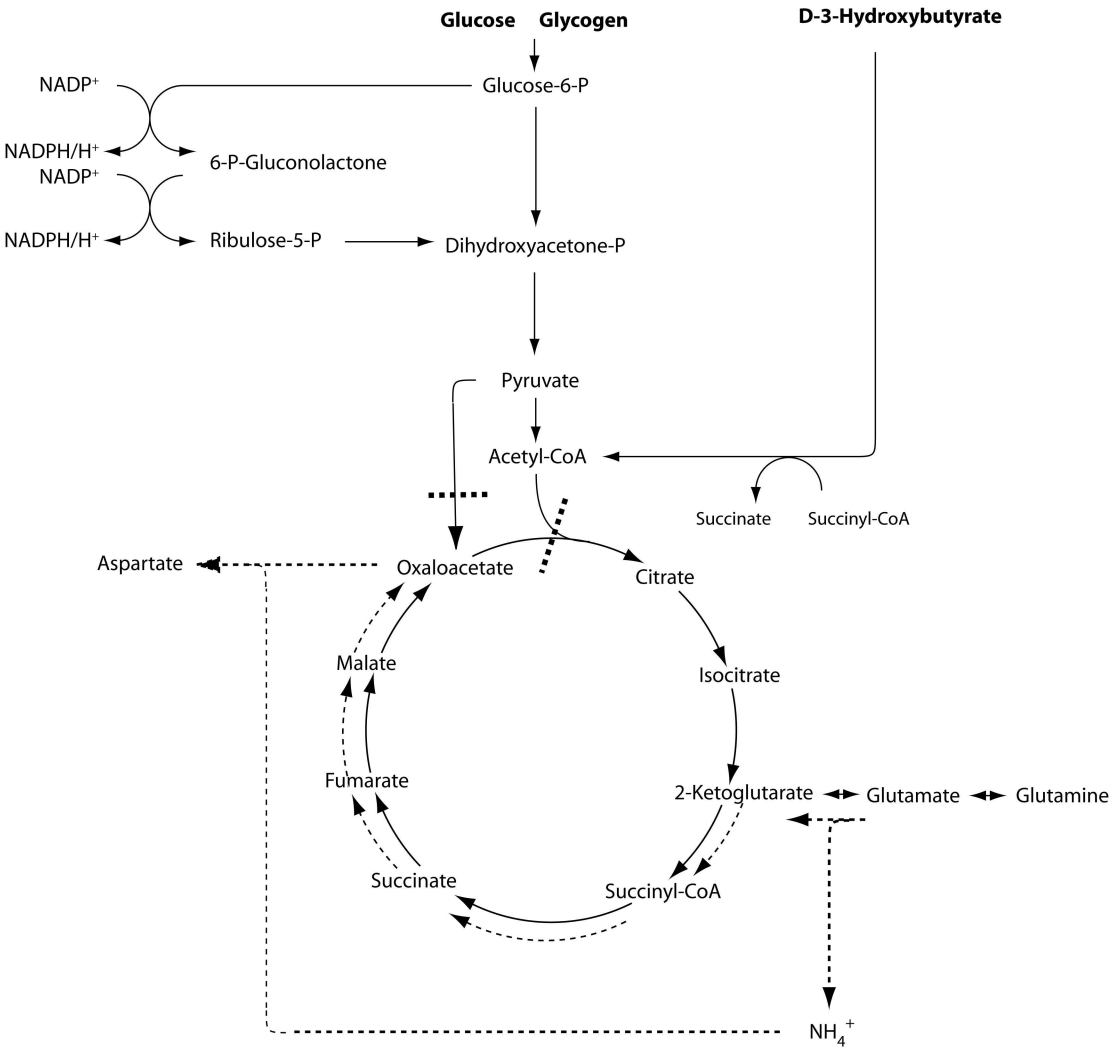

Figure 1.1: Pathometabolism during hypoglycemia

Energy metabolism during hypoglycemia – schematically. Glycolysis serves several metabolic functions, including the generation of acetyl-CoA for oxidation, the generation of NADPH for redox defences, and the generation of oxaloacetate for anaplerosis. 3OHB catabolism can provide acetyl-CoA for oxidation only. During hypoglycemia a lack of pyruvate results in reduced rates for oxaloacetate and acetyl-CoA generation. Insufficient acetyl-CoA can block citrate production in the citric acid cycle, resulting in a block. Glutamate can be utilized as endogenous energy substrate (dashed lines). Following de- or transamination to alpha ketoglutarate, it enters the citric acid cycle and is converted to oxaloacetate. A shortage of acetyl-CoA blocks citric acid synthesis from oxaloacetate. Instead, oxaloacetate is aminated to aspartate, so that the citric acid cycle appears to be only partially active (Sutherland, et al., 2008). During severe hypoglycemia cerebral tissue glutamate concentrations are reduced whereas aspartate and free ammonia are elevated. Biochemically, aspartate might be considered a reservoir of oxaloacetate and ammonia.

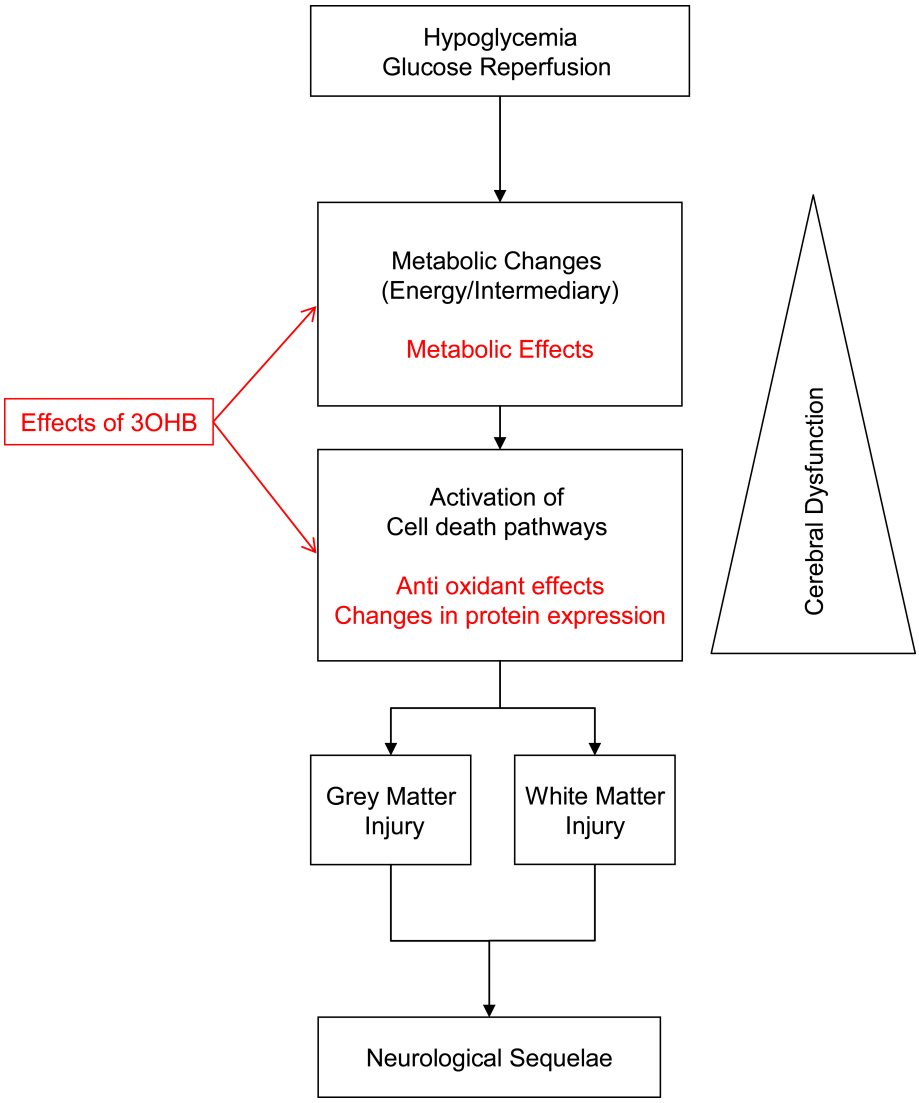

Figure 1.2: Levels of the pathogenesis of hypoglycemic brain injury

The pathogenesis of hypoglycemic brain injury comprises two aspects or levels: metabolic changes (glycogen depletion, acetyl-CoA depletion, aspartate and ammonia accumulation) and the subsequent activation of cellular death mechanisms and pathways (NMDA receptor activation, ROS production, apoptosis induction). Overlying these disturbances is a disruption of brain function (loss of alertness). 3OHB has effects on both levels of pathogenesis. Metabolically, it is a source of acetyl-CoA. On a cellular level it has anti-oxidant effects and appears to have a role in the regulation of anti apoptotic protein expression (section 1.6.3). Since changes in the pathometabolism may also alter the kind of cell death mechanisms triggered, an interpretation of any neuroprotective effect 3OHB might have during hypoglycemia can be expected to be complex.

In summary, during the hypoglycemic progression from full alertness to coma and EEG suppression, the pathobiochemical situation in the brain changes gradually from a state of metabolic compensation by utilizing endogenous glycogen and amino acids to a state of glycolytic and oxidative failure combined with glutamate depletion and cerebral ammonia accumulation. Metabolic failure is indicated by EEG suppression. These primary pathobiochemical changes and subsequent changes during glucose reperfusion eventually trigger cell death processes (excitotoxic NMDA receptor activation, zinc release, NADPH oxidase activation, ROS production, mitochondrial permeability transition, PARP-1 activation, caspase activation) resulting in neuronal death and apoptosis. The pathogenesis of hypoglycemic brain injury has thus two levels, firstly a pathobiochemical and secondly a resulting activation of cellular pathways mediating cell death (Figure 1.2).

1.5 Cerebral ketone metabolism and its animal models

Ketone bodies (D-3-hydroxybutyrate (3OHB), acetoacetate) are produced in the liver as a result of fatty acid β-oxidation. They enter the circulation and are then utilized by other organs, in particular the heart and brain. The production rate and plasma levels of ketones depends on the nutritional state of the organism, with high production during periods of starvation or on a high fat diet. The rate of utilization depends linearly on the arterial plasma concentration. Insulin reduces the rate of ketone production in the liver.

The brain relies mainly on glucose as metabolic fuel, but under some circumstances it also metabolizes ketone bodies to a considerable extent. Utilization of ketone bodies in the brain is broadly determined by two steps. First, their supply is controlled by transport processes across the blood brain barrier. Ketone bodies are transported across this barrier by the monocarboxylate transporter 1 (MCT-1). The density of this transporter in the blood brain barrier varies with developmental age and nutritional state. Second, ketone bodies are metabolically activated in the brain by an enzymatically catalyzed process called ketolysis. Ketolysis of 3OHB takes place in the mitochondrial matrix and is mediated by D-3-hydroxybutyrate dehydrogenase (3-HBD; conversion to AcAc with NADH production), succinyl-CoA:3-oxoacid-CoA transferase (SCOT; activation of acetoacetate to acetoacetyl-CoA by exchange transfer from succinyl-CoA) and mitochondrial acetoacetyl-CoA thiolase (T2; transfer of one acetyl unit from acetoacetyl-CoA to another CoA forming two acetyl-CoA). Activation of one molecule 3OHB yields two acetyl-CoA which are oxidatively metabolized in the citric acid cycle.

The rate of D-3-hydroxybutyrate utilization in the brain is generally proportional to the arterial D-3-hydroxybutyrate concentration. The slope of this dependence is determined by the capacity for D-3-hydroxybutyrate transport across the blood brain barrier.

In humans, the capacity of the brain to utilize ketone bodies is higher in infancy than in adulthood, with about fourfold higher extraction rates in infants than in adults. After 9 hours of starvation, ketone utilization accounts for about 13 percent of total energy generation in the brain of human infants, after a couple of days' starvation possibly for up to 30 percent (Kraus, et al., 1974). In addition, infants develop higher ketone plasma concentrations after the same time of starvation than adults (Bonnefont, et al., 1990).

This developmental pattern of ketone utilization in the brain has been studied extensively in the rat (Nehlig, 2004, Nehlig and Pereira de Vasconcelos, 1993). Suckling rats have high circulating ketone levels, which are sustained by the high fat content of rat milk. Their brains have a high capacity to extract ketone bodies from the circulation, which is reflected in higher expression of the MCT-1 transporter in the blood brain barrier as compared to adult animals, and they have higher enzyme levels for ketolysis as compared to adults. Both transporter and enzyme levels are reduced to adult levels at the end of the suckling period (Nehlig and Pereira de Vasconcelos, 1993, Vannucci and Simpson, 2003). During starvation, ketone bodies may supply about 30% of energy in the brain of infant rats (Dahlquist and Persson, 1976). There is thus a similar developmental pattern in humans and rats concerning the cerebral utilization of ketone bodies for energy production.

Other species are much less studied with respect to the developmental pattern of cerebral ketone metabolism. Many species appear to be less ketogenic than rodents and humans. Pigs, for instance, do not produce ketone bodies before the age of about nine days, and thereafter peak plasma D-3-hydroxybutyrate levels remain below 0.4 mM (Bengtsson, et al., 1969, Gentz, et al., 1970), as compared to 1-1.5mM in human infants and around 2.5 mM in rats. No in vivo studies have been published on the cerebral capacity for ketone utilization in swine, to our knowledge. Dogs and sheep are not ketogenic species and appear to be utilizing ketone bodies only if infused and then to a small extent, so they are physiologically dissimilar to humans and rats in this respect (Erecinska, et al., 2004).

1.6 Effects of 3OHB during hypoglycemia

Ketone bodies have effects at the two levels of the pathogenesis of hypoglycemic brain injury, aberrant metabolism and activation of cell death pathways (Figure 1.2). They have an effect on pathometabolic changes induced by glucose deprivation because they are an alternative substrate for

energy metabolism. Functional studies give an indication of 3OHB's capacity to support cerebral intermediary metabolism. They also have an effect directly on the susceptibility of neurons to cell death by influencing intracellular signalling pathways and ROS production. Published evidence for both types of effects is briefly reviewed.

1.6.1 Metabolic effects and functional studies

3OHB is oxidatively metabolized by the three main cell types of the brain: neurons, astrocytes, and oligodendrocytes (Edmond, et al., 1987). 3OHB's capacity to support a full range of functions in these cells in the absence of glucose has been investigated in brain slice and optic nerve preparations. Hippocampal synaptic activity in brain slices has been used to study the capacity of 3OHB to maintain electrophysiological activity in grey matter with discrepant results. While two studies found that 3OHB can maintain tissue ATP levels but fails to maintain synaptic activity in rat and guinea pig (Arakawa, et al., 1991, Wada, et al., 1997), one study found a good capacity to maintain electric activity in rat brain slices (Izumi, et al., 1998). Evidence also indicates a higher capacity to support synaptic function in slices from pre-weaning rats compared to adult rats (Izumi, et al., 1998, Wada, et al., 1997). Rat optic nerve preparations were used to study the capacity of 3OHB to maintain signal conduction in white matter in the absence of glucose (Brown, et al., 2001). 3OHB had very little capacity to maintain signal conduction but led to a small delay in conduction failure. This was in stark contrast to results for lactate which was able to maintain conduction over a period of 120 minutes in this study. These in vitro results suggest that 3OHB may have a capacity to maintain synaptic grey matter activity, whereas it is a poor substrate to maintain white matter function.

In vivo evidence suggests that 3OHB can sustain global brain function in the absence of glucose in weaning mice. Mice in insulin induced hypoglycemic coma were injected with 3OHB and this treatment resulted in the reversion to a conscious state (Thurston, et al., 1986). However, the study was not EEG controlled. The timing of 3OHB administration during the hypoglycemic progression to coma and the exact staging of this progression is important to define any effect 3OHB may have, because the availability of endogenous reserve substrates varies during the progression to EEG suppression and the effects of 3OHB can be expected to be biochemically different in the presence or absence of additional endogenous glycogen reserves. Glycogen reserves are generally depleted at the onset of EEG suppression.

After the injection of insulin, mice on a ketogenic, high fat diet develop hypoglycemic symptoms later than mice not on such a diet (Johnson and Weiner, 1978). In the latter study, ketone levels were not controlled. Insulin inhibits ketogenesis and therefore it is unclear whether ketone levels were continually elevated during hypoglycemia or were lowered. Overall studies on the

capacity of ketone bodies to sustain brain function during glucose deprivation demonstrate a certain effectiveness but are insufficient to assess the full potential and limitations of 3OHB as metabolic substrate for the brain. For this, studies with an EEG controlled animal model of hypoglycemia that allows monitoring of 3OHB concentrations are necessary (Project Objective B).

1.6.2 Neuroprotective effects

Ketone bodies have neuroprotective effects in a variety of cerebral injury types, including hypoxia ischemia (Suzuki, et al., 2002, Suzuki, et al., 2001), glutamate toxicity with glycolytic inhibition (Massieu, et al., 2003), and MPP toxicity (Kashiwaya, et al., 2000, Tieu, et al., 2003), a model of Parkinson Disease. These studies of 3OHB's neuroprotective potential in several disease models were partly motivated by the finding that the addition of ketone bodies to glucose as energy substrate improves mitochondrial oxidative phosphorylation and ATP generation in heart muscle, and was associated with increased cardiac output (Kashiwaya, et al., 1994, Sato, et al., 1995). This suggested that 3OHB could also improve ATP production in neurons and thus reduce their susceptibility to excitotoxic cell death. Since then the evidence clearly shows some neuroprotective effects, but also suggests that other mechanisms than improved ATP production may be responsible for the effect. These include in particular the reduction of oxidative injury and an increased expression of anti apoptotic proteins, as discussed in the next section.

There is little direct experimental evidence for neuroprotective effects of ketone bodies during hypoglycemia. Neuronal degeneration after glucose deprivation was reduced by 3OHB in brain slices from PND 15 and 30 rats, but not from PND 120 (Izumi, et al., 1998). Rats weaned onto a ketogenic diet showed less injury in a model of moderate hypoglycemia than rats weaned on to a carbohydrate rich diet (Yamada, et al., 2005). Although 3OHB plasma levels are elevated on a ketogenic diet, it is important to realize that neuroprotective mechanisms due to a ketogenic diet may differ from the effects of 3OHB alone because of differing availability and kind of plasma unesterified fatty acids in a ketogenic state (Maalouf, et al., 2009). Overall there is some consistent experimental evidence that 3OHB promotes survival of neurons during hypoglycemic states. The extent and determinants of this effect remain unknown. A well-controlled animal model of hypoglycemia in immature brain that allows 3OHB treatment could provide the basis for further studies (Project Objective B).

The interpretation of effects of 3OHB treatment on hypoglycemic neurodegeneration is complicated by issues of standardization of the severity of a hypoglycemic insult. To study effects of 3OHB on the susceptibility to hypoglycemic neuronal death presupposes a comparison of cell death rates in a similar pathometabolic environment. However, the presence of 3OHB changes the intermediary metabolism in cells during hypoglycemia and may thus change the pathometabolic

situation and resulting triggers of cell death processes involved, in addition to making cells possibly more resistant to cell death mechanisms. Investigations in other disease models allows certain conclusions as to protective mechanisms independent of any metabolic effects during hypoglycemia.

1.6.3 Neuroprotective mechanisms

Ketone bodies have shown neuroprotective potential in several types of injury suggesting mechanisms which target cell death pathways common to these injury types. Recent studies suggest antioxidant effects (Beskow, et al., 2008, Haces, et al., 2008, Kim do, et al., 2007, Maalouf, et al., 2007, Mejia-Toiber, et al., 2006). Antioxidant effects can be exerted at several levels, including the neutralization of existing reactive oxygen species (ROS) by direct chemical interactions, and the reduction of the production of ROS in mitochondria. One study describes a hydroxyl-radical scavenging capacity of both D and L isomers of 3OHB (Haces, et al., 2008). Evidence also exists that 3OHB reduces mitochondrial ROS production in neurons in response to glutamate toxicity *in vitro*, possibly by increasing the rate of NADH oxidation (Maalouf, et al., 2007). These results were obtained from cells utilizing glucose and 3OHB, and it is unclear whether these results could be extrapolated to glucose deprivation. A beneficial effect during hypoglycemia *in vivo* is suggested by the observation that 3OHB reduces hippocampal lipoperoxidation after hypoglycemia in adult rats (Haces, et al., 2008). The mechanisms involved have not been fully elucidated. Combining these indications that 3OHB has anti oxidant activity with the pathogenetic role of oxidative injury during hypoglycemia, especially in immature brain (Ballesteros, et al., 2003, McGowan, et al., 2006), confirms that 3OHB could be a promising neuroprotectant during hypoglycemia.

Effects of ketone bodies on cerebral protein expression can also reduce susceptibility to neuronal death. Treatment with 3OHB prior to an episode of focal ischemia increases hypoxia inducible factor 1α (HIF-1α) expression via metabolic regulation of intracellular succinate concentrations (Puchowicz, et al., 2008). Cytosolic succinate levels prevent the degradation of HIF-1α and increase with cerebral 3OHB utilization because the activation of 3OHB requires succinyl-CoA. In addition 3OHB treatment increases the expression of the anti-apoptotic protein bcl-2. This has been suggested to explain a reduced lesion volume after focal ischemia in rats treated with a ketogenic diet or intraventricular 3OHB administration (Puchowicz, et al., 2008). The treatment effect based on this mechanism may not necessarily rely on the availability of ketone bodies during an acute injury, but on prior ketone induced changes in protein expression. Since neuronal injury after hypoglycemia is largely apoptotic, one might expect that these effects could also contribute to neuroprotection after hypoglycemia.

1.7 Biochemical limitations of ketone bodies as a replacement of glucose

Although both 3OHB and glucose are a source of acetyl-CoA, they differ metabolically in many other respects. Glucose is metabolized in the cytosol and glucose derived carbons are metabolized in the mitochondrial matrix. Glucose provides cytosolic NADH and generates ATP glycolytically, it provides substrates for the pentose phosphate pathway and anaplerosis (pyruvate carboxylation to oxaloacetate). These metabolic processes support amongst others, neurotransmitter homeostasis, redox equilibrium (Banhegyi, et al., 2008), and oxidative defences. 3OHB is not an anaplerotic substrate, nor is it metabolized to glycolytic intermediates. It is a singular source of acetyl-CoA.

The metabolic comparison suggests that a replacement of glucose with 3OHB may result in an ongoing oxidative energy metabolism with concomitant suppression of glycolysis and associated pathways. The functional and pathogenetic consequences of a failure of metabolic support for glycolysis and its associated functions in the brain are unknown, but could contribute to imbalances of citric acid cycle intermediates, neurotransmitter homeostasis, and susceptibility to oxidative injury.

Glutamate is the major excitatory neurotransmitter in brain. Its metabolism is partitioned into an astroglial and a neuronal compartments. This compartmentalization forms the basis of the glutamate glutamine cycle. Glutamate is synthesized de novo from glucose in astrocytes via anaplerotic pathways (pyruvate carboxylase) and transamination with branched chain amino acids as nitrogen source. Glutamate converted to glutamine and subsequently transported to neurons through the extracellular space. Neurons reconvert glutamine to glutamate. During neurotransmission, glutamate is released from synaptic vesicles into the synaptic cleft. Uptake from the synaptic cleft is mainly into astrocytes, where glutamate is again converted to glutamine. This is the glutamate glutamine cycle that supports excitatory neurotransmission. Glutamate is lost from this cycle mainly because of ammonia detoxification (Cooper and Plum, 1987), oxidative metabolism of glutamate (Hertz and Hertz, 2003), and drainage into the intermediary metabolism of amino acids in the brain. Glutamate loss must be continually replenished by anaplerotic influx into the pool of citric acid cycle intermediates to generate alpha ketoglutarate as precursor, and an influx of nitrogen from branched chain amino acids. Metabolic flux measurements with isotope tracers have shown that about 30 % of the glutamine flow from astrocytes to neurons is de novo and supported by anaplerosis, whereas the remainder is supported by reuptake of glutamate from the synaptic cleft (Oz, et al., 2004, Patel, et al., 2005, Xu, et al., 2004).

The main substrate for anaplerotic reactions in brain is glucose, which is glycolytically converted to pyruvate and transformed to oxaloacetate. Rates for anaplerosis have been shown to vary with the degree of electroencephalographic activity in the cortex, demands on ammonia detoxification, and in response to cerebral trauma (Bartnik, et al., 2007, Sibson, et al., 1998, Sibson, et al., 2001). It has also been suggested that rates of glucose metabolism vary with electrophysiological activation patterns because of the demands on glutamate metabolism. Glucose plays thus a key role as anaplerotic substrate in supporting glutamate metabolism and for neurotransmitter homeostasis in the brain.

Ketone bodies cannot substitute for glucose in this respect because they are not an anaplerotic substrate. During ketone supplemented hypoglycemia, the lack of anaplerotic support could cause disturbances in the glutamate glutamine cycle with consequences for neurotransmission and brain function. Moreover, if insufficient anaplerosis had also an effect on the pool of citric acid cycle intermediates, this could impair flux through the cycle and NADH generation even though ketone bodies are available as a source of acetyl-CoA (Owen, et al., 2002). Possible consequences include functional failure of neurotransmission and impaired ATP generation with associated cellular injury. However, the relevance of these possible mechanisms during acute, ketone supplemented hypoglycemia is unknown. If they are relevant, then a combined supplementation with ketone bodies and a cerebral anaplerotic substrate could be superior in its ability to maintain brain function and integrity compared to ketone bodies alone (Project Objective C).

1.8 Project objectives

A) Develop an animal model of the effect of insulin induced hypoglycemia on immature brain in which the effect of 3OHB supplementation can be tested (chapter 2).
B) Study the clinical, electroencephalographic and neuropathological differences between 3OHB-treated and untreated hypoglycemic animals (chapter 3).
C) Study the effect of the additional provision of an anaplerotic substrate on the effectiveness of 3OHB supplementation (chapter 4).

1.9 Experimental design

Ketone bodies and glucose are metabolically not equivalent. Ketone bodies are an oxidative substrate, glucose is an oxidative substrate and a glycolytic substrate. Glycolysis supports cytosolic NADH generation, the pentose phosphate pathway, and anaplerosis. In particular intact pentose

phosphate pathway activity and anaplerosis could play in important part in the maintenance of redox and neurotransmitter homeostasis. Glycogen is an important cerebral reserve substrate during hypoglycemia that feeds into glycolysis and oxidative metabolism. In the absence of an external glucose supply from the bloodstream, glycogen is gradually used up. Adding ketone bodies as alternative energy substrate during hypoglycemia may, therefore, have differing metabolic effects according to the status of cerebral glycogen reserves. When glycogen is abundant, ketones might represent an additional oxidative substrate which allows sparing of glycogen reserves for the pentose phosphate pathway and anaplerosis by reducing the rate of its degradation (glycogen sparing). When glycogen is depleted, ketone bodies might only be able to compensate for a deficit of oxidative ATP generation and might not be able to compensate the glycolytic deficit. The associated functional and neuroprotective effects might also differ. It is, therefore, possible that 3OHB treatment during the hypoglycemic progression to coma has a stage specific metabolic effect. The experimental design has to take this into account and careful clinical and EEG staging of the effects of hypoglycemia on the brain will be important. EEG suppression indicates exhausted glycogen reserves.

In an *in vivo* situation, a spectrum of different grades of metabolic derangements and of grades of glycogen depletion is to be expected. At the beginning of a hypoglycemic episode animals are alert and cerebral metabolic disturbances are probably minimal despite low blood glucose levels, because they can be largely compensated for by endogenous reserves. At the other end of the spectrum, there is severe coma and onset of EEG suppression. In this situation glycogen reserves are depleted and metabolic aberrations are considerable. There are thus two basic possibilities for stage specific 3OHB treatment:

1) 3OHB can be supplemented from the start of a hypoglycemic episode. This might result in a combination of glycogen sparing and the provision of additional oxidative energy. It is unknown whether ongoing supplementation during hypoglycemia would result in a complete prevention of coma and EEG suppression or not. This design was chosen for the study in chapter 3 (Project Objective B).

2) 3OHB can be supplemented at the time when glycogen reserves are exhausted i.e. at the onset of EEG suppression. This might cause the provision of an oxidative substrate in a situation with very limited supply of glycolytic substrates. This experimental design can be expected to be suitable to test the additional effect of anaplerotic substrates, because endogenous anaplerosis from glycogen reserves should no longer be possible. This design was chosen for the study in chapter 4 (Project Objective C).

2. Model Development

The need for an *in vivo* model of hypoglycemia in infancy has been outlined in the previous section. At the time the research in this thesis was conducted, there were no published studies of well-controlled, sustained and severe hypoglycemia in developing brain and there were only few studies of the neuropathological effects of moderate hypoglycemia on infant brain (Grimaldi, et al., 2005, Kim, et al., 2005, McGowan, et al., 2005). These studies are, however, not representative of the clinical condition of aggressive hypoketotic hypoglycemia. The model development project was based on results from an adult rat model developed in the 1980s (Auer, et al., 1984a, Friberg, et al., 1998). Our objective was to induce sustained hypoglycemia and to monitor the clinical, EEG and neuropathological consequences on the developing brain. During hypoglycemia, plasma glucose and 3OHB levels must be monitored. Hypoglycemia should be terminated by glucose resuscitation and animals should survive. In addition, manipulation of 3OHB plasma levels during hypoglycemia must be possible. We chose insulin to induce hypoglycemia because this resembles persistent hyperinsulinemic hypoglycemia of infancy, a condition resulting in recurrent hypoketotic hypoglycemia in affected infants. This chapter presents the scientific rationale and results of several method development studies that finally contributed to an EEG controlled model of hypoglycemic coma in infant rats.

2.1 Choice of species and age

Rats are the only common laboratory species known to have a developmental pattern of ketone metabolism in brain similar to humans and we therefore chose rats as model species. A comparison of maturation of cortical metabolic rates for glucose (Kinnala, et al., 1996, Nehlig, et al., 1988) and of the ontogeny of EEG patterns (electrical activity is the most important determinant for energy expenditure in the brain) (Gramsbergen, 1976) between humans and rats suggests that rats on postnatal day 13-14 (date of birth as PND 0) are representative of human infants around 2-3 months of age in these respects. The details of this comparison are outlined below.

The brain of rats at birth is immature compared to the human brain at birth. Experiments should therefore be performed at an age of the rat pups at which brain development corresponds in important and model specific respects to that of humans in their first year. Widely used in experimental studies

to model injury to the developing brain is PND 7. The rationale for PND 7 is based on the observation that the point of maximal absolute brain weight gain as a percentage of adult weight in humans is at term while it occurs at PND 7 in rats (Hagberg, et al., 1997). Comparison of other parameters of cerebral maturation (enzymatic, synaptic) suggests that PND 12-13 can equally be considered as equivalent of term humans (Romijn, et al., 1991, Tucker, et al., 2009). To model hypoglycemic encephalopathy in developing brain a similarity with respect to energy requirement and glucose metabolism is important. A major determinant of cortical energy requirement and glucose metabolism is electrophysiological activity, which can be monitored by EEG recording (de Graaf, et al., 2004, Erecinska, et al., 2004, Sibson, et al., 1998).

Cortical rates for glucose metabolism and the pattern of EEG traces follow a maturational pattern in humans and rats (Figure 2.1). Glucose utilisation increases in an exponential-like pattern of gradual changes, making a precise comparison of stages difficult (Kinnala, et al., 1996, Nehlig, et al., 1988). EEG maturation, on the other hand, shows distinctive milestones of maturation which have been delineated in rats and humans. Initially, the EEG is monotonous and shows no organisation according to behavioural state (awake, quiet sleep, active sleep). At around 32 weeks of post-conceptional age in humans, quiet sleep acquires characteristic discontinuous higher amplitude characteristics, which gradually transform to continuous slow wave sleep. This transformation is completed around 44 weeks of post-conceptional age. Between 45 and 46 weeks, sleep spindles appear as a distinguishing characteristic of quiet sleep (Clancy, et al., 2003). In rats, quiet sleep patterns differentiate around postnatal day 12 (Frank and Heller, 1997, Gramsbergen, 1976, Mirmiran and Corner, 1982), and transform to a predominantly continuous slow wave sleep within about 2 days. Sleep spindles appear around postnatal day 14 (Frank and Heller, 1997, Gramsbergen, 1976). EEG maturation in the awake and active sleep states are less marked during this period, with a continuous mid to low amplitude, mixed frequency activity in humans after 32 weeks of post-conceptional age and in rats around postnatal day 8 (Gramsbergen, 1976). The developmental pattern of quiet sleep thus lends itself to a comparison and also reflects the functional maturation of the cortex with respect to the organisation of neurotransmission patterns (Watanabe, et al., 1974). According to this developmental comparison, postnatal day 13 to 14 in rats corresponds to around 45-46 weeks of post-conceptional age or 1.5-2 months after term birth in infants. We chose PND 13 for this project.

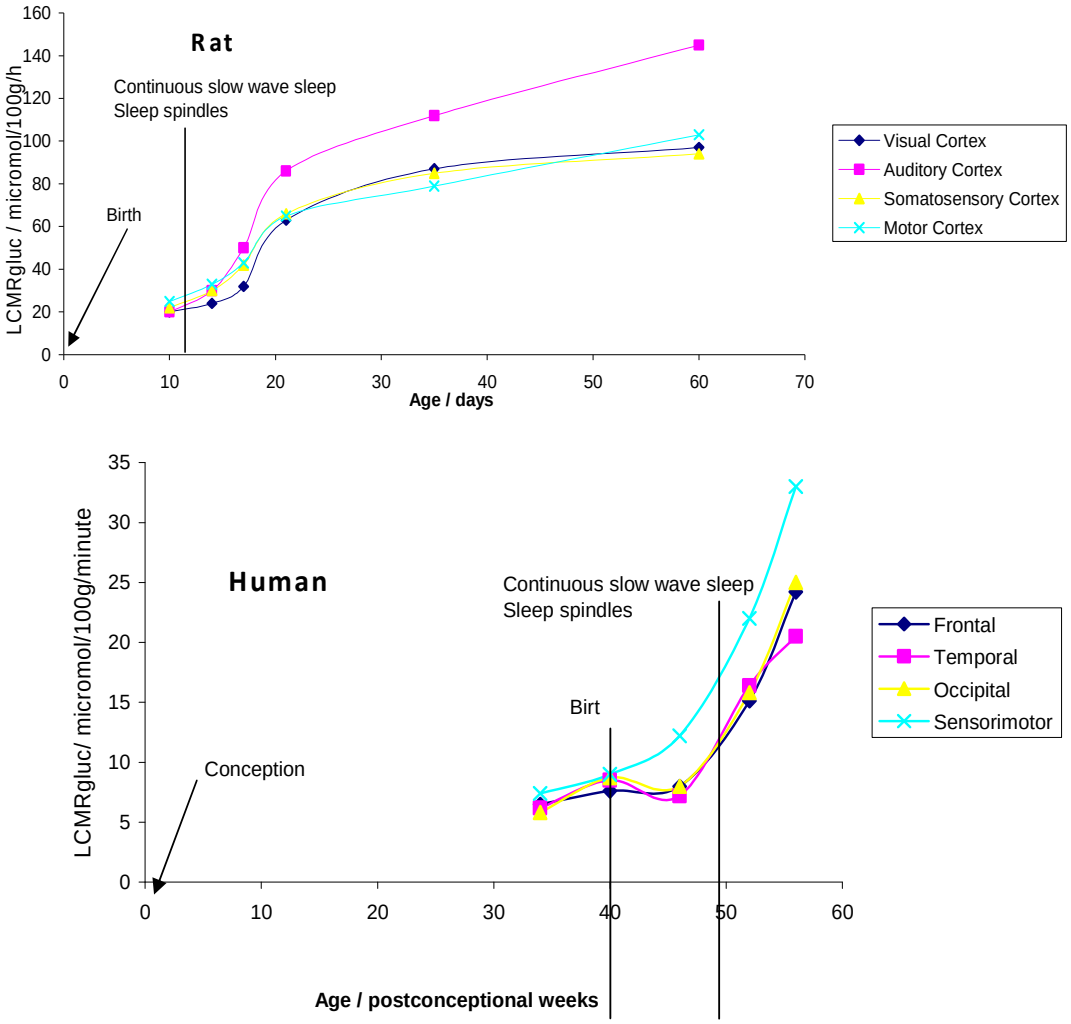

Figure 2.1: Postnatal development of glucose metabolism in humans and rats

Maturation of the rate of glucose utilization in the cortex of rats and humans. The gradual increase in rats between days 10 and 20 and in humans between postconceptional weeks 38 and 55 makes a direct comparison difficult. The appearance of continuous slow wave sleep and sleep spindles marks a milestone in EEG maturation that allows a direct comparison. Data from (Frank and Heller, 1997, Gramsbergen, 1976, Kinnala, et al., 1996, Nehlig, et al., 1988). LCMRgluc: local cerebral metabolic rate for glucose.

2.2 Technical requirements and method development

An *in vivo* model system of insulin-induced hypoglycemia with rat pups can be divided in various phases. The following may be distinguished:

- *Induction phase*: Injection of insulin until hypoglycemia (plasma glucose < 1 mM)
- *Hypoglycemic phase*: beginning of hypoglycemia until resuscitation by glucose injection
- *Resuscitation phase*: glucose injection until return to dam (righting reflex intact)
- *Recovery phase*: high risk phase after return to dam (2-3 hrs)
- *Survival phase*: end of recovery phase to sacrifice of the animal at 4 days post procedures.

Monitoring and standardization of the hypoglycemic phase in 13-day-old rats should include electroencephalographic (EEG), biochemical (plasma glucose and 3OHB levels) and clinical (alertness level) techniques. Rats at PND 13 are suckling. Weaning occurs only at day 20-21. Therefore animal husbandry and survival of rat pups creates additional technical challenges. Careful clinical monitoring of the reacceptance of the pups by the dam after hypoglycemia in addition to monitoring of signs of recurrent hypoglycemia during the recovery phase are important.

EEG recordings in experimental animals are usually done with surgically implanted epi- or subdural electrodes. To facilitate re-acceptance of the pups by the dam after the experiment and to reduce animal stress we sought a non-invasive technique for electrode placement. The development of a method for non-invasive EEG recordings is outlined in section 2.3.

Biochemical monitoring in our model requires repeat plasma glucose and 3OHB measurements from small blood samples. 3OHB measurements are possible in small sample volumes with a handheld meter (Precision Xtra, Abbott). No reports exist about the validity of such an approach in infant rats, and the procedure had to be validated before experiments. Since lactate is another potential alternative substrate for brain metabolism and a handheld lactate meter is available, we included this technique in the validation study in section 2.4.

For clinical grading of the alertness state of pups during hypoglycemia, we devised a scoring system based on the observed neurologic symptoms during hypoglycemia. For clinical monitoring of pups and dam after their return to the nest we devised a set of standardized monitoring sheets. These developments are presented in section 2.5.

The induction of hypoglycemia with insulin and manipulation of associated plasma 3OHB levels needed to be tested before any experiments. The dosing of insulin and the pharmacokinetics of

3OHB administration in 13 day old rats were tested and respective dosing schemes designed during model development and are reported in section 2.6.

Two potential confounding factors in our model could be a) changes in plasma lactate concentrations during insulin induced hypoglycemia, and b) shifts in electrolyte (sodium, potassium) concentrations in response to insulin injections and injections of sodium D-3-hydroxybutyrate. These were looked at in an additional study in section 2.7.

Finally, initial trials demonstrated that plasma 3OHB levels showed a less than expected reduction in response to insulin. The final part of the model development project was to explore potential pharmacological and nutritional strategies to achieve a greater reduction of ketone levels during hypoglycemia, summarized in section 2.8.

2.3 Electroencephalographic monitoring

2.3.1 Development of a technique for non-invasive EEG recordings

Background. To monitor cortical electrical activity during hypoglycemia in a research model for hypoglycemic brain injury in the developing rat, a non-invasive method for EEG recordings from infant rats is required. The least invasive electrode system are cutaneous electrodes, which are glued to the skin. The next stage of invasiveness is represented by subcutaneous electrodes, which are inserted with a needle resembling a subcutaneous injection and hooked in the subcutaneous space. There are no reports in the literature of recordings with cutaneous electrodes from infant rats.

Aim. To establish the technical basis for short term (2-3 hrs), non-invasive recording of the cortical electrical activity in 13-17 day old rats.

Objectives

Stage 1. Compare EEG recordings from small cutaneous electrodes with recordings from subcutaneous electrodes in anaesthetised animals. Optimise and select best system.

Stage 2. Evaluate selected system in awake animals, including stability of recordings over time and susceptibility to artefact.

Methods. *Animal source, transfer, and maintenance.* Timed pregnant Sprague Dawley rats were obtained from Charles River Laboratories, Canada, and arrived at the Animal Care Facility of the Child and Family Research Institute (CFRI) 7-10 days before parturition to allow for antepartal acclimatisation. Litters were culled to 8 animals between postnatal days 2 and 5.

Electrode Systems and Placement. Cutaneous electrodes were small Ag/AgCl electrodes (4mm diameter, Slimtrode, IVM, Healdsburg, USA). They were attached to the shaved and depilated (Nair crème) head either with an adhesive conductive gel (TacGel, IVM, Healdsburg, USA), or after mild

abrasion (Nuprep Gel, Weaver, USA) with conductive gel (Ten20, Weaver, USA) and a ring of collodion as glue (Collodion, Mavidon, USA). Collodion was applied through a 22G needle to the rim of the electrodes while they were held in place with pincers. In awake animals, cutaneous electrodes were protected with a custom made rubber cap (finger of laboratory glove with holes for the ears).

Subcutaneous electrodes were short subdermal wire electrodes (SWE, Grass Telefactor, Astro-Med, USA), consisting of 1cm long flexible insulated wires with a non insulated Ag/AgCl coated tip. Placement procedure resembles a subcutaneous injection with applicator needles. Subcutaneous electrodes were secured to the skin at their exit point with tissue glue (VetBond), medical tape, or collodion glue (Collodion, Mavidon, USA).

Two recording electrodes were attached symmetrically in biparietal location rostral to a line joining the anterior ear margins, roughly over the sensory motor cortex. The reference electrode was attached in midline position anterior or posterior to the these.

Amplification and Digitisation. Signals from the pair of biparietal electrodes and the reference were differentially amplified with Animal BioAmp (input impedance 1MOhm), digitised with PowerLab 8/30, and recorded with Chart 5.4 Software (all ADInstruments, USA). Amplification range was ±100 μV across a frequency range of 0.1-100 Hz. Digitisation rate was at 1000 Hz.

Anaesthesia. Inhalant anaesthesia was induced with isoflurane in oxygen at a concentration of 4-5% and maintained at 1-2%. Depth of anaesthesia was varied during EEG recordings to produce characteristic EEG changes. Anaesthesia was monitored pulse oximetrically (MouseOx, Starr LifeSciences, USA).

Experimental protocol.

Stage 1: Selection of best electrode system, and results on electrode placement and its mechanical stability. Selection criteria were signal quality, ease of placement, and invasiveness. Pups 13-16 days of age were removed from the nest, anaesthetised, respective electrode systems placed, signals monitored, and finally the depth of anaesthesia was increased and EEG changes were observed and compared to expectations (progression from continuous activity via burst suppression pattern to isoelectricity with increasing anaesthetic depth). This served to differentiate cortical signals from noise and simulated to some extent the changes expected during hypoglycemia.

Stage 2: Validation of recording technique selected in stage 1. Rat pups 13-17 days of age were removed from the nest, electrodes of the selected system were placed with suitable restraint, EEG was recorded continuously for 2 hours to obtain baseline EEG activity across different vigilance states, test for electrode stability over time, and monitor occurrence of artefacts. During the recording, rat pups were in a small cage and could move freely around. Concomitant notes on behavioural states were made.

Analysis. Visual analysis of recordings was done with consultative support from Dr Peter Wong, Director, Diagnostic Neurophysiology, BC Children's Hospital. His contribution is gratefully acknowledged.

Results and Discussion

Stage 1

Cutaneous electrodes. Tests of the various forms of electrode attachment showed that 1) mild abrasion of the skin under the electrodes is necessary to reduce electromagnetic noise from surroundings (reduction of impedance), and 2) that collodion provides far better stabilisation than TacGel. It also proved more convenient to attach the reference electrode in an occipital midline position and not in frontal location (Figure 2.2). With this technique, recordings were very satisfactory and the expected electroencephalographic patterns across different depths of anaesthesia could be clearly distinguished (Figure 2.3) (Akrawi, et al., 1996).

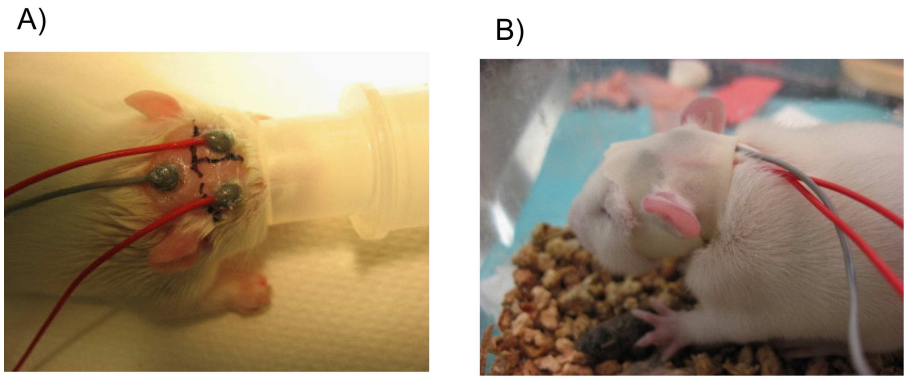

Figure 2.2: Electrodes in situ and protected with rubber cap

A) Cutaneous electrodes in biparietal position an occipital reference electrode attached with collodion glue. Black marks indicate midline and line joining anterior margin of the ears. B) Rubber cap made from glove finger to protect electrodes mechanically in awake pups.

Subcutaneous electrodes. Signals were strong and little electromagnetic background noise was apparent. However, it proved difficult to control the exact localisation of the tip of the wire electrode. Fixation of the wire to the skin for stabilisation with VetBond and/or medical tape was problematic. Collodion showed better stability. However, the arrangement proved very susceptible to movement artefacts, probably because the geometry of the electrode arrangement in the subcutaneous space is easily distorted (elasticity of tissue and bending of wires), and also very susceptible to electrocardiographic artefacts (better subcutaneous conduction). Considerable baseline drifts after

about 30 minutes were apparent in one recording, likely due to inflammatory reactions around the short subcutaneous wire tunnels, with subsequent fluid accumulation and changes in conductive properties.

Selection of electrode system. Based on good signal quality from the cutaneous system compared to a high susceptibility to movement/cardiac artefacts and distortions associated with subcutaneous trauma with the short wire electrodes, we selected cutaneous electrodes as best system.

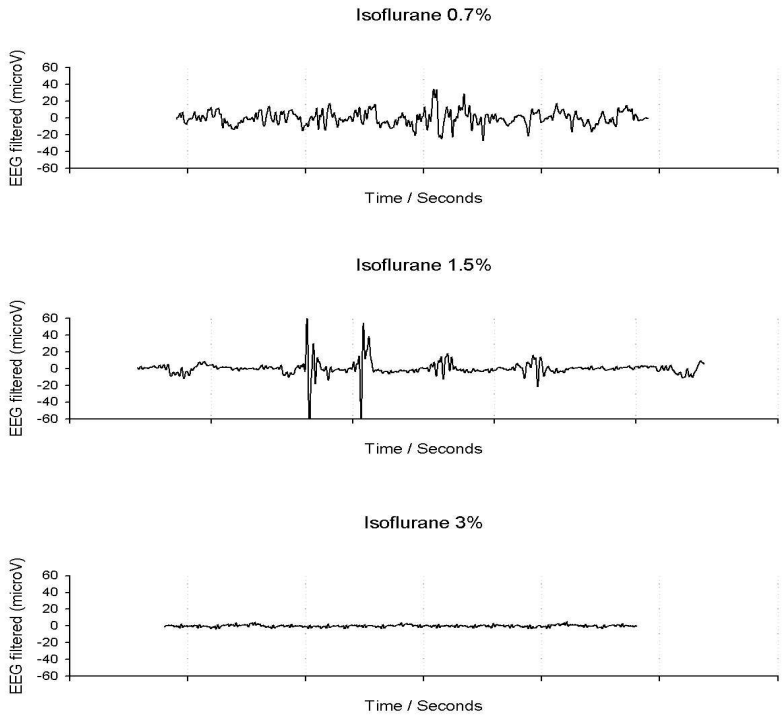

Figure 2.3: Validation of non-invasive EEG recording - EEG traces during isoflurane anaesthesia

Validation of non-invasive EEG recording technique across different anaesthetic stages. Raw signals were digitally filtered off-line with a band pass filter for 0.8-50 Hz. EEG recordings from the same animal across three different dosages of isoflurane during anaesthesia. Isoflurane 0.7%: continuous activity with intermittent slow waves. Isoflurane 1.5%: Burst Suppression pattern. Isoflurane 3%: Isoelectricity with visible electrocardiographic artefact.

Stage 2

Placement, mechanical, and electrical stability of cutaneous electrode system on awake animals. Placing small electrodes on the scalp and glueing them into place with collodion was done during short anaesthesia of the animals. After recovery, rat pups attempt to remove the electrodes by scratching/grooming. A rubber cap proved essential to prevent this (Figure 2.2). Recordings from four animals were stable over two hours, after which the experiment was terminated. Small baseline drifts were apparent after off-line analysis in one case, possibly caused by a) movement of electrode leads relative to each other, and/or b) sweating under the rubber cap. Bundling of leads and small perforations in the cap may improve this.

Differentiation of behavioural states. Observation of the animals after awaking from anaesthesia showed quick behavioural recovery. Initially the animals were alert and explored the new surroundings (new cage). After this, various behavioural states could be observed during the recording time. They fell roughly into four categories (Gramsbergen, et al., 1970): 1. Active wakefulness (eyes open, gross bodily movements such as grooming or sniffing, no locomotion), 2. Quiet wakefulness (eyes open, no gross bodily movements, no locomotion), 3. Locomotion (eyes open, walking around), 4. Quiet sleep (eyes closed, body posture maintained, no gross bodily movements), 5. Active sleep (eyes closed, body posture maintained, twitching of limbs or sniffing). EEG during these phase agreed with published results for electroencephalographic cortical activity of 15-17 day old rat pups in these states (Frank and Heller, 1997, Gramsbergen, 1976, Jouvet-Mounier, et al., 1970), in particular slow waves with high amplitude during quiet sleep, high frequency waves of lower amplitude during active sleep, mixed frequency continuous activity during quiet wakefulness, and an emphasis on higher frequency waves and suppression of slow waves during active wakefulness (Figure 2.4). These results were reproducibly obtained from four animals.

Conclusion

Cutaneous electrodes attached to depilated, mildly abraded scalp in developing rats are a stable, low noise system for short term electroencephalographic recordings from the parietal cortex in developing rats. For awake animals additional mechanical stabilisation with a rubber cap is necessary to protect electrodes from scratching/grooming. The final SOP for electrode attachment without anaesthesia can be found in the Appendix, section 7.2.1.

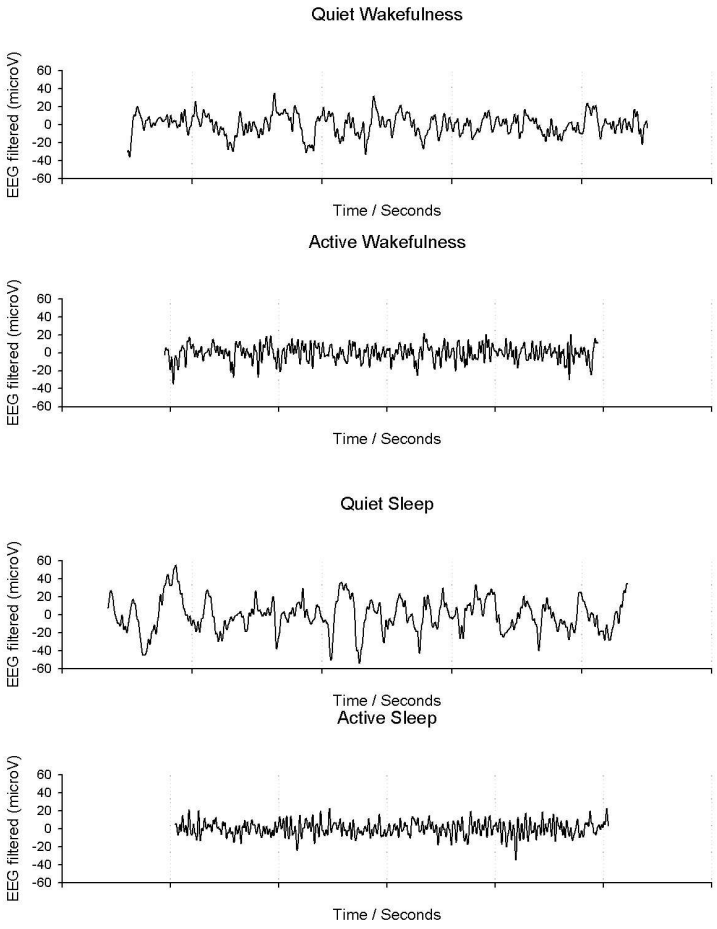

Figure 2.4: Validation of non-invasive EEG recording - traces in various behavioural states

Validation of non-invasive EEG recording technique across different behavioural stages. Raw signals were digitally filtered off-line with a band pass filter for 0.8-50 Hz. EEG recordings from a 17 day old rat pup across four behavioural states, about one hour after isoflurane anaesthesia. Quiet wakefulness: eyes open, no gross bodily movements, Active wakefulness: eyes open, gross bodily movements such as grooming or sniffing, no locomotion, Quiet sleep: eyes closed, body posture maintained, no gross bodily movements 5. Active sleep: eyes closed, body posture maintained, twitching of limbs or sniffing. Changes in amplitude and frequency are clearly visible.

2.3.2 Quantitative EEG analysis

EEG suppression is characteristic of the EEG pattern during severe hypoglycemic encephalopathy. EEG suppression has a gradual onset with short stretches of suppressed EEG activity interspersed with episodes of continuous EEG activity. With progressive severity, the extent of suppressed periods increases. To quantify the degree of EEG suppression, we calculated the suppression ratio (SR) online. The SR is the ratio of the duration of suppression to the total duration of any given EEG epoch. It was calculated according to Vijn's algorithm (Vijn and Sneyd, 1998) implemented on CHART 5 data processing software (ADInstruments, USA) for an epoch length of 8s (for programming details see appendix). The EEG was defined as suppressed if its derivative remained within a window of ± 0.4 mV/s for at least 200 ms. The choice of parameters was validated with awake animals, and with animals under isoflurane anaesthesia.

2.4 Validation of blood metabolite monitoring with handheld meters

Background. For accurate monitoring of plasma energy substrates a method was required that allows the measurement of glucose, D-3-hydroxybutyrate and preferably lactate in very small, repeatedly obtainable blood samples. Handheld meters are commercially available for all three metabolites. Sample volumes between 0.6 and 5 microliters were required. Repeat small blood samples can be obtained from 13 day old rats by puncture of the lateral tail vein. There are no data in the literature validating such an approach, especially for D-3-hydroxybutyrate and lactate. The aim of this preliminary study was to demonstrate that measuring circulating glucose, D-3-hydroxybutyrate, and lactate levels with handheld meters by peripheral venous puncture is acceptable for the model under development.

Method. *Study design.* Concentrations of respective metabolites were measured in 14 day old rats a) by handheld meters from a blood drop that emerges after puncturing a lateral tail vein, and b) by standard laboratory methods from a larger sample (0.5 – 1ml) obtained by cardiac puncture. To simulate the range of values expected later in the research model, animals were subjected to measurements 1) under physiological conditions, 2) after the injection of insulin, 3) after the injection of a D-3-hydroxybutyrate solution. Results from handheld meters and laboratory methods were compared. Total animal number was 48, chosen to obtain reasonably accurate 95% limits of agreement for the method comparison. All animals were anaesthetized during the experiment.

Animal source, transfer, and maintenance. Timed pregnant Sprague Dawley rats of conventional microbiological status were obtained from Charles River Laboratories, Canada, and

arrived at the CFRI Animal Care Facility 7-10 days before parturition to allow for antepartal acclimatisation. Litters were culled to 8 animals between postnatal days 2 and 5.

Anaesthesia. Pups aged 13-16 days were removed from the dam and weighed. Inhalant anaesthesia with isoflurane/oxygen was induced at 4-5% isoflurane concentration in an anaesthetic chamber, and maintained at 1-2.5% isoflurane with a face mask or in the anaesthesia chamber for longer duration. The animals were kept on a warming blanket.

Insulin injection. Pups were injected subcutaneously in interscapular location with 5-14 U/kg regular human insulin (Humulin R, Eli Lilly, USA) or fast acting insulin aspart (NovoRapid, Novo Nordisk, Canada). Blood samples were drawn between 45 and 120 minutes after insulin injection.

D-3-Hydroxybutyrate injection. Pups were injected subcutaneously in interscapular location with 5 or 10 ml/kg 600mM sodium D-3-hydroxybutyrate (Sigma) solution. The solution was of neutral pH and had been sterilised by 0.22 micrometer filtration. Anaesthesia was maintained and monitored for 15 - 50 minutes.

Peripheral venous puncture of the lateral tail veins. The lateral tail veins are best suited for venous puncture in 14 day old rats (results from preliminary trials with Karen Nelkenbrecher at the UBC Animal Care Centre). Animals were anaesthetised. Lateral tail veins were visible on the sides of the tail in many instances. Puncture is performed by pricking the side of the tail with a 22 G needle, preferably under visual control, sometimes blindly if the tail vein is invisible. After successful puncture, a blood drop emerged which was large enough for one set of measurements of glucose, D-3-hydroxybutyrate, and lactate.

Cardiac puncture. Cardiac puncture was performed according to SOP 006 of the UBC Animal Care Guidelines.

Deproteinisation. 0.5 ml blood were mixed with 0.5 ml ice cold 1M perchloric acid, vortexed, and left on ice until centrifugation (16,000g for 10 minutes at 4 degree Celsius). Clear supernatant was neutralised with 0.35 volumes of 0.7M tripotassium phosphate solution, centrifuged (16,000g, 10mins, 4 degree Celsius), and supernatant was conserved at -20 degree Celsius until analysis. Dilution resulting from deproteinisation was 1:2.7. All laboratory measurements were made in deproteinized extract.

Glucose measurement. The handheld meter was a Precision Xtra glucometer (Abbott, USA) with test strip technology based on the oxidation of glucose by glucose dehydrogenase. The laboratory method used for comparison was standard method in BC Children's Clinical Biochemistry laboratory, based on the oxidation of glucose by glucose oxidase, concomitant generation of hydrogen peroxide, and colorimetric measurement of the latter (Vitros GLU slides, Orthos Clinical Diagnostics, GB).

D-3-hydroxybutyrate measurement. The handheld meter was a Precision Xtra ketometer (Abbott, USA) with test strip technology based on the oxidation of D-3-hydroxybutyrate by D-3-hydroxybutyrate dehydrogenase. The laboratory method was based on the same enzymatic reaction, NADH was detected spectrophotometrically by measuring the change in absorption at 340 nm over 1 minute and conversion of kinetic data to D-3-hydroxybutyrate concentrations (RANBUT Kit, Randox, GB).

Lactate measurement. The handheld device was a Lactate Pro lactometer (Arkray, Japan) with test strip technology based on the oxidation of lactate to pyruvate by lactate oxidase. The laboratory method used for comparison was the standard method in BC Children's Clinical Biochemistry Laboratory, based on the oxidation of lactate by lactate oxidase with concomitant generation of hydrogen peroxide, which was measured colorimetrically (Vitros Lac slides, Orthos Clinical Diagnostics, GB).

Statistical Analysis. Method comparison data were plotted linearly for inspection one method against the other. Statistical comparisons were made by Bland Altman plots and calculation of 95% limits of agreement. Data for glucose demonstrated increasing deviation with higher values and were therefore log transformed before calculation of limits of agreement. All calculations were performed with Microsoft Excel.

Results

Glucose

Meter measurements correlated well with lab results (Fig. 2.5 and 2.6). Meter results tended to be smaller than lab results with a mean bias of -1.1mM. The lower 95% limit of agreement was -33%, the upper 6%, based on log transformed data.

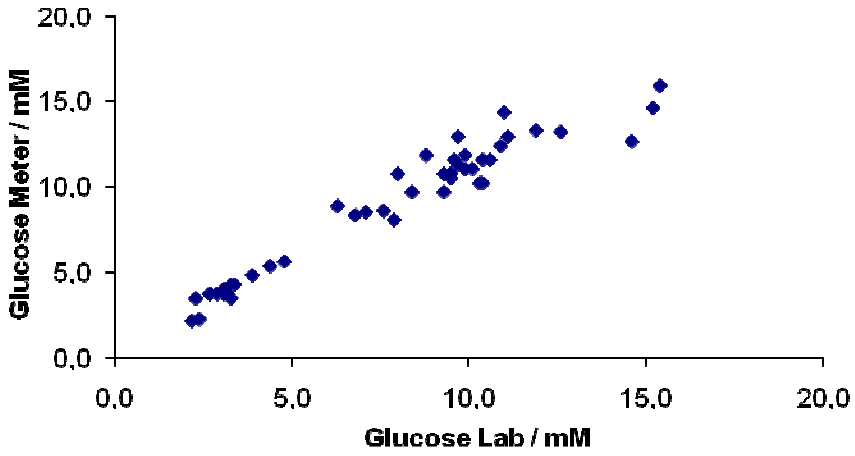

Figure 2.5: Linear plot for the validation of Precision Xtra glucose measurements

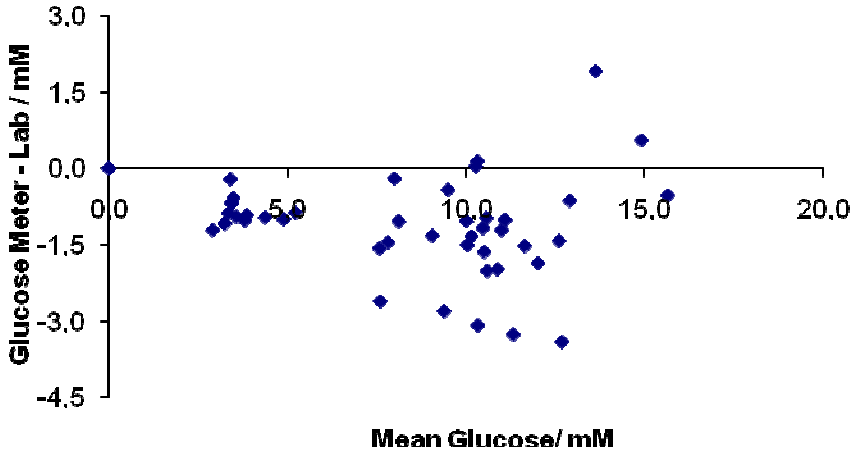

Figure 2.6: Bland Altman plot (difference vs. mean of meter and lab measurement) for validation of Precision Xtra glucose measurements

D-3-Hydroxybutyrate

Meter measurements correlated well with lab results in a range from 1 to 4 mM (Figures 2.7 and 2.8). Meter measurements had a mean bias compared to the lab method of +0.13mM, the lower 95% limit of agreement was -0.69mM, the upper was 0.95mM.

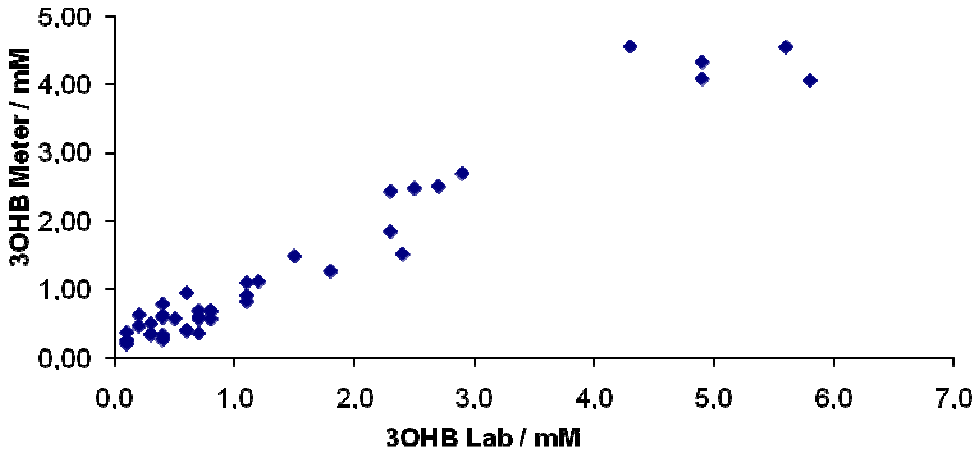

Figure 2.7: Linear plot for validation of Precision Xtra 3OHB measurements

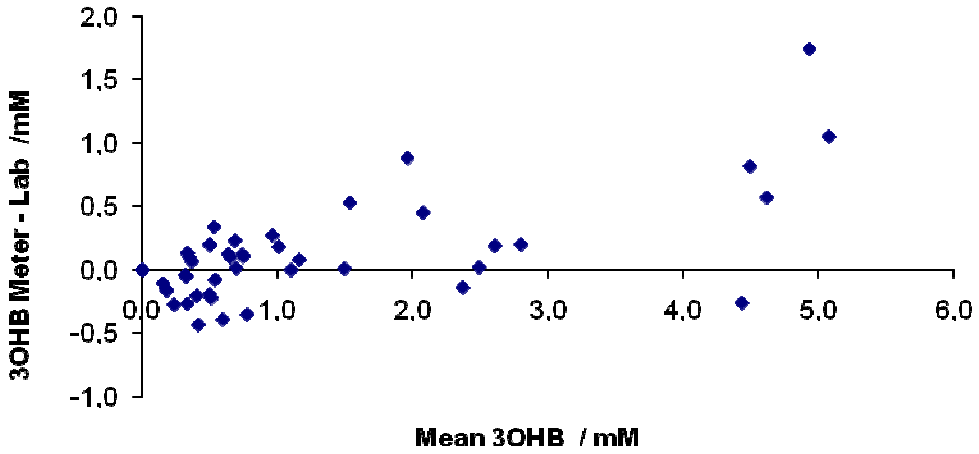

Figure 2.8: Bland Altman plot (difference vs. mean of meter and lab measurement) for validation of Precision Xtra 3OHB measurements

Lactate

The number of samples for a linear method comparison was limited by the measurement range of the lab method (0.5mM-12mM) and the dilution resulting from the deproteinisation procedure

(effective lower measurement limit 1.35 mM, 30 samples below, 18 above). Meter measurement did not correlate in any significant degree with lab measurements (Figure 2.9 and 2.10).

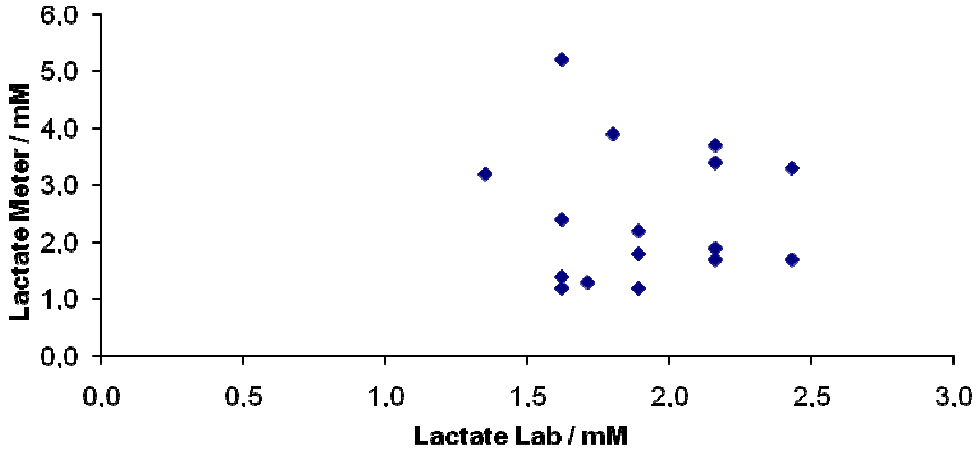

Figure 2.9: Linear plot for validation of handheld lactate measurements

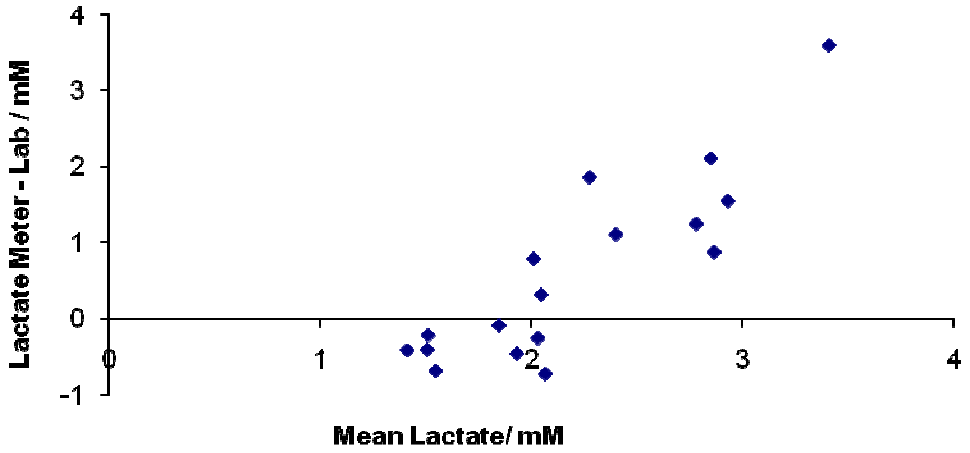

Figure 2.10: Bland Altman plot (difference vs. mean of meter and lab measurement) for validation of handheld lactate measurements

Comparison of those lab samples below the measurement range to respective meter measurements was based on a categorisation as either <1.35mM or >1.35mM. Kappa as statistical measure of the agreement of both methods on this basis was 0.19, indicating very poor correlation.

Because of the poor correlation we tested the lactometer in other settings and found a variability for repeat measurements of a single sample of heparinised human blood of 9.4% CV (mean 1.1mM, n=10), for repeat measurements from capillary samples obtained by repeated finger pricks from different fingers of the same subject a CV of 23% (mean 1.3mM, n=13), with one falsely elevated measurement of 3.9mM. Repeat measurement of a Randox quality control serum level 2 (expected value 4.4mM, range 3.5-5.3) resulted in a mean of 4.7mM, CV 3.9% (n=10).

Discussion

Glucose

Meter measurements correlate well with lab measurements. However, the large systematic bias of -1.1mM of meter vs. lab result was unexpected and various factors may have contributed.

Inaccuracy of the Precision Xtra device compared to reference methods in previous studies showed a bias of -0.1mM in one investigation (Ho, et al., 2004) and a mean bias of -10% compared to reference method measurement in another (Kristensen, et al., 2005). The bias found in this study was larger, especially for the small concentration range, and relatively constant across the whole concentration range (see Bland Altman Plot).

Regional kinetics of glucose metabolism and physiology may cause site specific sample differences in glucose levels. In humans, venous whole blood and capillary whole blood glucose measurements during the postabsorptive state after a glucose meal may differ by up to 1mM (Kuwa, et al., 2001). Capillary values largely reflect arterial levels prior to metabolism in tissues, and peripheral venous levels reflect post tissue metabolism values. Tail vein puncture in developing rats yields largely venous blood (post tissue metabolism in the tail) mixed with tissue fluid, whereas cardiac puncture yields (arterial or venous) pooled blood and is subject to whole body glucose homeostasis, inclusive of gluconeogenic output from the liver and glucose absorption from the gastrointestinal system (in this study, rats were not fasted). This could potentially explain the direction and magnitude of the bias found in our study.

In conclusion, Precision Xtra glucose measurements in tail vein samples correlate well with the reference method applied to cardiac samples. However, sampling site specific differences may have to be taken into account when interpreting the values obtained.

D-3-Hydroxybutyrate

Bias and limits of agreement found in our tests agree with published evaluations of the Precision Xtra ketometer in human studies (Byrne, et al., 2000, Ham, et al., 2004). Specifically, deviations of the meter readings greater than 4.5mM have been described in diabetic children (Ham, et al., 2004). Below this threshold, limits of agreement found in our test were around ± 0.5 mM. The main purpose of D-3-hydroxybutyrate monitoring in our model was to distinguish between a ketotic

group (2-3mM) and a hypo-ketotic group (0-0.5mM). Our comparison data indicate that this is well possible with the Precision Xtra ketometer and lateral tail vein puncture.

Lactate

There was no significant correlation between meter measurements and laboratory measurements. Inspection of the correlation plot suggests that the laboratory method produced values between 1.5 and 2.5mM, whereas meter measurements had a range of 1-5mM, with no systematic relationship between the two. Data from the additional tests on finger prick blood, human venous samples and control sera indicate that precision and accuracy of the Lactate Pro lactometer itself are acceptable. The lack of correlation between meter measurements and reference method results are therefore most likely due to preanalytic and sampling site specific problems. These could have two causes:

1. Regional kinetics of lactate metabolism. Venous lactate concentrations depend on the arterial concentrations of lactate entering the tissue, the net balance between lactate production and extraction in respective tissues from which venous blood is collected, and the production of lactate by erythrocytes. Production rates of lactate in tissues depend on the oxygen content of arterial blood and perfusion. Cardiac samples, on the other hand, reflect whole body lactate metabolism. Lactate content of tail veins will thus be determined by the perfusion of the tail (affected possibly by anaesthetic parameters or occlusion during the sampling procedure) and possibly by the position of the puncture site along the tail (the tip could be less well perfused/supplied with oxygen compared to the base with a resulting proximal to distal gradient). This may account for unsystematic variability of meter measurements. In addition, literature data suggest that measurements from small volumes of blood from a skin prick may be occasionally falsely elevated (Saunders, et al., 2005).

Regardless of the interpretation, small samples from the tail vein sampling in developing rats do not reflect central lactate concentrations. We conclude that cardiac samples are necessary for lactate determinations and the experimental design will have to reflect this.

Conclusion

Monitoring of circulating glucose and D-3-hydroxybutyrate levels by handheld meters and tail vein sampling is acceptable for the research model under development. The measurement of lactate levels requires cardiac puncture under metabolically appropriate anaesthesia.

2.5 Clinical monitoring

2.5.1 Alertness score

Initial observations of hypoglycemic rat pups identified several characteristic neurological symptoms during the progression of the hypoglycemic encephalopathy. Four major parameters to grade the alertness and severity of the hypoglycemic encephalopathy proved useful: the type of spontaneous movements, resting body posture and muscle tone, the righting response, and the tail pinch response. Based on consistent observations we developed a scoring system for quantification (Table 2.1).

2.5.2 Recovery phase

After resuscitation with glucose, pups recovered the righting reflex mostly within 20 -60 minutes. As soon as the righting reflex was intact pups, were returned to the nest to enable suckling and stabilize hypoglycemic recovery. During the initial phase after their return to the nest of about 3-4 hours pups and dam were monitored hourly using a clinical evaluation sheet (see appendix section 7.1.2) for early detection of recurrent hypoglycemia, rejection by the dam, or neurological injury that could possibly interfere with suckling and survival.

Spontaneous Movement	Score	Righting response	Score
Walking, head movements strong	3	Righting within 10s	3
Crawling, head movements weak	2	Coordinated, but failing	2
Dystonic or rhythmic myoclonic	1	Dystonic or rhythmic myoclonic	1
None (no movement after prodding)	0	No response	0
Resting posture and muscle tone	Score	Tail pinch response	Score
Legs tugged under body, rounded back	2	Directed flight	3
Legs spread out, flat back	1	Coordinated, but ineffective	2
Floppy animal	0	Dystonic or rhythmic myoclonic	1
		Slight twitch	0

Table 2.1: Alertness score

Table 2.1 continued
Alertness score (A-score) for clinical staging of the effects of hypoglycemia in 13-day-old rat pups. Points are added to obtain the final score. 11: full alertness, 10-9: mildly, 8–5: moderately, 4–0: severely reduced alertness (coma). The righting response was assessed after turning the animal on its back. The pain response was assessed after a slight tail pinch. Dystonic posturing in response to either stimulus included truncal flexion or extension, and leg extension and crossing; rhythmic myoclonic patterns included hind limb paddling and simultaneous hind limb pushing. Note that observations of resting posture and muscle tone identified only three characteristic stages during the clinical progression. Resting posture is the posture adopted by animals during inactivity. In floppy animals truncal muscle tone was severely reduced, so that they appeared completely limp during handling.

2.6 Insulin and D-3-hydroxybutyrate dosage selection

2.6.1 Insulin dose

To select a suitable dose for insulin treatment that causes glucose levels below 1 mM and allows recovery of glucose levels after the experiment we treated 13 day-old rat pups with different doses of insulin (Humulin R, Eli Lilly, Canada; freshly diluted with sterile saline to 3 U/ml) and monitored blood glucose levels with handheld meters. Results showed that 10 U/kg was the smallest dose to induce sustained severe hypoglycemia at about 90 minutes after injection with spontaneous recovery after about 150 minutes (Figure 2.11). We therefore selected treatment with 10 U/kg to induce hypoglycemia in this model with a repeat injection after 120 minutes unless signs of a severe hypoglycemic encephalopathy were present (severe coma, EEG suppression).

Observations of animals under isoflurane anaesthesia after insulin injection showed that the response to insulin is blunted considerably by isoflurane with lowest levels after 14 U/kg between 2 and 4 mM (Figure 2.12). It is known that isoflurane impairs glucose tolerance, increases gluconeogenesis and hampers peripheral glucose utilization (Carli, et al., 1993, Diltoer and Camu, 1988, Horber, et al., 1990, Laber-Laird, et al., 1992, Tanaka, et al., 2005). Our observations confirmed these findings for 13 day old rats. Moreover, the effect of isoflurane on glucose homeostasis lasted at least until 2-3 hours after termination of anaesthesia. We therefore avoided isoflurane anaesthesia during any preparatory stages and during the experiment itself.

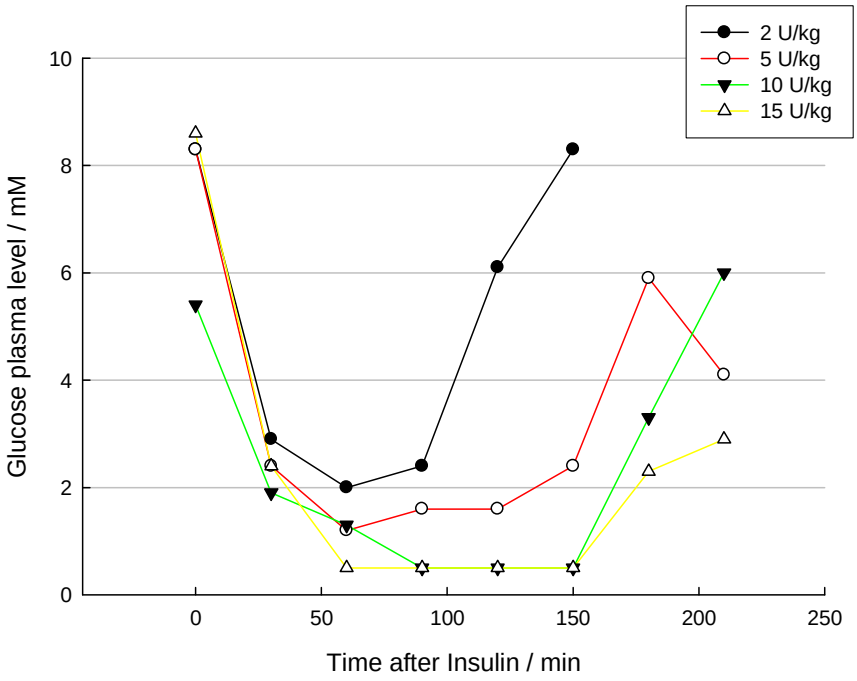

Figure 2.11: Plasma glucose after insulin treatment in various doses

Plasma glucose levels in response to various insulin doses administered s.c. at time 0 minutes in awake 13-day old rats. Symbols represent serial measurements from single animals.

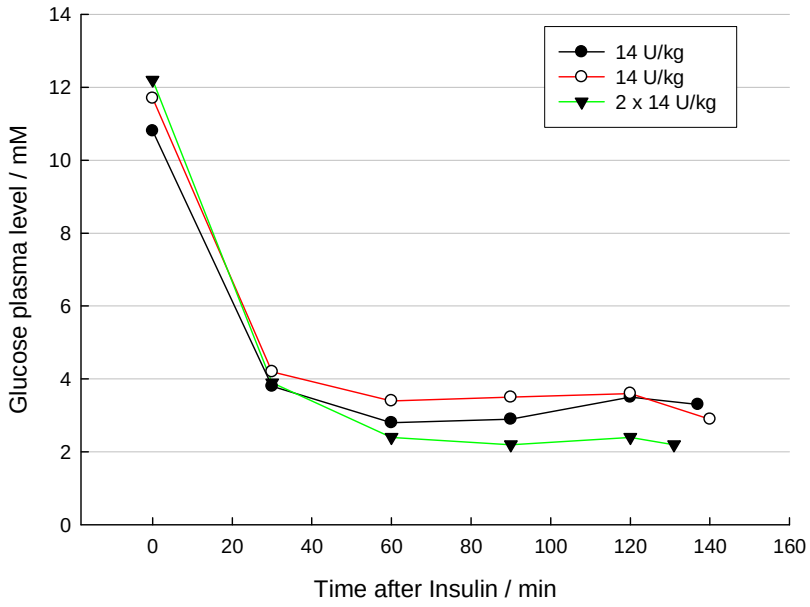

Figure 2.12: Plasma glucose levels after insulin treatment during isoflurane anaesthesia

Plasma glucose levels in response to various insulin doses administered s.c. at time 0 minutes in 13-day old rats during isoflurane (2%) anaesthesia. Symbols represent single animals.

2.6.2 Dosage of D-3-hydroxybutyrate

Subcutaneous injection of 3OHB causes a temporary elevation of plasma levels in adult rats (Langhans, et al., 1985). We monitored 3OHB plasma levels in response to subcutaneous injection of a sterile, neutralized solution of 600mM sodium D-3-hydroxybutyrate (3OHB; Sigma-Aldrich, USA) in doses of 5 mmol/kg and 10 mmol/kg. Figure 2.13 shows increase in 3OHB plasma levels above baseline. Baseline levels are around 1.5 mM, so that peak values reached after 10 mmol/kg were around 5-6 mM. Our tests confirmed that s.c. injection of 3OHB increases plasma levels in developing rats in a dose dependent manner with a steep initial increase over a time span of abut 20-30 minutes. To achieve a target range of high physiologic levels of 3-4 mM, a loading dose of 6 mmol/kg and maintenance doses of 3 mmol/kg every 30 minutes proved effective.

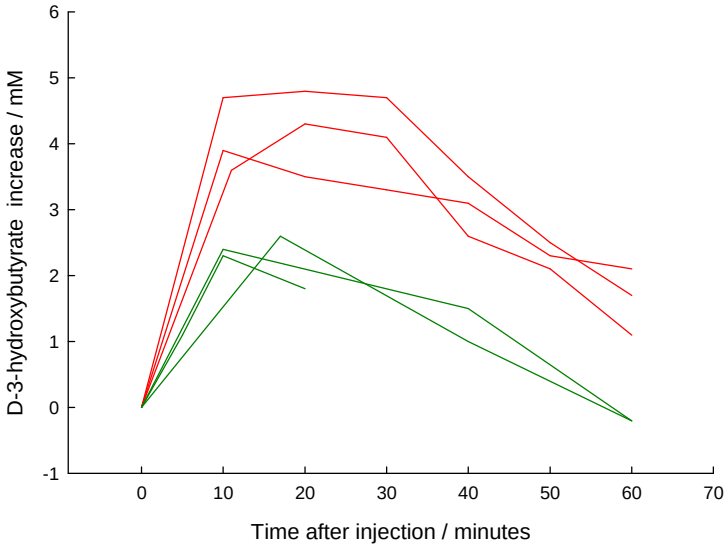

Figure 2.13: Plasma 3OHB concentrations after single dose 3OHB treatment

Increase in D-3-hydroxybutyrate plasma levels above baseline in response to s.c. injection of 5 mmol/kg (green) or 10 mmol/kg (red) of a 600 mM solution in 13-day-old rats. Each line represents measurements from one animal.

2.7 Lactate and electrolytes in response to insulin and 3OHB treatment

Background. Lactate is an alternative substrate for energy metabolism in developing brain in rats and other species (Dombrowski, et al., 1989, Fernandez and Medina, 1986, Hellmann, et al., 1982, Thurston, et al., 1983, Vicario and Medina, 1992). It is transported across the blood brain barrier by the monocarboxylate transporter 1 (MCT-1), the same transporter as 3OHB. The response of blood lactate levels to insulin treatment in infant rats is not known from the literature. Increased transport of glucose into muscle and liver cells in response to insulin could increase rates for glycolysis and lactate production. If lactate levels were significantly elevated during insulin induced hypoglycemia, this could be an important confounding determinant for the progression of a hypoglycemic encephalopathy in this model.

Plasma sodium and potassium levels are known to be affected by insulin (which has a tendency to lower potassium and increase sodium levels) and possibly by treatment with 3OHB. 3OHB treatment is administered as 600 mM solution of sodium D-3-hydroxybutyrate, thus creating an extra sodium load. The extent to which plasma electrolyte levels vary in response to insulin and 3OHB injection is unknown. However, electrolyte imbalances can cause osmotic imbalances in the brain or impair cardiac excitation and conduction. Especially hypernatremia of sufficient extent and speed of onset may result in cerebral myelinolysis in rats. The ability of PND 13 rats to maintain plasma electrolytes in response to insulin and 3OHB treatment is therefore an important prerequisite for this model.

Aim. To evaluate the stability of lactate, sodium, and potassium plasma levels in response to insulin and 3OHB treatment in this model.

Method. A total of 45 PND 13 rat pups from 6 litters were randomly assigned to 7 groups for the measurement of plasma lactate, sodium, and potassium levels as well as glucose and 3OHB measurements. Groups were measured 1) at baseline, 2) at 1 hr after insulin injection, 3) at 2 hrs after insulin, 4) at 1 hr after insulin and 3OHB treatment, 5) at 2 hrs after insulin and 3OHB treatment, 6) at 1 hr in untreated controls, and 7) at 2 hours in untreated controls. Insulin (Humulin R, Eli Lilly, USA) was administered at a dose of 10U/kg after a fasting period of 3hrs. 3OHB (600mM sodium D-3-hydroxybutyrate (Sigma) solution, sterile and neutral) was injected 30 min after insulin at a loading dose of 10 ml/kg followed by 5 ml/kg every 40 minutes according to group.

Heparin blood samples for lactate, sodium and potassium measurements were obtained by cardiac puncture after deep isoflurane anaesthesia, blood was drawn into a heparinized syringe. An aliquot of the sample was immediately deproteinized with perchloric acid and kept on ice for lactate measurement in BC Children's Hospital Laboratory. The remainder was centrifuged and plasma was submitted for determination of sodium and potassium levels to BC Children's Hospital Laboratory. Glucose and 3OHB were measured after lateral tail vein sampling by handheld meters (Precision Xtra, Abbott). Since the lower limit of measurement for glucose is 1mM with this system, all glucose measurements lower than 1 mM were assigned a value of 0.5 mM for statistical evaluation. Mean values were compared by one way ANOVA and Bonferroni post hoc test.

Results and Discussion. *Lactate.* Blood lactate levels were not elevated above baseline in any of the treated groups (Figure 2.14). At 2 hrs after insulin injection, levels were significantly lower than baseline. However, control levels at 1 hr and 2 hrs after injection were also slightly lower than baseline, and compared to those, levels were not significantly lowered. Results suggest that the effect of insulin in 13 day old rats does not include raised lactate levels. The increased intracellular glucose availability in liver and muscle is probably compensated by increased glycogen synthesis, so that

surplus glucose is stored rather than channelled into glycolysis with concomitant lactate production. Stable or respectively decreased lactate levels 2 hrs after insulin injection demonstrate that a hypothetical increase of lactate in response to insulin treatment is not a major confounding factor in this model.

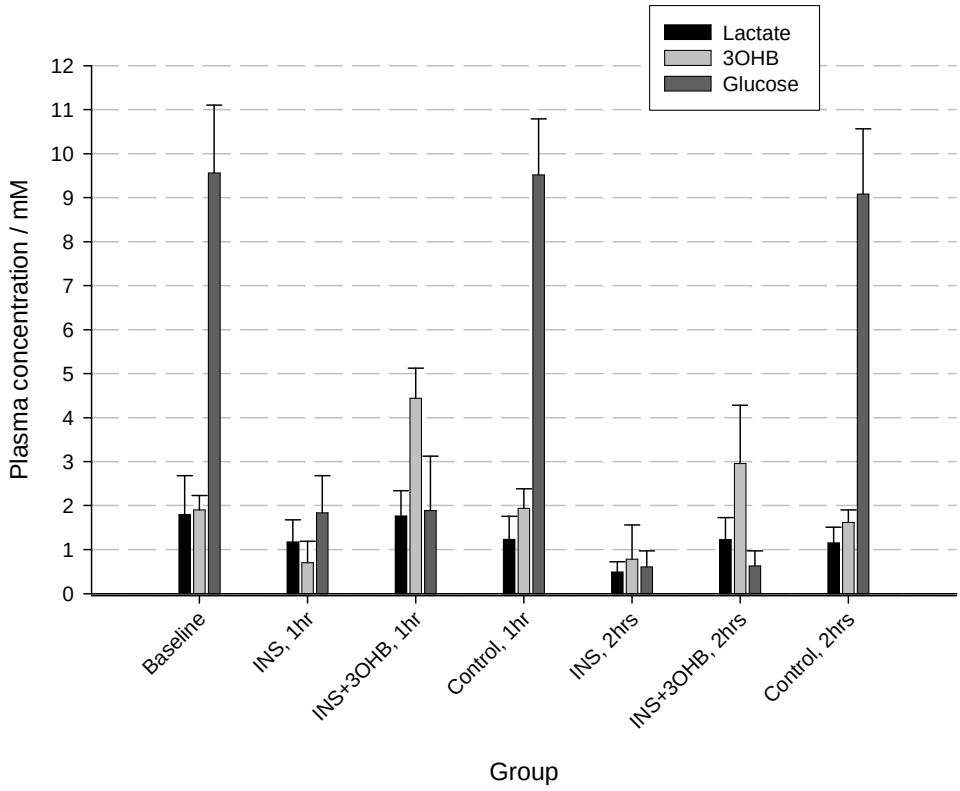

Figure 2.14: Plasma glucose, lactate, and 3OHB after insulin treatment

Plasma levels of glucose and 3OHB, and blood lactate levels at various time points after insulin treatment (10 U/kg) alone or in combination with 3OHB (for details see text). *N* = 6-7; error bar = 1SD.

Sodium. Sodium plasma levels in insulin treated animals at 1 and 2 hrs after treatment were not significantly elevated above respective control levels ($p = 1.0$ and $p = 0.29$ respectively, Figure 2.15). In 3OHB treated groups, however, levels were significantly elevated above controls at both time points. At 2 hrs of 3OHB treated insulin induced hypoglycemia sodium levels were 140 ± 2 mM compared to 132 ± 2 mM (mean ± 1SD) in controls, corresponding to a mean difference of 8 mM. This increase is probably caused by the additional sodium load from 3OHB injections. Reports from adult rats suggest that a much higher elevation of more than 28 mM is necessary to induce

myelinolysis in normonatremic animals (Soupart, et al., 1996). Since the physiologic mechanisms for the control of brain osmolarity are matured in PND 12 rats (Trachtman, et al., 1995), it may be assumed that an increase of 8 mM in sodium concentrations is below a range that can induce severe brain injury in this model. The sodium load due to 3OHB injections, however, can apparently not be completely controlled by increased renal excretion. This emphasizes the importance of 3OHB treated control animals in experiments with this model to exclude possible confounding effects from sodium overload.

Potassium. Potassium plasma levels in insulin treated animals at 1 and 2 hrs after treatment were not significantly lower than respective control levels, neither were levels in insulin + 3OHB treated animals 1 hr after insulin treatment . In the insulin+3OHB treated animals 2 hrs after insulin treatment, however, plasma potassium levels were significantly lower than in controls (3.4 ± 0.3 vs. 4.6 ± 0.2 mM (mean ± 1SD), p = 0.001, Figure 2.15). Insulin generally lowers plasma potassium levels by shifting extracellular potassium ions into cells. A tendency toward lower potassium levels in insulin treated animals at 1 and 2 hrs is apparent, although this trend did not reach statistical significance. The fact that insulin + 3OHB treated animals showed a significant decrease might suggest a synergistic effect on potassium levels, possibly mediated by simultaneous hypernatremia. Severe hypokalemia (less than 2.5 mM) can be associated with muscle weakness. Severe hypokalemia also facilitates cardiac arrhythmias in the presence of other triggers. Moderate hypokalemia, in contrast, is generally asymptomatic, so levels around 3.4 mM in this model are not expected to cause symptoms. Nevertheless, there appears to be a synergistic effect between treatment with sodium 3OHB solutions and insulin on potassium plasma levels with significantly lowered plasma levels in animals receiving both treatments.

Conclusion

Insulin treatment with or without 3OHB administration does not increase blood lactate levels in 13 day old rats above baseline. Blood lactate is therefore an unlikely cause of variability in the course of a hypoglycemic encephalopathy with or without 3OHB treatment. Although insulin treatment in combination with 3OHB administration causes increased plasma sodium and decreased potassium levels, the magnitudes of the changes are comparatively small and can be expected to remain asymptomatic. However, these effects emphasize the importance of 3OHB treated control groups in experiments.

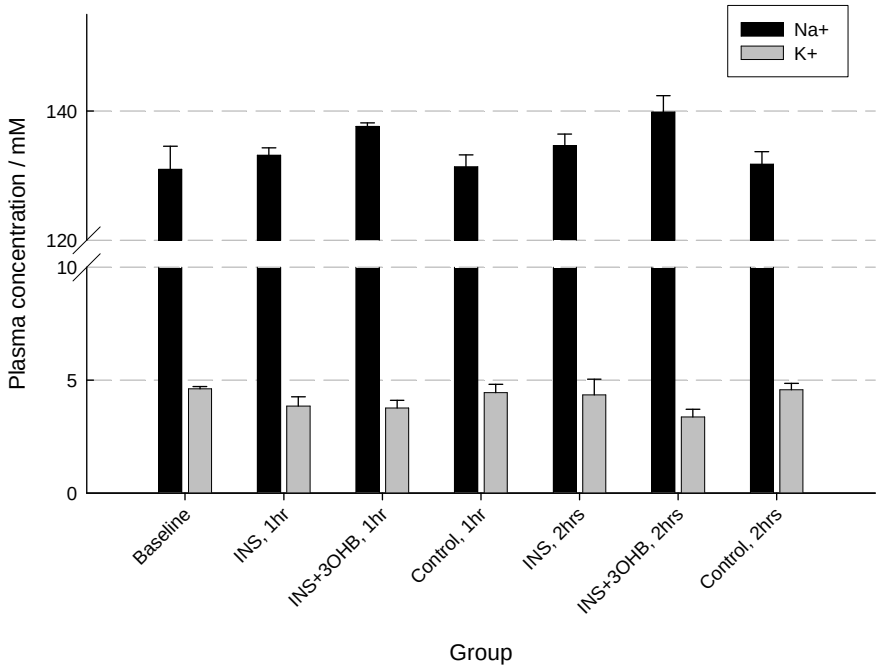

Figure 2.15: Plasma sodium and potassium concentrations after insulin treatment

Plasma sodium and potassium levels at various time points after insulin treatment (10 U/kg) alone or in combination with 3OHB in 13-day-old rats (for details see text). *N* = 6-7; error bar = 1SD.

2.8 Preliminary neuropathological observations

Little published information is available on neuropathological changes in infant rats after hypoglycemic episodes of different severity (Jones and Thomas Smith, 1971). Initial observations in our model showed that insulin induced hypoglycemia results in a characteristic clinical progression from complete alertness to deep coma accompanied by EEG changes and increasing EEG suppression. On a preliminary basis we resuscitated two PND 13 rat pups when the suppression ratio approached 1 and one pup at a suppression ratio of 0.5. For comparison we used two control pups. Animals survived for 3 days after resuscitation and were sacrificed by intracardial perfusion. Experimental and control animals showed no differences in behavioural patterns or weight gains at the time of sacrifice. Brains were analyzed after haematoxylin eosin or Fluoro Jade C staining of

paraffin sections at several anatomic levels. There were no indications of neuropathological changes in any of the experimental animals after these stains, in particular no signs of selective neuronal death in cortex (Figure 2.16) or hippocampus (Figure 2.17).

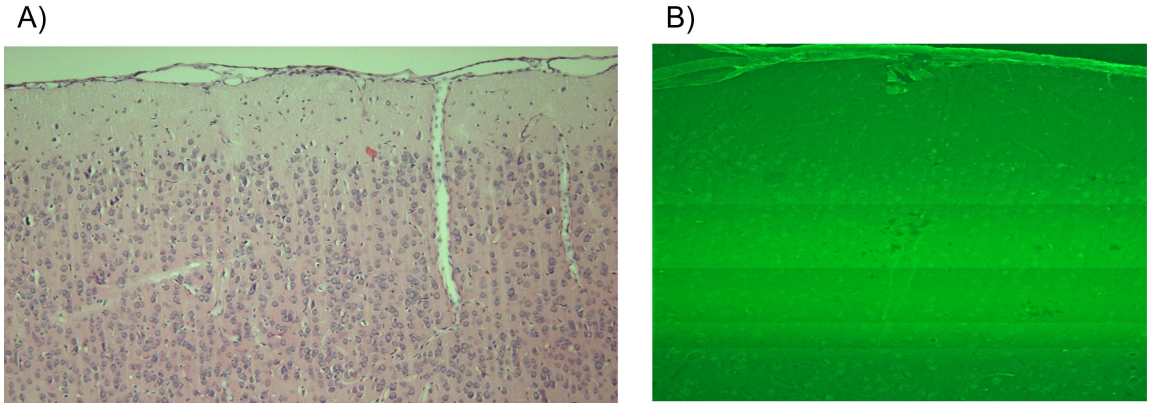

Figure 2.16: Histological sections from cortex after hypoglycemia

Preliminary neuropathological evaluation of parasaggital cortex of a 13-day-old rat after insulin-induced hypoglycemia, glucose resuscitation at the time of burst suppression coma, and 3 days survival. The animal was sacrificed by fixation perfusion with 10% phosphate buffered formalin for 45 minutes. Paraffin sections from several coronary levels across the brain were stained according to standard protocols with haematoxylin-eosin (HE) or Fluoro-Jade-C (FJC). There was no evidence of selective neuronal death or other neuropathological changes. A: parasaggital cortex, HE; B: parasaggital cortex, FJC.

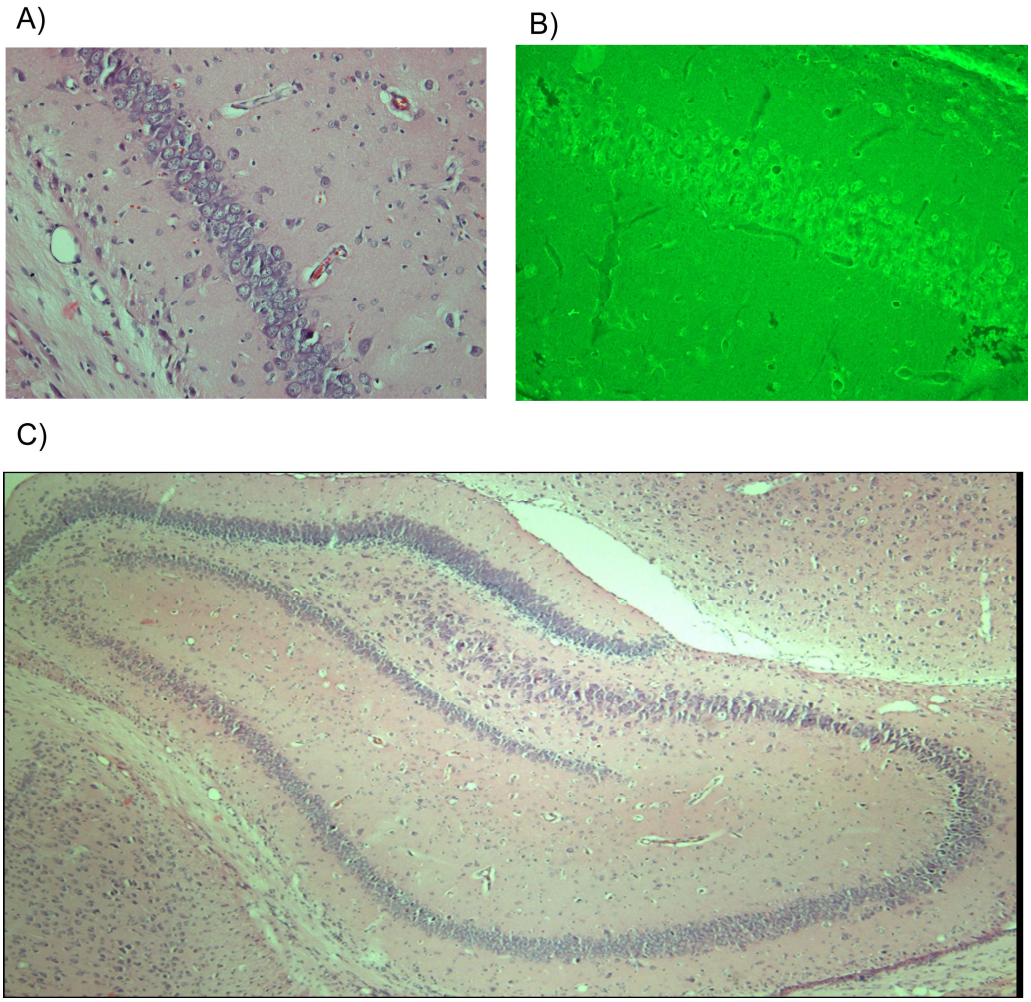

Figure 2.17: Histological sections from hippocampus after hypoglycemia

Preliminary neuropathological evaluation of hippocampus of a 13-day-old rat after insulin-induced hypoglycemia, glucose resuscitation at the time of burst suppression coma, and 3 days survival. The animal was sacrificed by fixation perfusion with 10% phosphate buffered formalin for 45 minutes. Paraffin sections from several coronary levels across the brain were stained according to standard protocols with haematoxylin-eosin (HE) or Fluoro-Jade-C (FJC). There was no evidence of selective neuronal death or other neuropathological changes. A) Hippocampus, CA1 region, HE; B) Hippocampus, CA1 region, FJC; C) Hippocampus, overview, HE.

This result was surprising, given that reports from adult rats suggest that selective neuronal death occurs after a period of burst suppression EEG (Auer, et al., 1984a), and that even moderate hypoglycemia in young (20-24 day old) rats results in increased neuronal death in parasaggital cortex (Yamada, et al., 2004). This effect in young rats, however, is abolished when they are weaned at 20

days onto a ketogenic diet and not a carbohydrate rich diet (Yamada, et al., 2005). Rat pups before weaning are also in a ketogenic state because of the high fat content of rat milk. The absence of neuronal injury in our model may therefore be related to the ketogenic state pre-weaning of rat pups. Such an effect may be mediated by several mechanisms, including elevated ketone levels during hypoglycemia.

Insulin induced hypoglycemia is generally considered hypoketotic because insulin reduces hepatic ketone production. This was also to be expected in animals that are in a ketogenic state prior to insulin treatment, like rat pups. However, 3OHB levels during insulin induced hypoglycemia in rat pups were higher than levels reported for adult rats (0.8 mM vs. < 0.1 mM; see also Figure 2.14), suggesting that the effect of insulin on ketone production was incomplete. These moderately elevated 3OHB plasma levels could have had a neuroprotective effect in our model. If this was correct, then further reduction of 3OHB plasma levels during hypoglycemia would be associated with neuronal injury. We therefore tested pharmacological and dietary strategies for a further reduction of 3OHB plasma levels during insulin induced hypoglycemia (section 2.9).

2.9 Testing of additional ketone reduction strategies

2.9.1 Regulation of ketone levels and ketogenesis in developing rats

Plasma ketone levels reflect the balance of ketone production in ketogenic organs and peripheral ketone consumption. Ketone consumption is generally determined by plasma ketone availability and transport capacities. The physiologic regulation of plasma ketone levels is achieved by controlling ketogenesis. In developing rats, ketogenesis occurs in liver and small intestine (Arias, et al., 1997, Ferre, et al., 1978, Hahn and Taller, 1987). Whereas the production of hepatic ketones contributes mostly to the plasma ketone pool, the fate of ketones produced in the small intestine is less clear. They could be used for local consumption or for distribution in the bloodstream, details are unknown.

Ketone bodies are produced from partial degradation of long and medium chain fatty acids (LCFA and MCFA). These stem either from dietary sources or are liberated from adipose tissue. Transport of fatty acids into ketogenic cells, in particular into hepatocytes, differs according to chain length and source.

Dietary LCFA are transported from gut to liver via chylomicrons and VLDL lipoproteins. These lipoprotein bound triglycerides are cleaved by endothelial hepatic lipase resulting in a release of non-esterified fatty acids which are taken up by hepatocytes. Dietary MCFA are transported as non-esterified fatty acids from the gut to the liver and are taken up by hepatocytes directly. During

fasting conditions, LCFA are liberated from adipose tissue by hormone sensitive lipase and transported in the bloodstream as non-esterified fatty acids, as are MCFA from adipose tissue.

Rat milk is both high in MCFA (ca 35%) and LCFA (ca 65%) (Brandorff, 1980, Fernando-Warnakulasuriya, et al., 1981, Wells, 1985). The availability of fatty acids for ketogenesis is one determinant of the ketogenic rate. Ketogenesis from MCFA is favoured in the presence of both substrates in suckling rats (Frost and Wells, 1981). The first step of ketogenesis is degradation of fatty acids.

Degradation of fatty acids takes place in the mitochondrial matrix, requiring prior transport from the cytosol. Mitochondrial entry of LCFA is mediated by a transport system comprising three enzymes, carnitine palmitoyl transferase I (CPT I), carnitine/acylcarnitine translocase, and carnitine palmitoyl transferase II (CPT II). The system is controlled at the first step CPT I. MCFA can bypass this transport system and can enter the mitochondrial matrix independently. Acetyl-CoA from partial degradation of FAs in the mitochondrial matrix can be channelled into ketogenesis, which is mediated by mitochondrial HMG-CoA synthase (mHS) and HMG-CoA lyase. mHS is the final regulatory step of ketogenesis. mHS activity is regulated at the mRNA and protein expression level. One regulatory factor is the fat content of the diet and with increased mHS protein expression on high fat diets (Fukao, et al., 2004). This transcriptional regulation is in part mediated by the peroxisomal proliferator activator receptor α (PPAR- α), which is relevant for regulatory effects of dietary fat content on hepatic protein expression (Mandard, et al., 2004, Patsouris, et al., 2006).

mHS activity is also reduced by insulin. In developing rats, insulin reduces ketogenesis in liver and small intestine, mainly by reducing mHS activity (Arias, et al., 1997, Hahn and Taller, 1987, Yeh and Zee, 1976). There are indications that the effect of insulin on mHS expression is mediated by the transcription factor FKHRL1 (Nadal, et al., 2002). Insulin treatment of developing rats, however, results only in partial reduction of total ketogenesis (about 30%) in these organs (Arias, et al., 1997). This is in accord with our findings of a partial reduction of plasma 3OHB levels after insulin treatment. Insulin is also reported to have limited effects on the plasma concentration of unesterified fatty acids in suckling rats in the fed state (Yeh and Zee, 1976), suggesting that reduced availability of plasma unesterified fatty acids does not contribute to the effect of insulin on ketogenesis.

Insights into the regulation of ketogenesis in developing rats formed the basis for the selection of additional pharmacological and dietary strategies to reduce ketone levels during insulin induced hypoglycemia. Promising strategies target ketogenic control points other than those affected by insulin. We chose to try four strategies targeting four different mechanisms to lower plasma ketone levels robustly: a) Nicotinic acid to reduce availability of unesterified fatty acids in plasma; b)

Etomoxir to inhibit CPT I activity; c) the PPAR- α inhibitor GW6471 to further reduce mHS expression and activity, and d) maternal high fat diet to reduce MCFA content of rat milk.

2.9.2 Inhibition of lipolysis with nicotinic acid

Nicotinic acid (niacin) in pharmacological dosage lowers the rate of lipolysis in adipose tissue, probably by binding to the G-protein coupled receptor GPR109A (Gille, et al., 2008). Single or repeat doses of 25 mg/kg body weight lowers plasma levels of unesterified fatty acids in adult rats by more than 50% about 30 minutes after administration (Dhalla, et al., 2007, Reaven, et al., 1988a, Reaven, et al., 1988b). 50 mg/kg lowers ketone plasma levels in fasting adult rats by about 80% (Mayor, et al., 1967).

To gauge any additional effect of nicotinic acid treatment on plasma ketone levels during insulin induced hypoglycemia we measured 3OHB levels and serum unesterified fatty acid levels in 13 day old rat pups after 3 hrs fasting, and after 1, 1.5 and 2 hrs of treatment with insulin (10 U/kg). Two animals were treated additionally with 25 mg/kg nicotinic acid (Sigma, USA) 1 hr after insulin injection. Measurements samples for these animals were taken at 1.5 hrs after insulin injection. 3OHB plasma concentrations were measured by test strips from lateral tail vein puncture, as described, unesterified fatty acids concentrations were measured in serum by a commercial kit as per manufacturer instructions (Wako NEFA-HR(2), Wako Chemicals, USA). Serum samples were obtained by cardiac puncture after isoflurane anaesthesia.

Results for insulin treated animals are graphed in Figure 2.18. The two insulin and nicotinic acid treated animals had serum unesterified fatty acid levels of 0.26 and 0.18 mM, respectively, and 3OHB concentrations of 0.4 and 0.5 mM at 1.5 hrs. This is well within the range of insulin only treated animals as displayed in Figure 2.18. Nicotinic acid treatment appeared thus unsuitable to achieve robustly lower 3OHB plasma levels.

The apparently small or non-existent effect of nicotinic acid treatment suggests that further inhibition of lipolysis in adipose tissue does not reduce any further unesterified fatty acids in *insulin-treated* rat pups. It thus brings dietary fatty acids as a source for residual ketogenesis into play, especially given the high fat content of rat milk.

The reduction of unesterified fatty acid levels after insulin treatment we found in rat pups (Figure 2.18) is in contrast to a previous report that insulin has no effect on FFA levels in rats (Yeh and Zee, 1976). This apparent contradiction may be due to the fact that the study by Yeh et al. was conducted with fed animals, whereas rat pups in this model were fasted for 4.5 and 5 hrs at the time of measurement. The nutritional state may thus be connected to the effect observed.

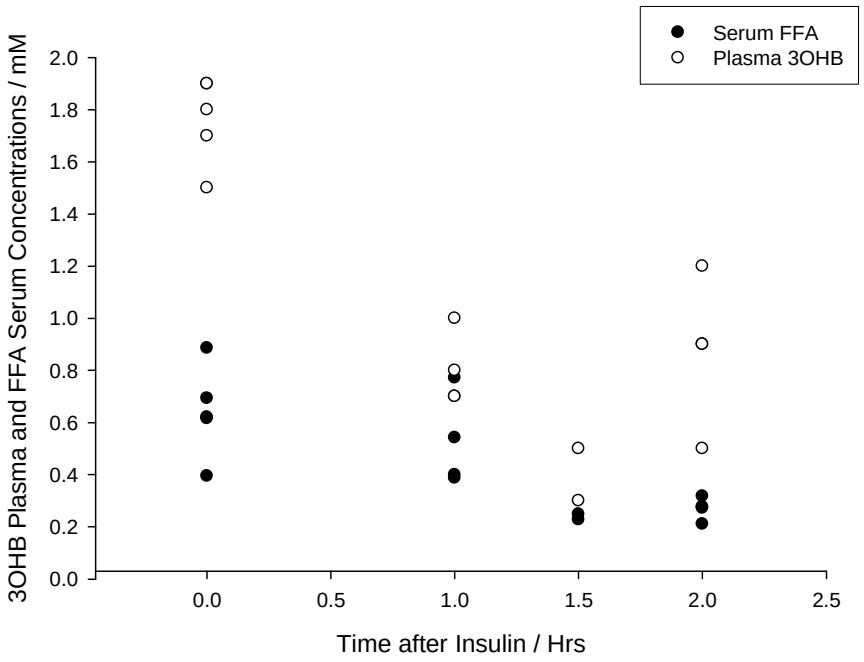

Figure 2.18: Free fatty acid and 3OHB plasma concentrations in response to insulin treatment

Serum free fatty acids (FFA, filled circles) and plasma D-3-hydroxybutyrate (open circles) concentrations after the injection of insulin (10 U/kg) in 13-day-old rats. Each symbol represents a measurement from one animal (for details see text).

2.9.3 Reduction of mHS activity by PPAR alpha inhibition (GW6471)

The peroxisomal proliferator-activated receptor α regulates hepatic fatty acid metabolism, in particular it promotes expression of mHS. PPAR α also mediates the activating effect of fibrates on fatty acid metabolism. The PPAR α antagonist GW6471 was developed in 2002 (Xu, et al., 2002). There are no reports of *in vivo* applications in the literature. However, cell culture experiments have used GW6471 for manipulation of PPAR α in concentrations of 0.1-10 micromole/l in culture media (Ding, et al., 2007, Poleni, et al., 2007). To test whether GW6471 could be suitable for further reduction of 3OHB levels in our model we treated animals with various dosages of GW6471 and observed changes in 3OHB plasma concentration in response. GW6471 (Sigma, USA) was dissolved in fresh DMSO at a concentration of 20 µmol/l and injected i.p. at dosages of 40, 80, and 160 µmol/kg bodyweight, resulting in injection volumes of 0.07, 0.13, and 0.26 ml. One control animal was injected with 0.1 ml DMSO only. 3OHB levels were determined as described.

Results are presented in Figure 2.19. These data suggested that GW6471 in various doses had no substantial effect compared to the animal injected with DMSO only. The transient reduction in 3OHB plasma levels in all animals is possibly caused by hepatotoxic effects of DMSO. These data suggested that GW6471 is unsuitable to achieve further reduction of 3OHB levels in the model under development. Moreover, hepatotoxic side effects of DMSO administration are undesirable as additional confounding factor.

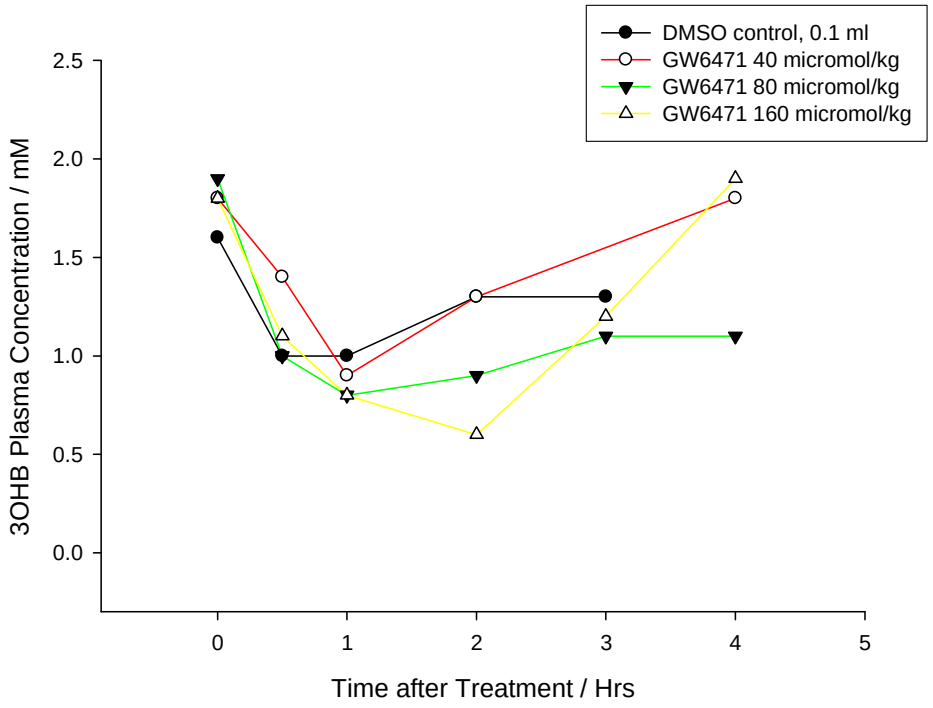

Figure 2.19: 3OHB plasma concentrations in response to GW6471 treatment

Plasma D-3-hydroxybutyrate levels in response to the injection various doses of the PPAR alpha antagonist GW6471 in DMSO and one control DMSO injection (for details see text). Each symbol represents serial measurements from a single animal.

2.9.4 Inhibition of CPTI by etomoxir

Etomoxir inhibits CPT I activity in the outer mitochondrial membrane and reduces the entry of LCFA into the mitochondrial matrix (Zarain-Herzberg and Rupp, 2002). In adult rats this results in

lowering of plasma 3OHB concentrations (Kruszynska and Sherratt, 1987, Schmitz, et al., 1995). Since MCFA enter mitochondria independently of CPT I, etomoxir is expected to inhibit ketogenesis from LCFA but not from MCFA. Since insulin reduces mHS activity in the liver of developing rats and thus reduces ketogenic output, combined treatment with insulin and etomoxir should lead to a synergistic effect and to a further reduction of 3OHB plasma levels. As a proof of principle test we treated one animal with etomoxir only and two animals with etomoxir and with insulin injection 30 minutes after etomoxir treatment. Based on previous studies (Hayashi, et al., 2001, Kruszynska and Sherratt, 1987, Penna, et al., 2005, Schmitz, et al., 1995) we chose a dosage of 20 mg/kg etomoxir (Sigma, USA) in water s.c.. All animals were fasted for 3hrs before the experiment.

Results are displayed in figure 2.20. Etomoxir alone resulted in agreement with reports from adult rats in a considerable reduction of 3OHB plasma levels by 83 % after 30 minutes. However, combined treatment with insulin did not reduce 3OHB plasma levels any further. Animals treated with etomoxir and insulin had ketone levels in the range of 0.5 to 0.7 mM. Thus there were no indications in these preliminary tests that combined treatment with insulin and etomoxir results in robustly lowered 3OHB levels below the effect of insulin alone. Given the relatively high MCFA content of rat milk, this could be explained by residual ketogenesis form MCFA. To test this hypothesis in a further step, we reduced MCFA content of the milk the pups received from their dams by feeding the dams a high fat diet.

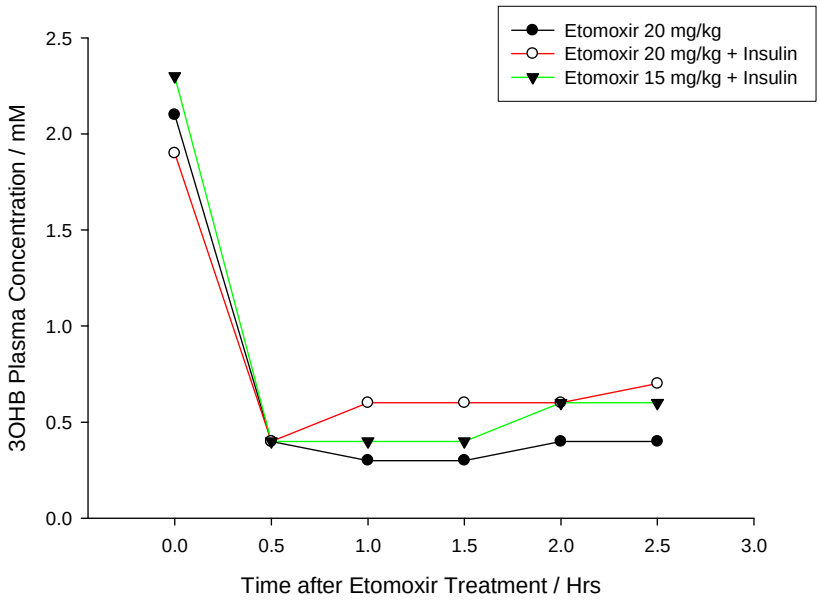

Figure 2.20: 3OHB plasma concentrations in response to combined etomoxir and insulin treatment

Plasma D-3-hydroxybutyrate levels in response to treatment with etomoxir alone or etomoxir and insulin in 13-day-old rat pups. Each symbol represents serial measurements from a single animal.

2.9.5 Dietary reduction of medium chain fatty acids in rat milk

Entry mechanisms of LCFA and MCFA into the mitochondrial matrix differ because LCFA are obligatorily transported by the CPT-transport system whereas MCFA may bypass this system. CPT I inhibition by etomoxir therefore reduces ketogenesis from LCFA, but probably not from MCFA. The proportion of MCFA in rat milk is normally about 30 % of all fatty acids. In order to further reduce ketogenesis by etomoxir treatment it could be useful to reduce the MCFA content in the milk of treated rat pups. MCFA content of rat milk is known to depend on the fat content of the maternal diet during lactation. The higher the fat content, the lower the MCFA content of milk (Grigor and Warren, 1980, Swithers, et al., 2001). We therefore compared the effect of etomoxir and insulin treatment between rat pups from dams on a conventional, high carbohydrate lab chow with pups from dams on a high fat diet. Support from Dr. Sheila Innis and her lab for this test is gratefully acknowledged.

Dietary reduction of medium chain fatty acids / triglycerides in maternal milk. Timed pregnant Sprague Dawley rats arrived at CFRI Animal Care Facility at gestational day 11. Following a 4-7 day

acclimatisation period (corresponding to 7-4 days before the estimated date of parturition) animals were placed on a high fat (16 % weight from fat) diet, with fat provided as safflower oil. This semi-synthetic diet was prepared in consultation with Dr Sheila Innis at her laboratory at CFRI. All ingredients were purchased from Harlan-Teklad. The animals had access to food and water ad libitum. Diet preparation was done by Elizabeth Novak in Dr Innis' lab.

Milk analysis. The lactating rat was anaesthetised with isoflurane, then 0.2 ml of 20IU/ml oxytocin were injected intraperitoneally. After 1-2 minutes, milk (100-200 µl) was expressed manually from the teats. Collected milk specimens were frozen at – 30 °C until analysis of fatty acid composition by gas chromatography mass spectrometry after methylation (Innis and Dyer, 1999) in Dr. Innis'lab.

Study Design. Three dams were placed on a high fat diet and compared to three dams on a laboratory chow diet. Pups were treated with etomoxir alone or in combination with insulin and results compared to data from previous experiments.

Results. Changes in fatty acid composition of rat milk from dams on a high fat diet are presented in Table 2.2: The content of MCFA (C6-12) was almost halved from 28.8 ± 1.5 molar % to 16.4 ± 3.9 molar % (mean ± 1SD, $n = 3$, $p = 0.007$, Student's t-Test). Mean baseline 3OHB plasma concentrations were comparable in pups from dams in both groups (1.9 ± 0.3 vs. 2.1 ± 0.3 mM, mean ± 1SD, $n_1 = 5$ and $n_2 = 9$).

There were no indications that plasma 3OHB levels after treatment with etomoxir were lower in pups from dams on a high fat diet compared to chow (Figure 2.21). Similarly, there were no indications that 3OHB levels were lower after combined treatment with etomoxir and insulin (Figure 2.22). Although animal numbers were small for these preliminary tests, results were not encouraging and so we did not pursue the strategy of reducing ketone levels by a combination of CPT-I inhibition and reduction of dietary MCFA content.

Discussion. Reduction of MCFA content of rat milk from 28 % to 16 % did not result in an appreciable reduction of 3OHB plasma levels after etomoxir treatment. This finding was surprising but may be explained in several ways. Either the reduction of MCFA in rat milk was quantitatively insufficient, or the etomoxir inhibition of CPT I in rat pups is only partial, or both. Etomoxir inhibits CPT-I by competitive but irreversible binding of its acetyl-CoA-ester to the catalytic centre (Kiorpes, et al., 1984). In a ketogenic state this might cause a partial inhibition only because of an abundance of fatty acid carnitine esters. Whatever the explanation may be, etomoxir and dietary reduction of MCFA in milk are unsuitable to achieve a robust further reduction of 3OHB plasma levels during insulin induced hypoglycemia in PND 13 rats.

	CHOW / % molar			High Fat Diet (20% Safflower) / % molar		
C 6:0	1,14	±	0,63	1,65	±	0,81
C 8:0	6,51	±	1,56	3,01	±	0,51*
C 10:0	14,09	±	0,46	7,01	±	1,59*
C 12:0	7,03	±	1,36	4,77	±	1,34
C 14:0	5,84	±	0,87	6,17	±	1,28
C 14:1	0,10	±	0,07	0,12	±	0,09
C 16:0	16,05	±	1,94	12,36	±	1,01
C 16:1n9	0,25	±	0,00	0,22	±	0,03
C 16:1n7	1,36	±	0,13	1,03	±	0,33
C 18:0	4,68	±	0,71	3,11	±	0,27*
C 18:1n9	18,10	±	2,05	15,53	±	2,03
C 18:1n7	1,66	±	0,11	1,05	±	0,19*
C 18:2n6	17,73	±	1,50	37,50	±	0,55*
C 18:3n6	0,13	±	0,10	0,96	±	0,22*
C 18:3n3	1,33	±	0,09	0,29	±	0,02*
C 18:4n3	0,06	±	0,02	0,04	±	0,03
C 20:0	0,08	±	0,02	0,14	±	0,03
C 20:2n6	0,51	±	0,09	0,90	±	0,08*
C 20:3n9	0,06	±	0,05	0,12	±	0,03
C 20:3n6	0,20	±	0,07	0,64	±	0,06*
C 20:4n6	0,79	±	0,13	1,95	±	0,17*
C 20:5n3	0,36	±	0,03	0,19	±	0,05*
C 22:0	0,06	±	0,02	0,23	±	0,26
C 22:1n11	0,05	±	0,03	0,10	±	0,01
C 22:1n9	0,09	±	0,06	0,02	±	0,01
C 22:4n6	0,05	±	0,01	0,18	±	0,03*
C 22:5n6	0,04	±	0,01	0,08	±	0,07
C 22:5n3	0,37	±	0,10	0,09	±	0,05*
C 22:6n3	0,73	±	0,18	0,09	±	0,04*
C 24:0	0,08	±	0,05	0,05	±	0,04
C 24:1	0,00	±	0,00	0,00	±	0,00
Saturates	55,56	±	1,99	38,49	±	3,32*
Monoenes	22,07	±	2,26	18,47	±	2,62
n-6	19,45	±	1,79	42,22	±	0,78*
n-3	2,86	±	0,37	0,70	±	0,07*
PUFA	22,38	±	2,19	43,03	±	0,70*
mg total fat per ml milk	134,97	±	27,45	186,78	±	73,63
Medium chain (C6-12)	**28,77**	**±**	**1,26**	**16,44**	**±**	**3,23***

Table 2.2: Diet dependent fatty acid composition of rat milk

Fatty acid composition of rat milk from dams on conventional lab chow and on a high fat diet; for details see text. Mean ± 1SD, $n = 3$, *: $p < 0.05$, Student's t-Test.

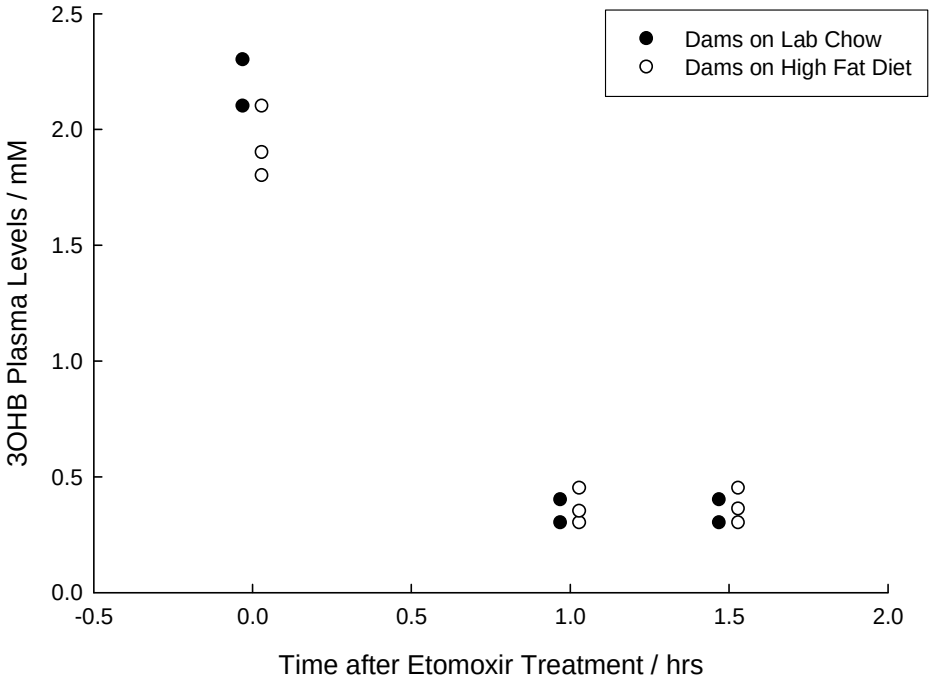

Figure 2.21: 3OHB plasma levels after etomoxir treatment and high fat maternal diet

3OHB plasma levels in response to treatment with etomoxir in 13-day-old rat pups receiving rat milk with physiological MCFA content (dams on chow) or rat milk with reduced MCFA content (dams on high fat diet). Each symbol represents a measurement from one animal.

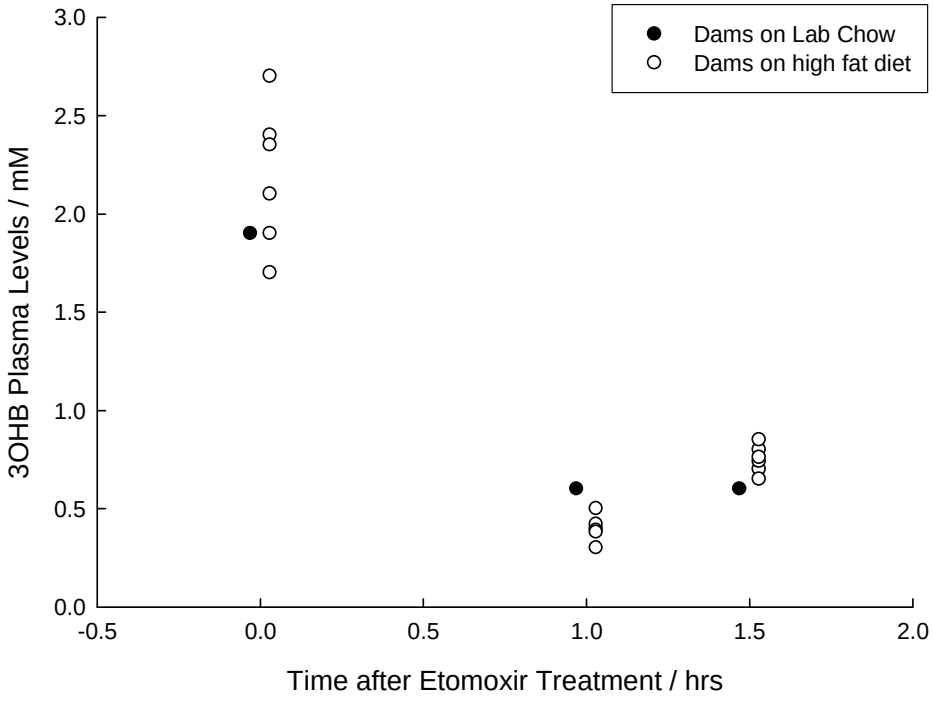

Figure 2.22: 3OHB plasma levels after combined etomoxir and insulin treatment and high fat maternal diet

3OHB plasma levels in response to treatment with etomoxir + insulin in 13-day-old rat pups receiving rat milk with physiological MCFA content (dams on chow) or rat mil with reduced MCFA content (dams on high fat diet). Each symbol represents a measurement from one animal.

2.9.6 Summary of additional ketone reduction strategies and further perspectives

None of the four tested additional ketone reduction strategies (nicotinic acid, GW6471, etomoxir, MCFA reduction) had a robustly lowering effect on plasma 3OHB levels during insulin induced hypoglycemia. In the absence of promising pharmacological strategies we decided to characterize the effect of ketone supplementation in this model as it is, i.e. with slightly raised plasma 3OHB concentrations in the hypoketotic group. The absence of brain injury on initial neuropathological examination must therefore presently be considered as part of this model.

Slightly raised 3OHB plasma levels, however, may not be the only cause of the absence of hypoglycemic injury in this model. Another cause may be the effect of the high fat milk diet on cerebral protein expression and mitochondrial biogenesis. A ketogenic diet increases mitochondrial biogenesis and the expression of mitochondrial uncoupling proteins, both with potentially neuroprotective effects (for a review see (Bough and Rho, 2007)). Uncoupling proteins are also increased in suckling compared to adult rats (Sullivan, et al., 2003). Constantly elevated 3OHB levels increase the expression of anti-apoptotic mitochondrial proteins (Puchowicz, et al., 2008). These effects could increase the resistance to hypoglycemic injury independently of 3OHB levels during hypoglycemia in our model.

2.10 Overview of the model and further observations

Development of a non-invasive EEG technique was pivotal to devise a model of EEG-controlled, insulin-induced hypoglycemia in 13 day old rats which allows survival of pups after an episode of sustained hypoglycemia. Monitoring of plasma glucose and 3OHB levels are possible by lateral tail vein puncture and measurement with handheld meters, the alertness state of an animal can be quantified with an alertness score. Figure 2.23 shows a typical example of changes in the alertness score and EEG suppression ratio during hypoglycemia. The timeline of the model is given in Figure 2.24.

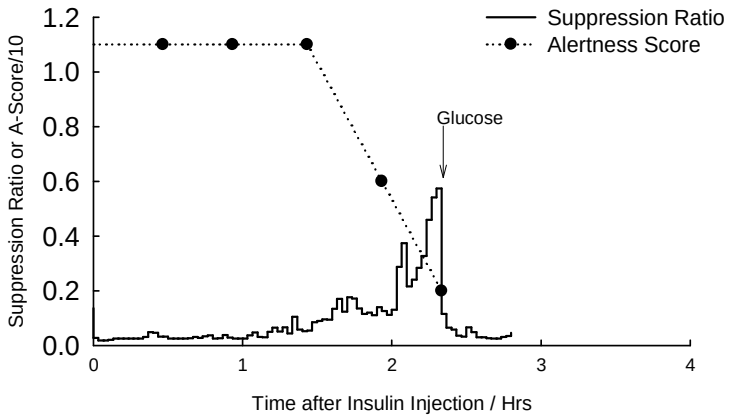

Figure 2.23: EEG suppression and alertness score after insulin injection

Typical changes in EEG suppression ratio (black line) and alertness score (A-score; filled circles) after 10 U/kg insulin at time 0 in 13-day-old rats. Plasma glucose levels have fallen below 1mM at 1 hr. A small increase in EEG suppression ratio between 1 and 2 hrs is followed by a more rapid increase after 2 hrs. The EEG improves promptly after glucose resuscitation. Clinical recovery typically lags behind with improved alertness 15-20 minutes after glucose resuscitation (alertness score after resuscitation not shown).

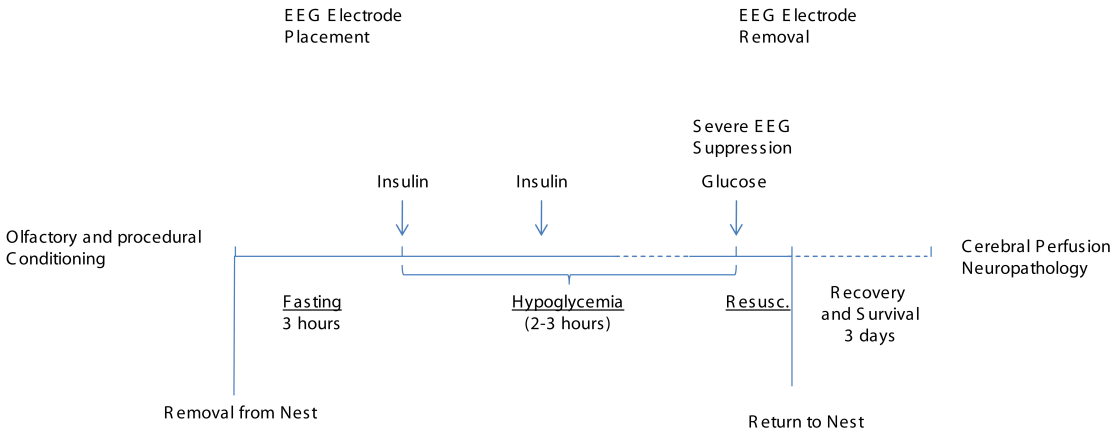

Figure 2.24: Timeline of hypoglycemia model

Timeline of the model of hypoglycemia in infant rats. Pups are fasted before the experiment for 3 hours. During the fasting period, EEG electrodes are placed. Insulin is administered twice to produce sustained hypoglycemia (see insulin dose selection in text). After resuscitation (Resusc.) and clinical stabilization of the animal, the electrodes are removed with acetone and animals are returned to the nest. They are closely monitored for 3 hours for recurrent hypoglycemia or rejection by the dam. After the survival period animals are sacrificed by intracardial perfusion according to standard techniques.

Heart rate and oxygen saturation of pups were monitored with a MouseOx Pulse oximeter. Pups tended to develop bradycardia during hypoglycemia which could be avoided with atropine. We therefore administer atropine routinely one hour after insulin injection.

Preliminary tests showed that the degree of EEG suppression correlates with the respiratory rate of the rat pups (Figure 2.25). Baseline values for the respiratory rate are around 120 min^{-1} for PND 13 pups, lowest values before successful resuscitation at the time of burst suppression coma around 10 min^{-1}. The respiratory rate is thus a marker of the severity of the hypoglycemic encephalopathy in this model.

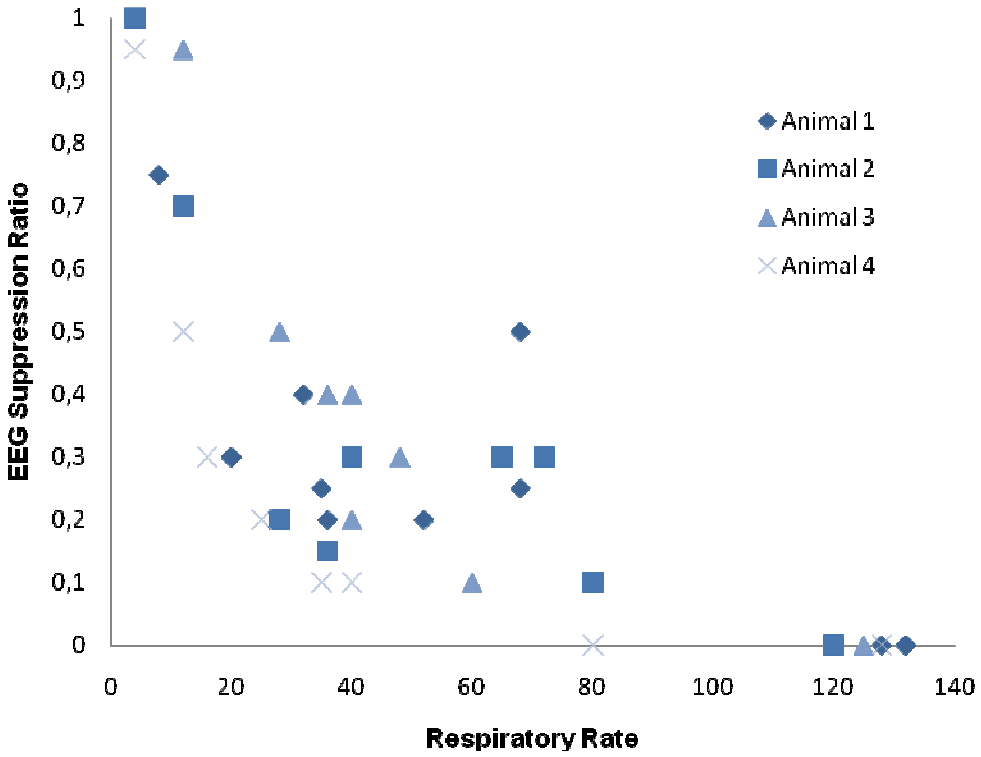

Figure 2.25: Suppression ratio and respiratory rate

Correlation of EEG suppression ration with respiratory rate during hypoglycemia in 13-day-old rats. Baseline respiratory rates are 120-140 min^{-1}. During the progression of the effects of hypoglycemia respiratory rates decrease. This decrease correlates with increased EEG suppression rates. Respiratory rates below 10 min^{-1} were generally associated with considerable EEG suppression. Rates between 20 and 80 showed a range of EEG suppression ratios between 0.1 and 0.5.

The progression of the pups to bradypnea and finally respiratory failure is a limiting characteristic of this model. Animals were given oxygen by face mask when respiratory rates were less than 30 per min to ensure sufficient oxygen saturation during hypoglycemic coma. Monitoring of oxygen saturation confirmed that this strategy stabilizes blood oxygen saturation at low respiratory rates. However, without resuscitation respiratory failure occurs eventually. This limits the duration of experimental hypoglycemic coma in this model. Preliminary trials showed that reliable resuscitation was possible from a state of severe burst suppression coma. In this state, the animals show gasping respiration at a rate of about 8-10 min^{-1}. The EEG is completely suppressed between gasps but shows activity bursts at the time of the gasp. The activity bursts may be the cause of the respiration, alternatively they may represent a consequence or an artefactual potential. A distinction between both possibilities was not possible in our experiments. However, for operational reasons we used this state as EEG defined experimental endpoint for our studies.

Glucose resuscitation is performed by combined subcutaneous and intraperitoneal glucose injections (10 ml/kg 10% dextrose in 0.9% saline s.c. and 15 ml/kg 25% dextrose in 0.9% saline i.p.). This regime resulted in a restoration of plasma glucose levels to around 3-5 mM, prompt EEG improvement, and clinical recovery over a period of about 30 minutes.

Returning animals to the nest after hypoglycemia was generally unproblematic. However, because of recurrent hypoglycemia it proved useful to routinely administer subcutaneous glucose 1 and 2 hours to hypoglycemic animals after their return to the nest. For resuscitation details see study 1. To facilitate re-acceptance of the pups by the dam, pups and dam were conditioned to handling and olfactory stimuli daily on days 7 to 13 before the experiment.(2 exposure episodes daily of five minutes with handling and characteristic smells, e.g. electrode glue, gloves, acetone used for electrode removal).

Initial neuropathological examination showed that there are no signs of 1 neuropathological changes upon haematoxylin-eosin and Fluoro Jade C staining after hypoglycemia and resuscitation at severe burst suppression coma in this model (see section 2.8). Behavioural observations of experimental and control animals after 3 day survival after the hypoglycemic episode showed no apparent differences. These observations were confirmed in the systematic experiments of chapter 3.

3. Effects of D-3-Hydroxybutyrate Treatment on Hypoglycemic Coma in Rat Pups

3.1 Introduction

Hypoglycemia is a frequent condition in neonates and infants. Long term neurological sequelae, including psychomotor deficits and seizure disorders, develop in 30-60% of patients (Burns, et al., 2008, Meissner, et al., 2003, Menni, et al., 2001). Hypoglycemia in the absence of ketone bodies (hypoketotic hypoglycemia) is perceived as particularly aggressive. Hypoketotic hypoglycemia is a characteristic manifestation of persistent hyperinsulinemic hypoglycemia of infancy (PHHI) or inborn errors of fatty acid oxidation. It is also the main form of hypoglycemia occurring in preterm and small for gestational age neonates. Cerebral glucose transporter (Glut-1) deficiency is another example of cerebral glucose deprivation. It presents with intractable seizures, developmental delay, and ataxia.

Ketone bodies (D-3-hydroxybutyrate (3OHB) and acetoacetate) are an energy substrate alternative to glucose for the brain. Ketone bodies are transported across the blood brain barrier by the monocarboxylate transporter 1 (MCT-1), and are subsequently metabolized to acetyl-CoA as oxidative substrate (Morris, 2005). Cerebral ketone body utilization is especially effective in the neonatal and early infantile period (Nehlig, 2004). In pre-weaning rats physiological ketone utilization accounts for about 20% of cerebral energy requirements, and is related to the high fat content of rat milk. Post weaning, ketone utilization is virtually zero in a fed state and on a carbohydrate rich diet (Cremer and Heath, 1974, Hawkins, et al., 1971).

Evidence from several experimental studies suggests that treatment with ketone bodies or ketosis induced by high fat diet are neuroprotective during hypoglycemia: 3OHB treatment improves the alertness of hypoglycemic mouse pups (Thurston, et al., 1986) and reduces hippocampal lipid peroxidation in hypoglycemic adult rats (Haces, et al., 2008). Furthermore, ketosis induced by a high fat diet delays the onset of neurological symptoms in adult hypoglycemic mice (Johnson and Weiner, 1978) and reduces neuronal death in post-weaning rats (Yamada, et al., 2005). Yet, clinical translation of 3OHB treatment has been limited to a few single case studies (Plecko, et al., 2002, Van Hove, et al., 2003). No clinical trials have been performed in neonates and infants, the population most susceptible to hypoglycemic brain damage.

Prerequisite for future clinical use of 3OHB in the protective treatment of hypoglycemia is an understanding of its capacity and limits to compensate for cerebral glucose deficiency in the developing brain. We thus investigated the effect of 3OHB treatment on the onset of insulin induced hypoglycemic coma in rat pups (clinical and electroencephalographic) and the effects of prolonged ketotic hypoglycemia on the subsequent clinical course and on the neuropathological outcome. Since rat pups pre-weaning have a physiologically high capacity for cerebral 3OHB utilization (Nehlig, 2004), they are suitable to explore the maximum effectiveness of 3OHB treatment.

3.2 Materials and methods

Animals. All experiments were performed according to the guidelines of the Canadian Council on Animal Care, and were approved by the University of British Columbia Committee on Animal Care. Timed pregnant Sprague Dawley rats were obtained from Charles River, Canada. We used female pups on postnatal day (PND) 13. Age selection was based on age-specific EEG patterns during postnatal development in rats and on the importance of EEG changes for the staging of the effect of hypoglycemia on the brain (Auer, et al., 1984a, Lewis, et al., 1974b): EEG activity before PND 8 is discontinuous, comparable to a gestational age of 32 weeks or earlier in humans, and unsuitable for staging. EEG patterns in rats on PND 13 are continuous and suitable for staging. They are comparable to 2-3 month old humans (Frank and Heller, 1997, Gramsbergen, 1976, Tucker, et al., 2009, Volpe, 2001). Other parameters of cerebral maturation in PND 13 rats (enzymatic, synaptic) correspond to the early postnatal period in humans (Hagberg, et al., 1997, Romijn, et al., 1991). From a metabolic point of view, PND 13 rats are exclusively milk fed and have high cerebral ketone utilization rates (Nehlig, 2004). Adaptation to a carbohydrate rich diet occurs during weaning from PND 17 to PND 21 or later. As there is no evidence on sex-specific effects of hypoglycemia on the brain, we used only female pups in order to standardize experimental conditions.

Induction of hypoglycemia and resuscitation. For the duration of the experiment pups were removed from the nest and kept in an incubator at 32°C. This ambient temperature stabilizes body temperature of PND 13 rats at 36-37°C as shown by our own preliminary tests and in agreement with previous reports (Conklin and Heggeness, 1971). After a fasting period of 3 hours, animals were s.c. injected with 10 U/kg regular human insulin (Humulin R, Eli Lilly, Canada). Because initial trials showed a tendency toward spontaneous recovery of blood glucose levels after 2 hours, the insulin injection was repeated after 2 hours, unless suppression of EEG activity had occurred prior to that time point. Atropine (1 mg/kg s.c., Bimeda-MTC) was administered 1 hour after the first insulin dose to prevent bradycardia, and oxygen was administered by facemask when respiratory rates were less than 30 min^{-1} to avoid hypoxia. Animals were resuscitated by administration of 10 ml/kg 10% glucose in 0.9%

saline s.c. and 15 ml/kg 25% glucose in 0.9% saline i.p., followed by hourly repeat s.c. injections of glucose for 3 hours. Animals were returned to the nest after they had recovered their righting reflex, and were monitored clinically at hourly intervals for 3 hours. Re-acceptance of the pups by the dam was unproblematic as animals had been conditioned to handling procedures and olfactory stimuli before experiments.

3OHB Treatment. We determined the ideal dosage of 3OHB (D-3-hydroxybutyrate, Sigma Aldrich, USA) in a pilot study. We chose a 600 mM 3OHB solution for subcutaneous injections in order to administer a maximal amount of 3OHB in a minimal volume. Subcutaneous administration of solutions with an osmolality up to 1400 mOsm/kg, corresponding to 700 mM 3OHB, has been reported to be safe (Bellin, et al., 2002, Elam, et al., 1991). We did not observe any tissue necrosis or other adverse effects after subcutaneous injections during the pilot study. In order to determine the dosage of 3OHB, we subcutaneously injected test doses of 10 mmol/kg (n = 3) and 5 mmol/kg (n = 3), which resulted in a dose and time dependent increase of 3OHB plasma levels. Levels peaked between 10 and 20 minutes and returned to baseline at around 60 minutes. Total increase above baseline was 4.3 ± 0.4 mM and 2.4 ± 0.1 mM respectively, resulting in peak levels of around 6.5 mM and 4.5 mM. Experimental target levels were in the high physiological range of 3-4 mM. For the final experiments we therefore chose a 6 mmol/kg loading dose and a 3 mmol/kg maintenance dose every 30 minutes, which proved effective in maintaining target levels.

Experimental Design. From each of 5 litters, four female pups were randomly assigned to one of four groups, resulting in 5 animals per group. Group 1 was given insulin to induce hypoglycemia (hypoG); Group 2 was given insulin and the resulting hypoglycemia was treated with 3OHB (hypoG+3OHB); Group 3 was a saline treated normoglycemic control (normoG); Group 4 was a normoglycemic control treated with 3OHB (normoG+3OHB). Hypoglycemic (hypoG and hypoG+3OHB) animals were resuscitated with glucose when the EEG showed severe suppression of electrical activity that was interrupted only by short bursts associated with gasps of the comatose animal (burst-suppression coma), or after a maximum time of 5 hrs after insulin injection. Normoglycemic animals (normoG and normoG+3OHB) were treated with saline or 3OHB for the same time as respective hypoglycemic littermates (hypoG and hypoG+3OHB). Thus 3OHB-treated normoglycemic controls received the same total amount of 3OHB as their 3OHB-treated hypoglycemic littermates. Animals which had stabilized after resuscitation were returned to the nest and brains were harvested for histological analysis after 24 hrs. Animals which did not stabilize after resuscitation were euthanised and their brains were harvested shortly after resuscitation.

Clinical Score. In pilot experiments we found a consistent pattern of changes in neurological and vital functions in correlation with the duration of the hypoglycemic state. Based on these observations we developed an alertness score (A-Score) including spontaneous motor activity, postural reflexes and

muscle tone and used it to assess brain function clinically during hypoglycemia (Table 2.1). Criteria of the score were based on consistent clinical presentations of the rat pups in preliminary experiments. Total score 11 denotes an alert animal, 10-9 a slight, 8-5 a moderate, and 4-0 a severe reduction of alertness.

Biochemical and Vital Sign Monitoring. Glucose and 3OHB plasma levels were measured with PrecisionXtra glucose- and ketone-test strips (Abbott Diabetes Care, UK) from a blood drop obtained by puncture of a lateral tail vein. Lower limit of measurement for glucose was < 1mM. The accuracy of test strip measurements had been validated by a comparison to enzymatic measurements of plasma samples for both substances (data not shown) in preliminary experiments. Heart rate and oxygen saturation were measured by pulse oximetry (MouseOx, Starr Life Sciences, USA). Temperature was monitored with a rectal probe attached to a PowerLab data acquisition system (ADInstruments, USA).

Electroencephalography. Ag-AgCl skin electrodes of 4 mm diameter (Slimtrode, InVivoMetric, USA) were attached to the depilated, slightly abraded (Nuprep, Weaver, USA) scalp with collodion glue (Mavidon, USA) and conductive paste (Ten20, Weaver, USA). Two electrodes were placed symmetrically 2 mm from the midline and about 2 mm anterior to a line joining both ears, situated above the cortex of both hemispheres. The reference electrode was placed on the occipital midline. Electrodes were stabilized with a rubber cap. Signals were amplified with an Animal Bio Amp (ADInstruments, USA) and digitized with a PowerLab data acquisition system (ADInstruments, USA) at 1 kHz, for a full-scale range of 100 µV and a frequency band pass from 0.3-50 Hz.

The digitized EEG was processed online to extract the suppression ratio (SR). The SR is the ratio of the duration of EEG suppression and the total duration of any given EEG epoch. It was calculated according to Vijn's algorithm (Vijn and Sneyd, 1998) implemented on CHART 5 data processing software (ADInstruments, USA) for an epoch length of 8s. The EEG was defined as suppressed if its derivative remained within a window of ± 0.4 mV/s for at least 200 ms. The choice of parameters was validated during pilot experiments with awake animals, and with animals under isoflurane anesthesia. To correlate the suppression ratio with the alertness score at a given time point, a 5 minute window of the EEG centered at this time point was inspected, the most stable part without artifacts was chosen, and the mean SR was determined.

Brain histology. Rat pups were deeply anaesthetized with 4% isoflurane and perfused intracardially with 10% phosphate buffered formalin for 45 minutes, as previously described (Popken, et al., 2004), and brains were dissected. Brains from animals euthanised shortly after resuscitation were dissected directly. After further immersion-fixation for 48-72 hours in the same fixative, paraffin sections (5 µm) were obtained from four coronal levels: A) Caudate-putamen, B) Anterior Hippocampus, C) Superior Colliculus, D) Cerebellum. One section per level was stained with Hematoxylin eosin, and one with Fluoro Jade C (Schmued, et al., 2005).

For immunohistochemistry, sections were incubated with rabbit anti-cleaved-caspase-3 (ClCasp-3) antibody (Cell Signaling # 9661, USA, 1:400) for 1 hr at room temperature after antigen retrieval in 10 mM Tris/EDTA buffer (pH 9, steamed for 20 min). Antibody detection was with a peroxidase based ABC Kit (Vector Laboratories, USA), with 3,3'-diaminobenzidine (DAB) as chromogenic substrate, and Hematoxylin as counterstain. The criterion for ClCasp-3-positive cells was the detection of cleaved-caspase-3 antigen in cytoplasm, because nuclear ClCasp-3 is not necessarily associated with apoptosis induction (Noyan-Ashraf, et al., 2005, Oomman, et al., 2004). For double labeling studies, sections were consecutively treated with rabbit anti-Olig-2 antibody (Chemicon AB9610, Denmark, 1:1000) and DAB as substrate, then with anti-ClCasp-3 antibody and Vector SG (Vector Laboratories, USA) as chromogenic substrate. For negative controls one or both of the primary antibodies were left out, without any non-specific staining. For immunofluorescent double labeling, sections were incubated with an antibody cocktail of rabbit anti-ClCasp-3, 1:200, with either mouse anti-CC-1 (Abcam ab16794, USA, 1:200), or mouse anti-GFAP (Chemicon MAB360, Denmark, 1:800). Detection was with suitable FITC and Alexa Fluor 594 conjugated secondary antibodies.

Statistical Analysis. Time to event data were analyzed by Kaplan Meier plots and logrank test, multiple comparisons for physiologic data and eosinophilic cell counts by one way ANOVA and Bonferroni post hoc test, changes in physiologic variables by paired T-tests, SR-ratios for alertness stages were compared by two sample T-tests, post resuscitation glucose levels by the Mann Whitney test, and correlation between apoptotic cells and time to EEG suppression by linear regression after natural logarithmic transformation. Post-resuscitation glucose levels below the lower level of detection (1 mM) were assigned a value of 0.5 mM for statistical analysis after we had confirmed the robustness of the Mann Whitney test for any values below 1 mM for our data. For all statistical analyses $p < 0.05$ was considered significant.

3.3 Results

Clinical and electroencephalographic characteristics of the hypoglycemic encephalopathy. Plasma glucose levels dropped to less than 1 mM 1.5 hr after insulin injection, and remained low during the clinical and electroencephalographic progression to coma. Clinically, animals progressed from an alert state with intact motor function, to ataxia and forelimb weakness, followed by clonus-like pushing with the back legs, loss of the righting reflex, progressive bradypnea, opisthotonus-like posturing, and finally minimal responsiveness to pain stimuli, severe bradypnea, and truncal flaccidity. The EEG passed through the characteristic stages of slow background activity during this progression and ultimately showed severe suppression with occasional bursts or slow waves (Figure 3.1). Within 5-10 minutes after glucose resuscitation, the EEG reverted to a continuous background activity, and animals typically

returned to a clinically alert state after 15-30 minutes. Animals did not develop clinical or electroencephalographical evidence of seizures at any stage during hypoglycemia.

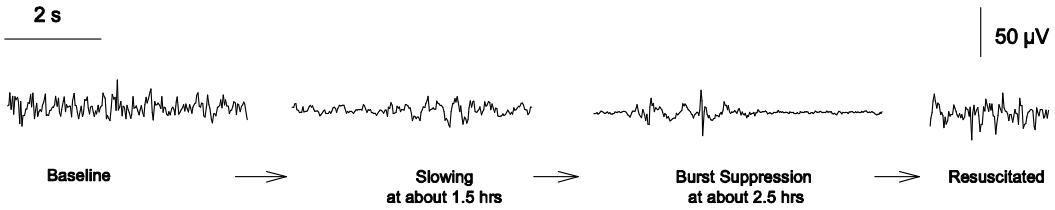

Figure 3.1: EEG changes during hypoglycemia

EEG changes during insulin-induced hypoglycemia in 13-day-old rats. Approximate time course is given for untreated animals in hours after insulin injection. Plasma glucose levels were < 1 mM one hour after the administration of insulin.

Time course of clinical and electroencephalographic progression to coma in hypoG+3OHB and hypoG animals. HypoG+3OHB pups showed sustained hyperketonemia, demonstrated by 3OHB plasma levels of 3-4mM 1.5 hrs after insulin and at the end of the experiment (Table 3.1). The onset of severe clinical coma (A-score < 4) was delayed by 70 minutes in hypoG+3OHB compared to hypoG (189 ± 18 vs. 116 ± 13 min, mean ± SD, n = 5, p = 0.015, Figure 3.2 A). Burst-suppression coma occurred about 50 minutes after the onset of severe clinical coma in hypoG+3OHB, compared to 30 minutes in hypoG. Overall, the onset of burst-suppression coma was delayed by 90 minutes in hypoG+3OHB compared to hypoG (238 ± 18 vs. 148 ± 12 min, mean ± SD, n = 5, p = 0.002, Figure 3.2 B). HypoG+3OHB pups showed greater preservation of continuous EEG activity at a given alertness score during the clinical progression to coma (Figure 3.2 C), whereas at the end point of the experiment and prior to resuscitation the degree of EEG suppression was comparable in both groups (SR: 0.85 ± 0.24 in hypoG+3OHB, 0.76 ± 0.11 in hypoG; mean ± SD). All groups were similar with respect to body temperature, oxygen saturation and heart rate at baseline and at resuscitation (Table 3.2). HypoG animals received oxygen for a total of 20-30 minutes during respiratory depression during coma, hypoG+3OHB animals received oxygen for a total of about 0-10 minutes because respiratory rates were generally higher during coma. This regime resulted in normal oxygen saturation rates at the time of resuscitation in both groups (Table 3.2). Normoglycemic control animals treated with 3OHB (normoG+3OHB) had normal alertness scores and regular EEG activities at all times during the experiment. In summary, clinical and electrophysiological tolerance to hypoglycemia was increased in hypoG+3OHB animals. This resulted in a significantly longer exposure to hypoglycemia before resuscitation compared to hypoG.

	Glucose			3OHB		
	Baseline	1.5 hrs	Endpoint	Baseline	1.5 hrs	Endpoint
Group		mmol / l			mmol / l	
HypoG	6.0 ± 1.5	< 1.0*	< 1.0*	2.0 ± 0.4	0.9 ± 0.2	0.8 ± 0.1
HypoG+3OHB	7.4 ± 1.5	< 1.0*	< 1.0*	2.0 ± 0.7	3.6 ± 0.9*,†	3.8 ± 0.8*,†
NormoG	6.4 ± 1.2	6.7 ± 1.0	5.3 ± 1.1	2.0 ± 0.4	0.8 ± 0.3	1.1 ± 0.4
NormoG+3OHB	6.5 ± 0.9	5.5 ± 0.3*	5.2 ± 0.9	1.5 ± 0.3	3.5 ± 0.5*,†	4.8 ± 0.8*,†
ANOVA $F_{3,16}$	0.9	n/a	n/a	1.1	37.4	52.8

Table 3.1: Glucose and 3OHB plama levles

Glucose and 3OHB plasma levels (mean ± 1 SD) at baseline, 1.5 hours after insulin injection, and at the endpoint of the experiment (burst suppression coma for hypoG and hypoG+3OHB, respective timepoints for normoG and normoG+3OHB). Lower limit of measurement for glucose was 1 mM; < 1mM indicates all measurements in one group were below this limit. Mean ± 1 SD ; $n = 5$; * $p<0.05$ vs. normoG, † $p<0.05$ vs. hypoG (One Way ANOVA and Bonferroni post hoc test, F values in table).

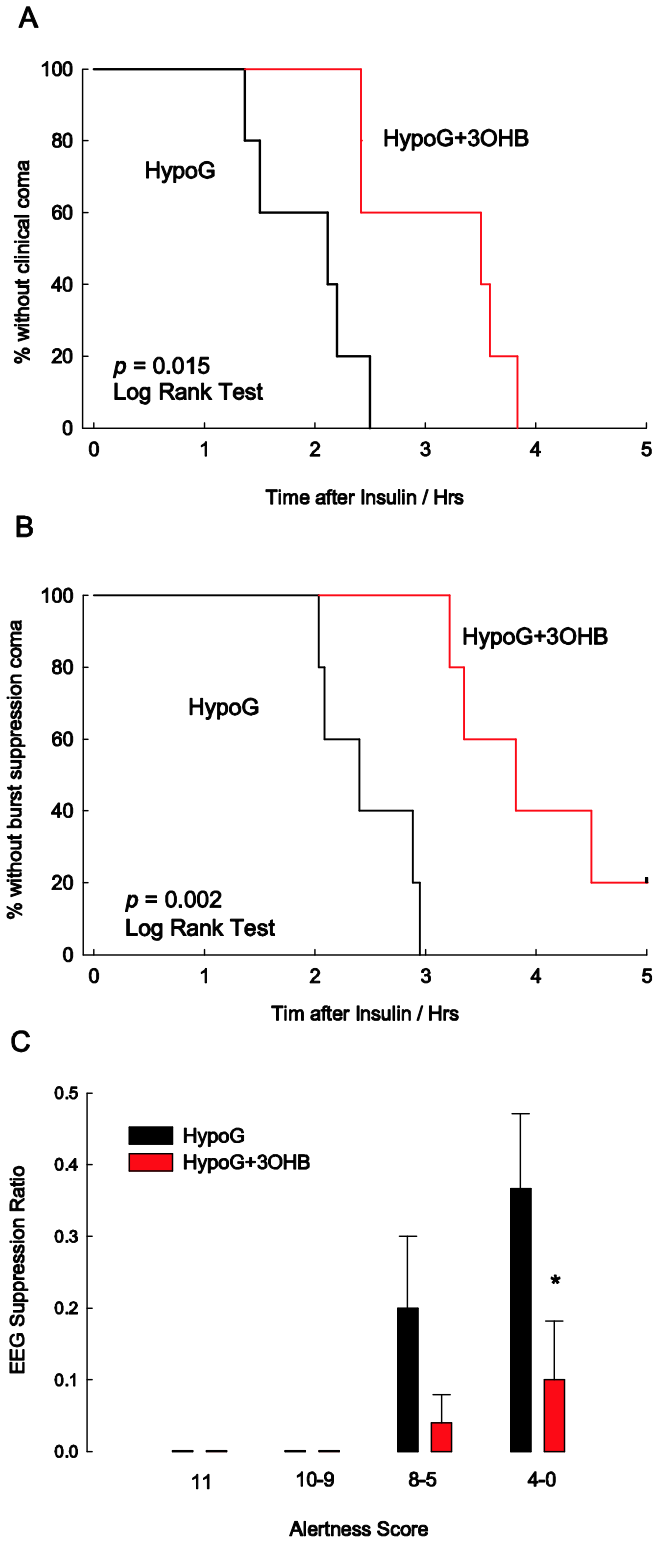

Figure 3.2: Progression of 3OHB treated and untreated hypoglycemic animls to clinical and EEG coma

Figure 3.2 (continued):
Progression of insulin-induced, hypoglycemic encephalopathy in untreated (hypoG, *n* = 5) and 3OHB-treated (hypoG+3OHB, *n* = 5) hypoglycemic 13-day-old rats. Normoglycemic controls (normoG and normoG+3OHB) showed no clinical or EEG changes during the experiment. A: Kaplan Meier Plot for time from insulin injection to the onset of clinical coma (Alertness score < 4). B: Kaplan Meier Plot for time from insulin injection to the onset of burst suppression coma. One treated animal reached the maximum time limit of the experiment of 5 hours after insulin injection without EEG suppression (censored observation). This animal was clinically comatose and developed a short episode of EEG suppression during glucose injection for resuscitation. C: EEG suppression ratios associated with different alertness states during the progression to coma (11: alert, 10-9: slightly reduced, 8-5: moderately reduced, and 4-1: severely reduced alertness) in hypoG and hypoG+3OHB rat pups. Error bars = 1SD; * $p < 0.05$, t-Test.

	TEMPERATURE		RESPIRATORY RATE		OXYGEN SATURATION		HEART RATE	
Group	Baseline	Endpoint	Baseline	Endpoint	Baseline	Endpoint	Baseline	Endpoint
	ºC		min^{-1}		%		min^{-1}	
HypoG	36.6 ± 0.9	35.6 ± 0.4*	126 ± 12	10 ± 6*,†	98.4 ± 0.4	98.8 ± 0.9	387 ± 35	406 ± 31
HypoG+3OHB	36.6 ± 1.3	36.5 ± 1.3	130 ± 12	59 ± 19$^{*,\#,}$	98.6 ± 0.5	98.9 ± 0.5	432 ± 67	479 ± 58
NormoG	37.7 ± 0.6	36.3 ± 1.3*	129 ± 21	112 ± 6	97.7 ± 1.3	97.7 ± 1.2	391 ± 43	429 ± 56
NormoG+3OHB	37.4 ± 0.9	36.2 ± 0.8*	136 ± 17	115 ± 11	98.4 ± 0.9	98.3 ± 0.6	411 ± 39	448 ± 48
ANOVA $F_{3,16}$	1.2	1.6	0.3	88.9	2.7	1.2	1.3	2.6

Table 3.2: Vital parameters

Physiologic parameters (mean ± 1 SD) for 13-day-old rat pups from hypoG, hypoG+3OHB, normoG, and normoG+3OHB groups. Endpoint: burst suppression coma for hypoG and hypoG+3OHB, respective timepoints for normoG and normoG+3OHB; * $p < 0.05$ vs. baseline (paired T-test). No significant inter-group differences at baseline and endpoint except for respiratory rates: $^{\#}$ $p < 0.05$ vs. normoG, normoG+3OHB, hypoG, † $p < 0.05$ vs. normoG, normoG+3OHB, hypoG+3OHB (one-way ANOVA and Bonferroni post hoc test; F values in table).

Resuscitation and Survival. Upon onset of EEG burst suppression we terminated the hypoglycemic state by combined s.c. and i.p. administration of glucose. This treatment resulted in a

recovery of EEG background activity in both hypoG and hypoG+3OHB animals. Concomitant recovery of clinical alertness occurred in 80% (4/5) of hypoG pups and these remained alive until the endpoint of the study 24 hours later (survival rate of 80%). In hypoG+3OHB only 40% (2/5) recovered clinical alertness after glucose resuscitation and this recovery was only transient because all animals in hypoG+3OHB developed recurrent coma, EEG suppression, and bradypnea, necessitating euthanasia 30-60 minutes after resuscitation. In summary, the 24-hour survival rate was 80% in hypoG and 0% in hypoG+3OHB ($p = 0.034$, Log Rank test).

Glucose levels after resuscitation were lower in hypoG+3OHB compared to hypoG animals (1.4 (1.5) vs. 3.5 (1.1) mM at 10 min after glucose, $p = 0.02$; 1.5 (1.2) vs. 4.6 (4.1) mM at 30 min after glucose, $p = 0.02$; median (interquartile range), Mann-Whitney test).

When hypoG+3OHB pups were resuscitated at the same time as their hypoG littermates (about 90 min earlier, data not shown, $n = 4$), they survived at the same rate as, and they also had similar post-resuscitation plasma glucose levels as untreated hypoglycemic animals (4.8 (2.7) mM 10 min after glucose, and 6.9(9.2) mM 30 min after glucose; median (interquartile range)). 3OHB administration without prolonged hypoglycemia thus did not result in resuscitation failure.

Neuropathology. Fluoro Jade C staining of sections from the four coronal levels examined showed that selective neuronal death had neither occurred in hypoG+3OHB nor in hypoG animals (see also section 2.8). H&E stained sections showed an increase in eosinophilic cells in white matter of hypoG+3OHB animals (Figure 3.3 A, B), indicating selective cell death. The mean number of eosinophilic cells in anterior corpus callosum, cingulum, and external capsule of 3OHB-treated hypoglycemic animals was 20-fold larger than in white matter of normoG, normoG+3OHB, and hypoG animals (Figure 3.3 C). HypoG+3OHB pups that were resuscitated at the same time as hypoG littermates showed no increase in white matter eosinophilic cells compared to hypoG, normoG, or normoG+3OHB animals ($n = 4$).

We used cleaved-caspase-3 (ClCasp-3) immunohistochemistry as a marker of apoptosis to further characterize this finding (Figure 3.3 D, E). Quantification of ClCasp-3-positive cells demonstrated apoptotic cells per section in corpus callosum in the following numbers (mean ± 1SD): hypoG+3OHB: 112 ± 68 ($n = 5$); hypoG: 1 ± 1 ($n = 4$); normoG: 5 ± 2 ($n = 5$); normoG+3OHB: 3 ± 1 ($n = 5$). HypogG+3OHB animals that were resuscitated at the same time as untreated hypoglycemic littermates had 1 ± 1 ($n = 4$) ClCasp-3-positive cells in corpus callosum per section. Thus, numbers of ClCasp-3-positive cells were similar to results from H&E staining (Figure 3.3 C). Correlation analysis of the number of ClCasp-3-positive cells in white matter per section with total time between insulin injection and resuscitation in hypoG+3OHB shows a clear increase of apoptotic cells with time (Figure 3.3 F; linear regression of logarithmically transformed cell numbers against time yields a regression coefficient of 1.8 ± 0.3 SE, $r^2 = 0.83$).

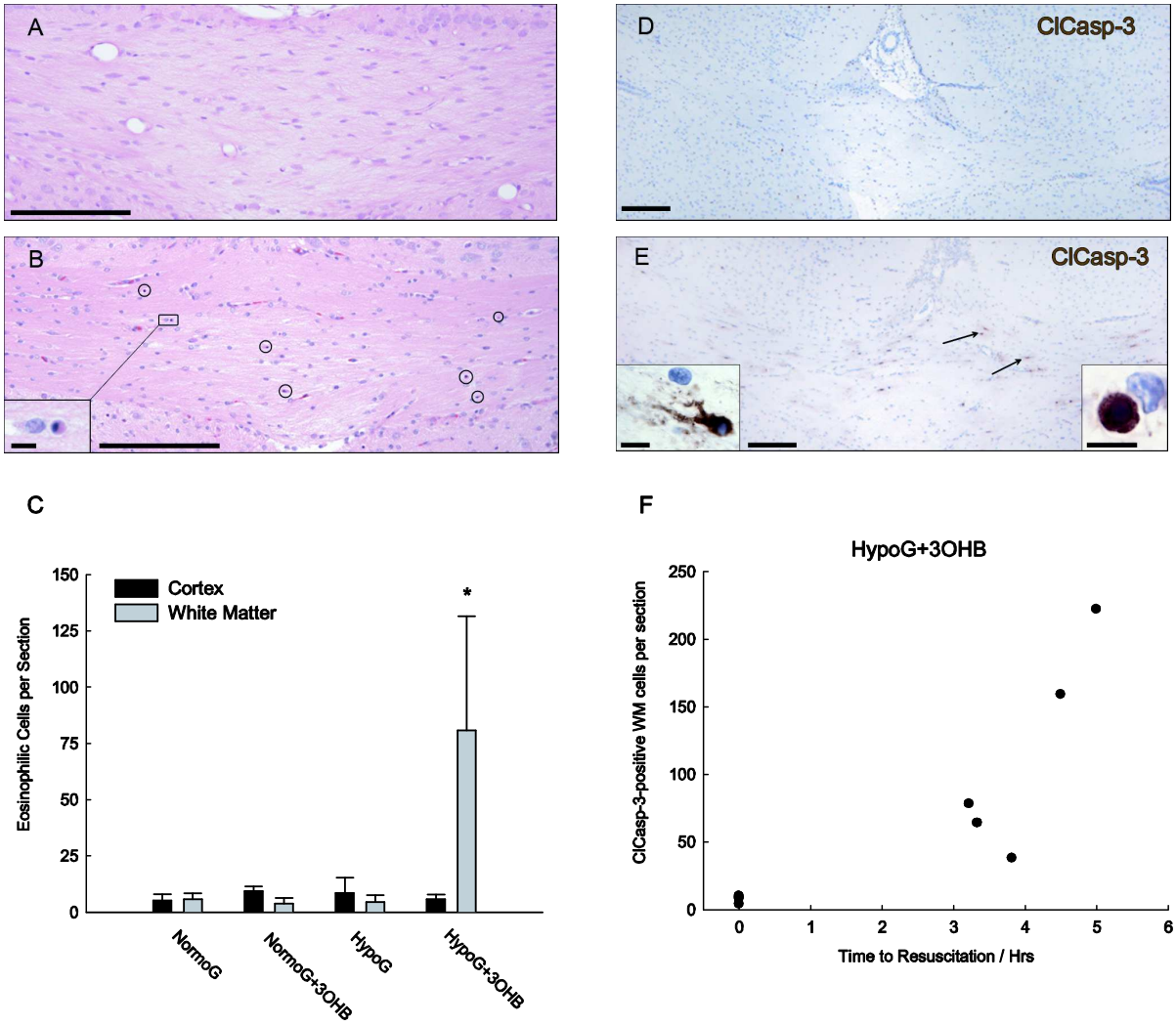

Figure 3.3: White matter injury after untreated and 3OHB treated hypoglycemia

Figure 3.3 (continued):
White matter injury after insulin-induced hypoglycemia in untreated (hypoG, n = 4, 1 resuscitation failure) and 3OHB-treated (hypoG+3OHB, n = 5) 13-day-old rats, compared to normoglycemic controls (normoG and normoG+3OHB). All analyses are from a coronal level of the anterior corpus callosum, corresponding to bregma -0.2 mm in adult rat brain (Paxinos, 1997). Scale bars: 200 µm for overview micrographs, 10 µm for insets. For quantification, cell counts per section were obtained from cortex (cingulate cortex to rhinal fissure) and white matter (corpus callosum, cingulum, and external capsule). A, B: Corpus callosum, H&E stain. A: normoG+3OHB; B: hypoG+3OHB; black circles indicate eosinophilic cells, inset shows typical eosinophilic cell with pink cytoplasm and pyknotic nucleus. C: Mean eosinophilic cell counts in cortex and white matter. Brains from hypoG, normoG, and normoG+3OHB animals were harvested 24 hrs after hypoglycemia, brains from hypoG+3OHB animals were harvested shortly after the hypoglycemic episode because of survival failure, * $p < 0.05$ (one way ANOVA and Bonferroni post hoc test, $F_{3,15}$ = 1.1 for cortex, $F_{3,15}$ = 10.0 for white matter). D, E: Corpus callosum, cleaved-caspase-3 (ClCasp-3) immunohistochemistry with hematoxylin counter stain. D: normoG+3OHB; E: hypoG+3OHB; insets show different typical morphologies of ClCasp-3-positive cells, possibly corresponding to different stages of apoptosis. F: Number of ClCasp-3-positive cells in white matter against duration of hypoglycemia (time between insulin injection and resuscitation) in hypoG+3OHB. For baseline cell counts (time 0 hrs), an additional set of completely untreated and age-matched animals (n = 4) was used to exclude physiological apoptosis on PND 13 and dissection or fixation artifacts as confounding factors. Brains of these control animals were immersion fixed only, like those of 3OHB-treated hypoglycemic animals.

To identify the type of dying cells, we used immuno-double-labeling for ClCasp-3 and the oligodendrocyte marker CC-1, the oligodendroglial lineage marker Olig-2, and the astrocyte marker GFAP respectively, and analyzed sections from the 3 most affected animals (Figure 3.4). 41 ± 10 % of ClCasp-3-positive cells co-labeled for CC-1, 16 ± 9 % for Olig-2, and none for GFAP. CC-1 typically identifies the somata of myelinating (mature) oligodendrocytes (Bhat, et al., 1996, Fuss, et al., 2000), whereas the transcription factor Olig-2 is expressed by pro-oligodendrocytes, pre-myelinating oligodendrocytes, and myelinating oligodendrocytes (Lu, et al., 2000, Nicolay, et al., 2007) in white matter structures. These data indicate that white matter injury in hypoG+3OHB is largely due to oligodendroglial apoptosis.

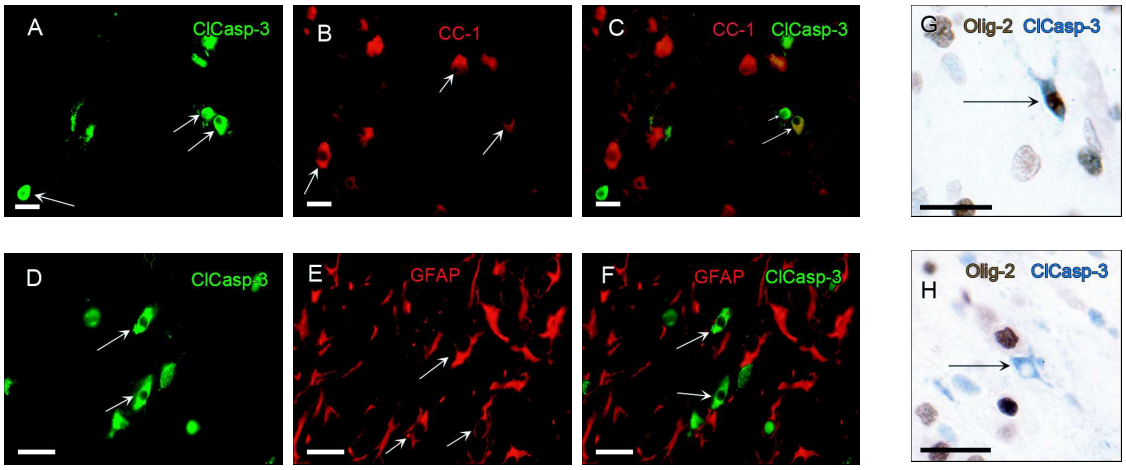

I

	HypoG+3OHB (*n*=3)	Control (*n*=3)
Cl-Casp-3 + CC-1	154 / 392 (40 ± 10 %)	2 / 19
Cl-Casp-3 + GFAP	0 / 388 (0 %)	0 / 10
Cl-Casp-3 + Olig-2	48 / 322 (16 ± 9 %)	5 / 13

Figure 3.4: Double labelling studies of apoptotic white matter cells

Characterization of apoptotic white matter cells from corpus callosum, cingulum, and external capsule in hypoG+3OHB rat pups by double labeling studies, compared to age matched controls. A-G: Representative micrographs from double labeling experiments for ClCasp-3 and three cell type markers, scalebars: 20 µm. A-D: Oligodendroglial marker CC-1; white arrows indicate ClCasp-3-positive cells in A, CC-1-positive cells in B, and one double-positive cell (yellow, long arrow) and one cell positive for ClCasp-3 only (green, short arrow) in D (superposition of A and B). E-F: Astroglial marker GFAP; white arrows indicate ClCasp-3-positive cells in D, GFAP-positive cells (perinuclear cytoplasm) in E, and ClCasp-3 only labeled cells in F (superposition of D and E). H-G: Oligodendroglial lineage marker Olig-2 (brown nuclei); black arrows indicate a ClCasp-3 only labeled cell in H, and a double-positive cell in G. I: Total number of double-positive cells per section as a proportion of total ClCasp-3-positive cells in white matter from three worst affected hypoG+3OHB animals, compared to three age-matched controls; mean percentages in brackets (mean ± 1 SD).

3.4 Discussion

Treatment with 3OHB prolonged the latency to onset of clinical and electrophysiological coma, but the longer exposure to hypoglycemia was associated with mortality after resuscitation and with white matter injury. The course of cerebral symptoms during hypoglycemia is determined by a gradual depletion of cerebral energy substrates resulting in bioenergetic failure and coma (Ghajar, et al., 1982, Lewis, et al., 1974b, Suh, et al., 2007b). The observed capacity of 3OHB to delay the development of cerebral symptoms during hypoglycemia, but not to prevent it, can be explained by the different metabolic functions of glucose and 3OHB. 3OHB is similar to glucose in that both are converted in the same ratio to acetyl-CoA. Acetyl-CoA serves as a major source for oxidative mitochondrial energy (ATP) generation. Continuously high 3OHB plasma levels in our experiment should therefore have provided a constant supply of oxidative substrate to the brain. 3OHB differs metabolically from glucose because it is not a substrate for glycolysis. Cerebral glycolysis is a major anaplerotic resource, and provides substrates for the pentose phosphate pathway. Cerebral anaplerosis via the formation of pyruvate and oxaloacetate is an important pathway for cerebral glutamate and neurotransmitter synthesis (Bartnik, et al., 2007, Oz, et al., 2004, Patel, et al., 2003). The pentose phosphate pathway is essential for the maintenance of cellular redox defenses through the generation of NADPH (Ralser, et al., 2007). Thus, from a biochemical point of view, 3OHB can provide acetyl-CoA and compensate for a lack of oxidative substrates, but it cannot support glycolysis, anaplerosis, and the pentose phosphate pathway. These biochemical limitations may explain why 3OHB treated hypoglycemic animals became eventually comatose, despite ongoing acetyl-CoA supply.

The stability of pulse rate and oxygen saturation throughout prolonged hypoglycemia suggest that 3OHB also had a cardio protective effect. Yet the mortality shortly after an initial electrophysiological response to i.p. glucose at the end of the experiment is difficult to explain. Glucose reperfusion injury via increased production of reactive oxygen species might be a reason (Suh, et al., 2007c). Effects of prolonged hypoglycemia on other organs were not investigated but could have contributed. For example, pulmonary edema has been described as a complication of prolonged hypoglycemia (Ortega, et al., 2000). The moderate increase of blood glucose levels after resuscitation is also difficult to explain. Impaired resorption from the peritoneal space due to sudden cardiovascular failure after prolonged hypoglycemia may have been one reason. Toxic effects of 3OHB as a cause of resuscitation failure are excluded because resuscitation failure did not occur when hypoG+3OHB animals were resuscitated at the same time as their hypoG littermates. Regardless of the unexplained mechanisms leading to resuscitation failure, its occurrence suggests that the pathophysiology underlying the comatose states in hypoG and in hypoG+3OHB animals differs. This may have implications for a clinical translation of 3OHB treatment.

We found a positive correlation between the number of apoptotic cells in white matter of hypoG+3OHB pups and the total time of hypoglycemia. NormoG+3OHB pups and hypoG pups did not develop white matter changes, probably because of a shorter exposure of white matter cells to glucose deprivation. The absence of white matter injury in hypoG+3OHB pups resuscitated at the same time as their hypoG littermates largely excludes toxic effects of 3OHB as a cause of white matter injury. The apoptotic cell population consisted largely of mature, myelinating oligodendrocytes, as shown by double labeling experiments with cell-type specific markers. 50% of cells were not identified by our labeling technique and could represent a different cell population, such as microglia, which was not targeted by the antibodies used. The high proportion of myelinating oligodendrocytes among apoptotic cells is mirrored by the predominance of this stage of oligodendrocyte development in rats on postnatal day 13 (Craig, et al., 2003). Myelinating oligodendrocytes are also the predominating oligodendroglial cell type in human brain after birth (Back, et al., 2001). *In vitro* studies have shown that myelinating mouse oligodendrocytes and oligodendroglial cultures from neonatal rats are vulnerable to glucose deprivation (Yan and Rivkees, 2006, Zuppinger, et al., 1981). Oligodendrocytes are highly susceptible to oxidative injury (McTigue and Tripathi, 2008). Suppressed glycolysis during hypoglycemia and an associated failure of the pentose phosphate pathway to maintain intracellular redox defenses may have contributed to cell death despite the availability of 3OHB as energy substrate.

We did not find signs of neuronal death even after prolonged hypoglycemia. This is in contrast to findings in adult rats where selective neuronal death directly correlates with the duration of EEG suppression (Auer, et al., 1984b). Induced by the high fat content of milk, rat pups are in a physiologically ketotic state which may have resulted in a selectively neurono-protective effect during hypoglycemia (Yamada, et al., 2005). Potential mechanisms include stabilization of the hypoxia-inducible-factor (HIF) 1α, a neuroprotective regulator protein, and upregulation of the anti-apoptotic protein Bcl-2 (Puchowicz, et al., 2008). Ketosis also increases the expression of cerebral mitochondrial uncoupling protein (UCP) 2, which is known to increase resistance to neuronal death (Mattiasson, et al., 2003, Sullivan, et al., 2004).

Resuscitation failure necessitated early euthanasia of 3OHB treated animals, resulting in two time points for brain collection after resuscitation. This complicates the interpretation of our neuropathological data, since cell death processes are time dependent. Oligodendroglial apoptosis in models of hypoxic ischemic injury in developing rats is histologically apparent 24 hrs after the insult (Back, et al., 2002, Follett, et al., 2000), suggesting that white matter injury in untreated hypoglycemic or 3OHB-treated euglycemic control animals would have been apparent on H&E or ClCasp-3 stains at 24hrs after resuscitation.

NormoG+3OHB animals showed no clinical impairment and no signs of cellular injury. HypoG+3OHB animals which were resuscitated at the same time as their hypoG littermates showed no

signs of cellular injury and no increased mortality compared to hypoG. Therefore toxic effects of 3OHB treatment in this study can largely be excluded.

In conclusion, 3OHB delays the onset of clinical and electrophysiological coma during hypoglycemia. Prolonged hypoglycemia is associated with high mortality and white matter injury. These observed limitations of the effect may be related to anaplerotic or glycolytic deprivation. They could be overcome by a combined administration of 3OHB with anaplerotic and gluconeogenic substrates. Further experimental studies in particular of the underlying pathobiochemistry will serve to find optimal treatments for patients at risk for hypoglycemic brain damage.

4. Protective Effects of D-3-Hydroxybutyrate and Propionate during Hypoglycemic Coma: Clinical and Biochemical Insights from Infant Rats

4.1 Introduction

Hypoglycemia is a frequent condition in neonates and infants which may result in long term neurological sequelae like psychomotor deficits and epilepsy (Burns, et al., 2008, Meissner, et al., 2003, Menni, et al., 2001). Hypoglycemia in the absence of ketone bodies is perceived as particularly aggressive. It typically occurs in small for gestational age and preterm neonates and in some inborn errors of metabolism, such as persistent hyperinsulinemic hypoglycemia of infancy (PHHI) and fatty acid oxidation disorders.

Ketone bodies, such as D-3-hydroxybutyrate (3OHB) and acetoacetate, are a cerebral energy substrate alternative to glucose. They are transported across the blood brain barrier by the monocarboxylate transporter 1 (MCT-1) and are subsequently metabolized to acetyl-CoA as an oxidative substrate. The extent of cerebral ketone utilization is especially high in the neonatal period (reviewed in (Nehlig, 2004)). Experimental evidence suggests that ketone bodies can sustain electrical responses in brain slices in the absence of glucose (Arakawa, et al., 1991, Izumi, et al., 1998, Wada, et al., 1997) and that 3OHB treatment improves the alertness state of mouse pups in a hypoglycemic coma (Thurston, et al., 1986). Still, the capacity of 3OHB to support brain function over extended periods of glucose deprivation is limited. We have shown recently that ketone body supplementation increases the latency to hypoglycemic coma in rat pups. We could also show that prolonged latency to electroclinically symptomatic hypoglycemia is associated with white matter injury (chapter 3). The biochemical background of these limitations is poorly understood. One possibility is that 3OHB cannot compensate for an anaplerotic deficit in the absence of substrates arising from glycolysis. In the brain anaplerosis is essential because the pool of citric acid cycle intermediates is the exclusive source of glutamate

synthesis, which is required for neurotransmitter metabolism and ammonia detoxification (Oz, et al., 2004, Sibson, et al., 2001, Xu, et al., 2004). Propionate is an alternative anaplerotic substrate because it is metabolized to succinyl-CoA, a citric acid cycle intermediate (Martini, et al., 2003, Nguyen, et al., 2007, Reszko, et al., 2003) (Figure 4.1). We hypothesized that treatment with propionate additionally to 3OHB improves cerebral anaplerosis and that this is associated with an improved treatment outcome. To address this hypothesis we investigated the clinical and biochemical effects of 3OHB supplementation during hypoglycemic coma and the potentials of additional propionate as an alternative anaplerotic substrate in an infant rat model of insulin induced hypoglycemia.

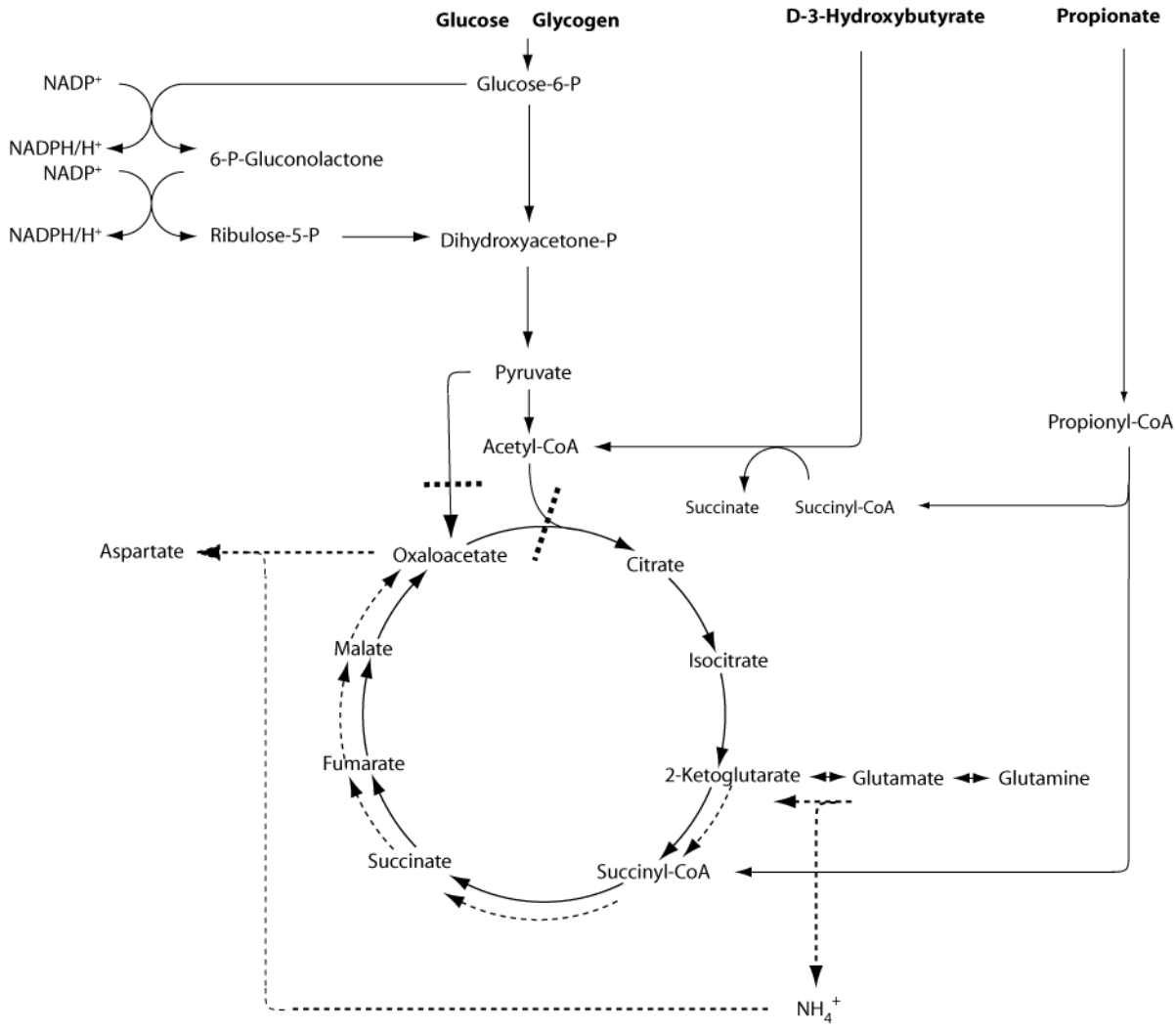

Figure 4.1: Metabolic pathways for glucose, D-3-hydroxybutyrate, and propionate

Metabolic pathways for glucose, D-3-hydroxybutyrate, and propionate. Glycolysis serves several metabolic functions, including the generation of acetyl-CoA for oxidation, the generation of NADPH for redox defenses, and the generation of oxaloacetate for anaplerosis. 3OHB catabolism can provide acetyl-CoA for oxidation only. Propionate is metabolised to succinyl-CoA and could thus represent an alternative anaplerotic source. Note that succinyl-CoA, which is produced by propionate metabolism, is not only a citric acic cycle intermediate but is also required for the ketolytic activation of 3OHB. During hypoglycemia glutamate is utilized as endogenous energy substrate (dashed lines). Following de- or transamination to alpha ketoglutarate, it enters the citric acid cycle and is converted to oxaloacetate. Glucose deprivation results in a shortage of acetyl-CoA, so that citric acid synthesis from oxaloacetate is blocked. Instead, oxaloacetate is aminated to aspartate, so that the citric acid cycle appears to be only partially acitve (truncation, (Sutherland, et al., 2008)).

4.2 Materials and methods

Experimental setting. All experiments were performed according to the guidelines of the Canadian Council on Animal Care, and were approved by the local Animal Care Committee.We used Sprague Dawley rat pups on postnatal day (PND) 13. At this age, in rat pups the cerebral metabolic rates for glucose undergo a steep increase, equivalent to 2 month old human infants (Kinnala, et al., 1996, Nehlig, et al., 1988). For induction, maintenance, and monitoring of hypoglycemia we used an experimental setting as previously decribed (chapters 2 & 3). Briefly, we induced and sustained hypoglycemia with a subcutaneous injection of 10 U/kg regular human insulin (Humulin R, Eli Lilly, Canada) at the start point of the experiment and a repeated dose after 120 minutes. We monitored heart rate and oxygen saturation by pulse oximetry and respiratory rates by observation.We administered atropine (1 mg/kg s.c.) 1 hour after the first insulin dose to prevent bradycardia. We administered oxygen by facemask when respiratory rates were less than 30 min^{-1} to avoid hypoxia. For assessment of clinical brain function we used an alertness score (A-score) evaluating voluntary movements, tone, posture, and reflexes as previously described (Table 2.1). Scores range from 11 and 9-10 denoting alertness and slight reduction of alertness to 4-0 denoting deep coma**.** For assessment of electrical brain function we used electroencephalography and quantitative analysis of the suppression ratio (SR) as decribed. The SR is the ratio of the duration of suppression and the total duration of any given EEG epoch.

Treatment Protocol. After the induction of hypoglycemia, animals progressed clinically and electroencephalographically through characteristic stages to a deeply comatose state. When the EEG showed burst-suppression coma, animals were treated in three groups with either a single dose of D-3-hydroxybutyrate (3OHB), or D-3-hydroxybutyrate combined with propionate (3OHB+Prop), or a single dose propionate (Prop). Treatment was given as subcutaneous injection of 6 mmol/kg sodium D-3-hydroxybutyrate (sterile, neurtalized solution of 600mM, Sigma, USA), 1.5 mmol/kg sodium propionate (sterile, neutralized solution of 350 mM, Sigma, USA), or equivalent amounts of saline in respective combinations.

Dose selection for 3OHB was based on target plasma levels in the high physiological range for rat pups of around 4 mM. The best dose to attain target levels was determined in a pilot study (Schutz, et al., 2011b). We chose a 600 mM 3OHB solution for subcutaneous injections in order to administer a maximal amount of 3OHB in a minimal volume. Subcutaneous administration of solutions with an osmolality up to 1400 mOsm/kg, corresponding to 700 mM 3OHB, has been reported to be safe (Bellin, et al., 2002, Elam, et al., 1991). There was no evidence of tissue necrosis in preliminary studies. Target plasma levels for propionate were chosen in analogy to studies on anaplerosis from propionate in pig heart and liver as 0.3-1 mM (Martini, et al., 2003, Reszko, et al., 2003). Observations showed that a dose of 1.5 mmol/kg produces serum levels in the target range.

Experimental Design. In a first set of experiments we investigated the clinical and electrical brain function during a period of 60 minutes following treatment. At the end of the experiment animals were euthanized. Each of the 3 groups was randomly assigned 7 pups (three littermates per experiment from a total of 7 litters). We performed a second set of experiments to analyze the brains biochemically at three time points: Before insulin injection; at the time of coma / prior to treatment; and 30 minutes after treatment with D-3-hydroxybutyrate alone or in combination with propionate. Each group was assigned 7 pups (four littermates per experiments from a total of 7 litters). At the end of the experiment animals were sacrificed by decapitation and heads were immediately frozen in liquid nitrogen for further biochemical analysis in brain homogenates.

Plasma glucose and D-3-hydroxybutyrate levels were measured from a blood drop obtained by puncture of a lateral tail vein at various time points during the experiments with PrecisionXtra glucose- and ketone-test strips (Abbott Diabetes Care, UK). Lower limit of measurement for glucose was ≤ 1mM. *For determination of serum propionate kinetics,* animals were s.c. injected with 1.5 mmol/kg sodium propionate and serum samples were obtained by cardiac puncture at 0, 7, 15, 30, and 60 minutes after injection (terminal procedure after isoflurane anaesthesia; $n = 3$ per timepoint). Propionate was measured by LC-MS using [$^2H_5$]propionate (CDN Isotopes, Canada) as internal standard, a C_{18}-HPLC analytical column for elution, followed by detection by mass spectrometry operating in the negative ionization mode. The lower limit of detection as determined in preliminary experiments was 10 µmol/l serum propionate**.**

For biochemical analysis of brain metabolites, samples were dissected on dry ice from frozen forebrain. *Brain acylcarnitine profiles* were determined by MS/MS as described by van Vlies et al. 2005 with minor modifications (van Vlies, et al., 2005). 60-100 mg tissue samples were extracted by sonication in 80% acetonitrile containing [$^2H_3$]L-carnitine, [$^2H_3$]propionyl-L-carnitine, [$^2H_3$]octanoyl-L-carnitine, and [$^2H_3$]hexadacanoyl-L-carnitine (obtained from Herman J. ten Brink, VU Medical Hospital, Amsterdam, The Netherlands) as internal standards. In contrast to the original publication of the method tissue samples were not freeze-dried, since initial trials demonstrated that freeze-drying had no advantage in our hands. We used propyl-derivatives instead of more commonly used butyl-derivatives because butylated acetyl-carnitine cannot be distinguished tandem mass spectrometrically from butylated glutamate. For determination of *brain amino acids, ammonia, and pentose phosphate* metabolites, 100 mg tissue samples were extracted with 0.5 ml 1N perchloric acid in a manual glass tissue grinder on ice. After centrifugation, the supernatant was neutralized with 0.7M tripotassium phosphate. Aminoacids (aspartate, alanine, valine, leucine, isoleucine, glutamate, glutamine) and GABA were measured as their fluorenylmethoxycarbonyl (FMOC) derivatives by HPLC-MS/MS after addition of respective stable isotope labeled internal standards (Mills, et al., 2006). The peaks for leucine and isoleucine were not resolved with our settings, and results are reported as a combined measurement for both. Ammonia

levels were determined with a kit as per manufacturer's instructions (Ammonia Assay Kit, Sigma Aldrich, USA). Intermediates of the pentose phosphate pathway were determined by HPLC-MS/MS as described by Wamelink et al. (Wamelink, et al., 2005).

Statistical analysis. Group comparisons for 2 groups were made by Student's T test, and for multiple groups by one way ANOVA followed by Tukey's HSD test. Clinical outcome in 3OHB and 3OHB+Prop groups was compared by Fisher's exact test. Differences were considered significant for $p < 0.05$. Data are given as mean ± 1 standard deviation.

4.3 Results

Plasma glucose levels dropped progressively to less than 1 mM at about 1.5 hr after insulin injection, and remained low during the entire experiment. Mean total time between insulin injection and treatment was 143 ± 26 minutes.

Course from induction of hypoglycemia to burst suppression coma: Plasma 3OHB levels dropped from 1.6 ± 0.4 mM at baseline to 0.6 ± 0.1 mM (mean ± 1SD) at the time of coma. Burst suppression coma was reached about 2-3 hours after insulin injection. Clinically, animals progressed from an alert, ambulatory state (A-Score 11) to ataxia and forelimb weakness (A-Score 9-10), followed by clonus, opisthotonus and loss of the righting reflex, and finally minimal responsiveness to pain stimuli, severe bradypnea, and truncal flaccidity (A-Score 4-0). The EEG passed through the characteristic stages of slow background activity during this progression and ultimately showed severe suppression with occasional bursts or slow waves (burst suppression coma). One animal from the 3OHB+Prop group died before reaching the comatose stage.

Effects of treatment with 3OHB and propionate. Respective treatments resulted in a 4-fold increase of plasma 3OHB and in a 100-fold increase of plasma propionate levels compared to baseline. Peak levels of 3OHB and propionate were reached 30 minutes and 7 minutes after treatment, respectively (Fig. 4.2). Mean plasma 3OHB peak levels were similar after 3OHB and 3OHB+Prop treatment (4.1 ± 0.4 mM in 3OHB and 3.8 ± 0.5 in 3OHB+Prop, mean±1SD). Both treatments resulted in reversal of EEG activity from burst suppression to complete continuity in all animals. This reversal occurred between 5-10 minutes after administration of 3OHB and lasted 40-50 minutes (Fig. 4.2). EEG suppression invariably recurred when plasma 3OHB levels fell again below 1.5-2 mM.

Clinically animals were severely comatose at the time of burst suppression coma with and alertness score < 4. Scores remained low in all 6 animals treated with 3OHB alone (1 animal died before it reached coma) but resolved to normal (A-Score > 9) in 5/7 (71%) animals treated with 3OHB+Prop ($p = 0.02$, Fisher's Exact Test). Improved alertness occurred at the time when maximum plasma 3OHB levels had been reached and cerebral C3 carnitine levels were high. (Fig. 4.2). Improved alertness lasted

15 ± 5 min. The two clinically unresponsive animals in the 3OHB+Prop group remained in a stable coma with reversion of EEG suppression to continuous activity within the 60 minute-observation period. *Pups treated with propionate only* showed neither an electroencephalographical nor a clinical response. They all developed isoelectric EEG and respiratory failure several minutes after treatment, necessitating euthanasia.

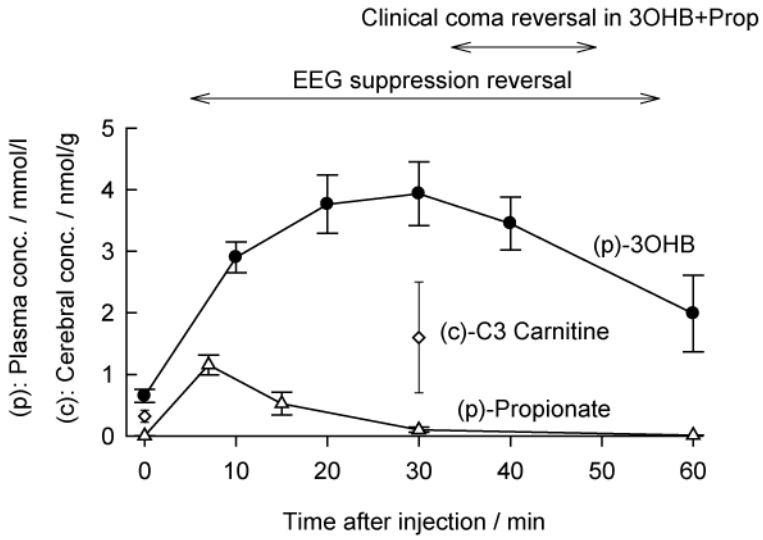

Figure 4.2: 3OHB and propionate plasma levels and clinical response

Levels of 3OHB and propionate in plasma and of propionyl-carnitine in brain after single dose subcutaneous injection of 6 mmol/kg 3OHB or 1.5 mmol/kg propionate in rat pups. 3OHB levels represent mean ± 1SD of serial measurements from the first experiment with injection at the time of burst suppression coma (n = 14). Propionate levels represent mean ± 1SD from an additional experiment with single measurements at each timepoint (n = 3). The period of reversal of EEG suppression and clinical coma are indicated by double arrows. Cerebral propionyl-carnitine (C3) measurements are elevated at 30 min, shortly before improvement of alertness starts.

The respiratory rate is a sensitive marker of the clinical state of the pups during hypoglycemia. Respiratory rates were severely reduced in burst suppression coma (9 ± 4 min^{-1} compared to 122 ± 6 min^{-1} at baseline). Treatment with 3OHB+Prop resulted in a normalization of the respiratory rate as long as 3OHB plasma levels remained elevated above 2 mM. 3OHB alone resulted in partial improvement of respiratory rates with significantly lower peak levels compared to 3OHB+Prop treatment (72 ± 17 vs. 120 ± 36, $p < 0.05$, t-Test) . Treatment with propionate only did not stop a further decrease in respiratory rates leading to respiratory failure about 10 minutes after treatment.

Results of biochemical studies are give in table 4.1. *Cerebral acyl-carnitine* profiles at the time of coma show depletion of short chain acyl-carnitines (C4: butyrylcarnitine and isobutyrylcarnitine; C4OH: hydroxybutyrylcarnitine and hydroxyisobutyrylcarnitine; C5: isovalerylcarnitine, 2-methylbutyrylcarnitine and dimethylpropionylcarnitine) and elevation of long-chain acyl-carnitines (C14: tetradecanoylcarnitine; C16: palmitoylcarnitine; C18: steaorylcarnitine; C18:1: oleylcarnitine). Metabolic pathways resulting in production of short chain acylcarnitines include degradation of valine and butyrate contributing to C4, degradation of valine and 3OHB contributing to C4OH, and degradation of isoleucine, leucine, and odd chain fatty acids contributing to C5.Metabolic pathways contributing to long-chain acylcarnitines include oxidation of long chain fatty acids. Treatment with 3OHB+Prop and 3OHB alone resulted in partial reversal of short chain acyl-carnitine depletion and in a further increase of long chain acylcarnitines. In the 3OHB + Prop treated group, we found an additional increase of *propionyl-carnitine*.(C3) levels. Increased cerebral propionylcarnitine levels were measured 30 minutes after treatment, shortly before the reversal of clinical coma had occurred in the observational group (Fig 2).

Aminoacids and ammonia. By the time of coma cerebral ammonia and aspartate levels were increased, while glutamate was decreased in comatose animals. These changes were reversed by 3OHB treatment (Fig. 5). Depletion of other aminoacids such as glutamine, alanine and branched chain amino acids valine, leucine, and isoleucine and of GABA was not reversed after treatment (Fig. 5). These findings were comparable in both the 3OHB and the 3OHB+Prop treatment groups.

Analysis of *pentose phosphate pathway intermediates* demonstrates that the oxidative part of the pathway is severely depleted in comatose animals (cf. glucose-6-phosphate, 6-phospho-gluconolactone, and ribulose/xylulose-5-phosphate in Fig. 3C), and that 3OHB treatment with or without propionate does not reverse this depletion.

Oxygen saturation and *body temperature* were similar in all groups at the time of sacrifice, except for a small reduction of body temperature to 34.3 ± 1.6 °C in comatose animals compared to 36.7 ± 0.6 °C at baseline.

	Baseline mM or nmol/g	**Coma** mM or nmol/g	**3OHB+NaCl** mM or nmol/g	**3OHB+Prop** mM or nmol/g
Plasma				
Glucose	7.6 ± 0.7	< 1	< 1	< 1
3OHB	1.9 ± 0.5	1.0 ± 0.3*	4.5 ± 0.7*	4.3 ± 0.6*
Brain				
Acylcarnitines				
C3	0.7 ± 0.2	0.3 ± 0.1	0.4 ± 0.3	1.8 ± 0.9*#
C4	2.0 ± 0.3	0.8 ± 0.2*	1.7 ± 0.4	1.6 ± 0.3
C4OH	0.9 ± 0.4	0.4 ± 0.1*	0.9 ± 0.2	1.1 ± 0.2
C5	2.2 ± 0.7	0.7 ± 0.1*	1.3 ± 1.0	1.5 ± 1.2
C12	0.9 ± 0.2	0.4 ± 0.1*	0.7 ± 0.1	0.7 ± 0.1
C14	1.7 ± 0.4	1.7 ± 0.4	2.8 ± 0.6*	2.9 ± 0.5*
C16	1.1 ± 0.1	1.7 ± 0.5*	3.2 ± 0.6*	3.4 ± 0.9*
C18	0.7 ± 0.1	1.1 ± 0.3	1.4 ± 0.2*	1.7 ± 0.4*
C18:1	1.1 ± 0.2	1.7 ± 0.5	2.2 ± 1.0*	2.4 ± 0.6*
Aminoacids				
Aspartate	2550 ± 470	5320 ± 1110*	3250 ± 360	3000 ± 400
Glutamate	6590 ± 690	3250 ± 440*	6330 ± 730	6220 ± 750
Glutamine	2910 ± 490	1500 ± 550*	2100 ± 160*	2060 ± 420*
GABA	670 ± 140	440 ± 100*	550 ± 80	560 ± 90
Alanine	840 ± 210	130 ± 30*	270 ± 110*	310 ± 220*
Valine	190 ± 40	120 ± 20*	120 ± 20*	130 ± 40*
Leucine/Isoleucine	230 ± 40	140 ± 20*	150 ± 40*	150 ± 50*
Ammonia	460 ± 150	1090 ± 240*	510 ± 120	470 ± 250
PPP				
Glucose 6 P	96 ± 16	29 ± 9*	31 ± 3*	51 ± 19*
6-P-Gluconolactone	33 ± 4	4 ± 1*	8 ± 3*	8 ± 3*
Ribulose/Xylulose 5 P	24 ± 3	5 ± 2*	9 ± 4*	5 ± 3*
Ribose 5 P	22 ± 3	23 ± 12	26 ± 4	21 ± 4
Seduheptulose 7 P	30 ± 8	17 ± 8*	15 ± 4*	22 ± 10
Dihydroxyacetone P	115 ± 13	48 ± 7*	61 ± 6*	53 ± 6*

Table 4.1: Biochemical parameters at baseline, coma, and 30 minutes after resuscitaiton with 3OHB or 3OHB+Prop

Table 4.1 (continued):
Plasma levels of glucose and 3OHB and cerebral tissue concentrations of acyl-carnitines, aminoacids, ammonia, and pentose phosphate pathway intermediates at baseline, at burst-suppression coma, and 30 minutes after treatment of comatose animals with 3OHB (n = 6) or 3OHB+Prop (n = 7). There were no statistically significant differences between 3OHB+Prop and 3OHB except for cerebral propionyl-carnitine (C3) levels. Lower limit of plasma glucose measurement was 1 mM. Plasma levels "< 1mM" indicates that all measurements were below 1 mM. * $p < 0.05$ vs. baseline, $^{\#}$ $p < 0.05$ for 3OHB+Prop vs. 3OHB, One Way ANOVA and Tukey's HSD Test, all values are mean ± 1SD.

4.4 Discussion

Prolonged insulin induced hypoglycemia resulted in clinical and electrical (burst suppression) coma. Coma was associated with depleted cerebral glycogen reserves (indicated by low glucose-6–phosphate levels) and a reduced 3OHB supply (indicated by low C4OH levels) (Choi, et al., 2003, Hack, et al., 2006, Oz, et al., 2009). Cerebral concentrations of several amino acids that serve as alternative energy substrates were also reduced at the time of untreated burst suppression coma (e.g. glutamate, glutamine and branched chain amino acids). Concomitantly, ammonia levels were elevated indicating ongoing amino acid deamination (Honegger, et al., 2002). Treatment with 3OHB resulted in reversal of EEG burst suppression but not of clinical coma, whereas combined treatment with 3OHB and propionate also led to reversal of clinical coma.

The limited capacity of 3OHB to restore cerebral function and the beneficial effect of additional propionate must relate to complementary roles of both substrates in energy and intermediary metabolism. 3OHB as the precursor of acetyl-CoA can compensate for a lack of oxidative substrates during hypoglycemia, while additional propionate, as the immediate precursor of succinyl-CoA, could support anaplerosis and possibly gluconeogenesis.

Results of biochemical analyses in brain tissue give more insight into the metabolic changes effected by both treatments. Treatment with 3OHB alone resulted in an increase of cerebral 3-hydroxybutyryl-carnitine (C4OH) while glycolytic substrates such as glucose-6-phosphate and dihydroxyacetone-phosphate remained depleted. Interestingly, 3OHB treatment also resulted in a correction of cerebral glutamate levels. This finding is best explained by the truncated citric acid cycle model proposed by Sutherland et al. (Sutherland, et al., 2008). During hypoglycemia, glutamate is deaminated to form alpha-ketoglutarate and thus becomes a major anaplerotic substrate. Alpha-ketoglutarate is converted to oxaloacetate. However, a shortage of acetyl CoA blocks its further conversion to citrate. Oxaloacetate cannot continue its flux through the cycle and is aminated to aspartate

instead. This mechanism explains the depletion of glutamate and accumulation of aspartate observed in our untreated hypoglycemic animals. When 3OHB is supplemented, this provides a new supply of acetyl-CoA enabling the conversion of oxaloacetate to citrate. This allows accumulated aspartate to be re-converted into oxaloacetate and further into alpha-ketoglutarate and glutamate (Fig. 1). The observed reduction of aspartate and the simultaneous increase of glutamate in the 3OHB treated animals is in line with the effects of 3OHB described above. The increase of cerebral glutamate levels upon 3OHB supplementation also explains the observed correction of ammonia levels (via formation of glutamine) as well as the reversal of GABA depletion (via glutamate decarboxylation).

Clinical improvement as demonstrated by the increase in alertness score and peak respiratory rate was only achieved after combined treatment with 3OHB and propionate and occurred at a time when propionyl-carnitine levels were elevated in brain. Propionate alone did not show any protective effect. Combined treatment with 3OHB and propionate did not result in a measurable redirection of propionate into gluconeogenetic substrates such as alanine, dihydroxyacetone-P, and glucose-6-P. There was also no effect of additional propionate on glutamate synthesis beyond the effects achieved by 3OHB treatment alone. This is in line with the results of a recent study demonstrating that anaplerotic metabolism of propionate in astrocytes resulted in a comparatively small contribution to amino acid synthesis (Nguyen, et al., 2007).

We were not able to measure succinyl-CoA or other citric acid cycle intermediates in brain homogenates, but we assume that propionyl-CoA has served to replenish citric acid cycle intermediates via formation of succinyl-CoA (Owen, et al., 2002). Apart from its anaplerotic role, succinyl-CoA is required for the activation of 3OHB to acetyl-CoA (Fig. 1). Thus a greater efficiency of 3OHB oxidation in the presence of propionate could explain the superior therapeutic effect of this combined treatment. Other compartment-specific metabolic effects of propionate on various pathways may have gone unnoticed in this analysis, since they would not necessarily change metabolite concentrations in tissue homogenates.

During untreated hypoglycemic coma we found an increase of long chain acyl-carnitines, especially palmitoyl-carnitine (C16), in brain homogenates. As the brain does not have triglyceride reserves, changes probably reflect a release of free fatty acids from membrane bound phospholipids via phospholipase activation (Agardh, et al., 1981, Strosznajder, 1984). Palmitoyl-carnitine has been ascribed a pathogenetic role in apoptosis induction (Mutomba, et al., 2000, Phillis and O'Regan, 2004). After treatment with 3OHB alone or in combination with propionate, long chain acyl-carnitines were further increased, suggesting that free fatty acid release was not reduced by either treatment. Phospholipase inhibitors could be a useful neuroprotective adjunct to 3OHB treatment (Farooqui, et al., 2006).

Taking all these results together, we could prove the hypothesis that additional supplementation of propionate improves the therapeutic effect of 3OHB treatment during hypoglycemic coma. The superior clinical effect of combined treatment occurred although additional propionate could not correct most of the biochemical changes associated with hypoglycemic coma over and above the corrections achieved by 3OHB alone. Further studies are needed to explore the exact mechanism of the effect of 3OHB and propionate on a cellular and subcellular level.

5. Conclusions and Future Work

5.1 Summary of results

Our research was aimed at exploring the protective potential of 3OHB treatment during hypoglycemia for the developing brain in a novel PND 13 rat model. Our results can be summarized as follows:

1. **Untreated** and sustained hypoglycemia in 13 day old rats resulted in progressive loss of alertness and coma, followed somewhat later by EEG suppression (burst-suppression coma; chapter 3). Burst suppression coma had the following characteristics:
    a. After glucose resuscitation at the time of burst suppression coma, the mortality rate was low (< 20 %; chapter 3).
    b. One day after glucose resuscitation, there were no signs of grey or white matter injury (chapter 3).
    c. Biochemically, burst suppression coma had the following characteristics (chapter 4):
        i. Glucose-6-phosphate was drastically reduced, indicating that endogenous glycogen is used up at this point.
        ii. Glycolytic intermediates and intermediates of the oxidative PPP were depleted, indicating reduced glycolytic activity.
        iii. Cerebral glutamate concentrations were decreased, aspartate and ammonia were increased, indicating that de- and transamination reactions took place to extract oxidative substrates from amino acids (truncated citric acid cycle).
        iv. Long chain acyl-carnitines were increased.
2. **Continuous treatment with 3OHB** during hypoglycemia resulted in increased latency to the onset of clinical coma and of burst suppression coma (chapter 4). Burst suppression coma in treated animals differed from untreated animals:
    a. After glucose resuscitation at the time of burst suppression coma, the mortality rate was 100%.
    b. After glucose resuscitation at the time of burst suppression coma, selective cellular white matter injury (predominantly oligodendroglial apoptosis) was present, its density depended on the total time of hypoglycemia; no signs of neuronal injury were apparent

   c. The preservation of EEG continuity was more pronounced than preservation of clinical alertness during the progression to coma.

3. **Single dose treatment with 3OHB** at the time of burst suppression coma reversed EEG suppression but had no effect on clinical coma (chapter 4); this is consistent with findings from continuous 3OHB treatment where 3OHB had shown greater capacity to preserve EEG continuity than clinical alertness. Single dose treatment showed the following characteristics:
   a. EEG reversion coincided with a period of elevated 3OHB plasma levels.
   b. Biochemically, 3OHB treatment at the time of burst suppression coma
      i. corrected changes in glutamate, aspartate and ammonia levels, indicating that glutamate is no longer oxidatively metabolized, a certain relief of energy stress, and a possible reconversion of aspartate to glutamate (chapter 4).
      ii. had no effect on intermediates of glycolysis and the oxidative pentose phosphate pathway, indicating glycolytic depression in treated animals.
      iii. did not decrease elevated long chain acyl-carnitines.
4. **Single dose treatment with 3OHB <u>and</u> propionate** at the time of burst suppression coma reversed clinical coma and EEG suppression (chapter 4). This effect had the following characteristics:
   a. EEG reversion showed the same course as after treatment with 3OHB alone, reversion of clinical coma started about 30 minutes after EEG reversion.
   b. Cerebral propionyl-carnitine levels were elevated at the time of clinical alertness, indicating active cerebral metabolism of propionate.
   c. 3OHB and propionate treatment at the time of burst suppression coma were not associated with biochemical corrections over and above those observed with 3OHB alone for the metabolites analyzed (amino acids, glycolysis, PPP, acyl-carnitines), suggesting that the mechanism underlying improved alertness may involve provision of citric acid cycle intermediates, enhanced ketolysis, or may be compartmental.
   d. Propionate treatment alone at the time of burst suppression coma had no effect on alertness or EEG suppression.

5.2 Conclusion 1: Limitations of 3OHB treatment

3OHB treatment prolonged the latency to the onset of clinical and burst suppression coma. There were several indications that the comatose state during 3OHB treated hypoglycemia differs in some way from untreated hypoglycemia: (1) the relationship between alertness state and EEG suppression ratio

differed (chapter 3), (2) coma after 3OHB treatment was associated with much higher mortality (chapter 3), (3) 3OHB given at burst suppression coma to untreated pups caused EEG normalisation, whereas prolonged 3OHB treatment eventually resulted in EEG suppression (chapters 3 and 4). Morphological data were compatible with a partial protective effect of 3OHB treatment on cell survival. Neuronal injury was not apparent after untreated hypoglycemia, and it was also not apparent after 3OHB treated, prolonged hypoglycemia. White matter injury, in contrast, was apparent after prolonged 3OHB treated hypoglycemia (chapter 3), suggesting that hypoglycemic grey and white matter injury are prevented to a differing extent by 3OHB treatment. Thus 3OHB treatment that elevated 3OHB plasma concentrations to a high physiological range had a limited capacity to sustain brain function during prolonged hypoglycemia in infant rats. Infant rats have a high capacity of cerebral ketone utilization. This suggests limiting biochemical factors rather than insufficient transport or enzymatic machinery.

These biochemical limitations could be related to difference between 3OHB and glucose as a metabolic substrate. Both substances are a source of the oxidative substrate acetyl-CoA. Glucose is in addition a substrate for glycolysis with associated fluxes through the pentose phosphate pathway and an anaplerotic pathway via pyruvate carboxylase. 3OHB cannot feed into any of these pathways. Our biochemical results showed that 3OHB treatment at the time of hypoglycemic burst suppression coma indeed cannot correct depleted intermediates of glycolysis or the pentose phosphate pathway (chapter 4), suggesting that during 3OHB treated hypoglycemia a glycolytic deficit evolves in the brain. Thus the pathobiochemical basis of untreated (hypoketotic) hypoglycemia is a deficit of glycolysis *and* oxidative energy production, whereas the pathobiochemical basis of 3OHB treated, hyperketotic hypoglycemia could be a primarily glycolytic deficit. The biochemical effect of a sustained glycolytic deficit probably includes insufficient anaplerosis and pentose phosphate pathway activity causing an imbalance of citric acid cycle intermediates and the intracellular redox equilibrium and redox defences. Thus, the pathobiochemistry underlying hypoketotic hypoglycemic coma may differ from that of highly ketotic hypoglycemic coma, which may explain the clinical, electroencephalographic and neuropathological findings.

The effect of a predominantly glycolytic deficit may be compartment specific. Glucose deprivation causes both a failure of gray and white matter function (Arakawa, et al., 1991, Brown, et al., 2001, Fern, et al., 1998, Izumi, et al., 1998, Wada, et al., 1997). 3OHB has a better capacity to keep up activity in grey matter compared to white matter *in vitro* (Arakawa, et al., 1991, Brown, et al., 2001, Izumi, et al., 1998, Wada, et al., 1997). In our experiments, 3OHB treatment alone resulted in an isolated reversal of EEG suppression without correlate in the alertness state of the animals. EEG activity reflects the intensity of neurotransmission in local areas of cortical grey matter, whereas clinical alertness reflects a complex CNS function integrating grey matter activity with white matter signal conduction. If the capacity to utilize 3OHB as alternative fuel is greater in grey matter compared to white matter, this could

explain the observed discrepancy between electroencephalographic and clinical improvement. The relative contribution of functional failure in grey matter and white matter in untreated and 3OHB treated hypoglycemic coma is unknown and could differ. However, current data do not allow conclusions in this regard. White matter injury after 3OHB treated hypoglycemia may suggest greater disturbances in white matter than in grey.

Hypothetical biochemical basis of ketotic hypoglycemic coma in infant rats

Our results indicate that during ketotic hypoglycemia in infant rats, glycolytic flux in the brain is depressed while oxidative energy substrates are being supplied. In the initial phase of hypoglycemia, cerebral glycogen stores are utilised to maintain glycolysis. In the presence of both 3OHB and glucose or glycosyl-units, 3OHB tends to reduce glucose consumption in the brain as it represents an alternative source for acetyl-CoA. Regulation is based on the inhibition of glycolysis and pyruvate dehydrogenation by increased acetyl-CoA availability (Randle cycle) (Hue and Taegtmeyer, 2009, Itoh and Quastel, 1970, LaManna, et al., 2009, Roeder, et al., 1984a, Roeder, et al., 1984b). Therefore, glycogen would be used at a slower rate during ketotic compared to hypoketotic hypoglycemia (glycogen sparing), prolonging the latency to coma. Once glycogen stores are depleted, glycolytic depression sets in and may cause disturbances in grey and white matter function culminating in a comatose state and white matter injury. In addition, anaplerotic failure may reduce citric acid cycle activity and ketolysis. This hypothesis ascribes a central role to glycolytic failure in the pathogenesis of 3OHB treated hypoglycemic failure. Whether this pathobiochemical derangement triggers cell death in the same way as hypoketotic hypoglycemic coma is presently unknown. These considerations presuppose a high physiologic capacity for cerebral ketone utilization.

5.2.1 Implications for treatment

The limited biochemical and clinical effectiveness of 3OHB therapy suggested that combination treatment with a complementary metabolic substrate may improve the capacity to sustain global brain function and prevent pathometabolic changes. Propionate is effective in this and chapter 4 represents a proof of concept for such an approach. Although we could not identify a mechanism for propionate's effectiveness, an increase in cerebral succinyl-CoA is a likely mediator. Increased succinyl-CoA may have enhanced ketolysis and may have helped to balance concentrations of citric acid cycle intermediates. The role of compartment specific effects in this remains unclear.

A combination of 3OHB with gluconeogenetic substrates like lactate, alternative carbohydrates like mannose or glycerol, or anaplerotically active C5 ketone bodies should be evaluated as combined therapy. The advantage of 3OHB as alternative substrate is essentially its energy density (ketolysis yields

2 acetyl-CoA) and its MCT-1 based transport into the brain. Lactate, on the other hand, yields less oxidative energy but can feed into gluconeogenesis and may support anaplerosis and pentose phosphate pathway activity to some extent. It is also transported by MCT-1 and is a physiological substrate for the brain during development (Dombrowski, et al., 1989, Fernandez and Medina, 1986, Medina, 1985, Medina and Tabernero, 2005, Tabernero, et al., 1996, Vicario and Medina, 1992). Lactate has also been reported as an alternative energy substrate for brain metabolism in a patient with glucose-6-phosphatase deficiency (Fernandes, et al., 1984). Mannose (Alton, et al., 1997, Ghosh, et al., 1972, Sloviter and Kamimoto, 1970) and glycerol (Sloviter, et al., 1966, Sloviter and Suhara, 1967) are reported to be metabolized in brain, but the cerebral capacity for glycerol or mannose utilization is unknown. C5 ketone bodies feed into the propionate pathway and yield one acetyl-CoA in addition to succinyl-CoA. Their cerebral utilization with beneficial effects has been shown in a patient with pyruvate carboxylase deficiency (Brunengraber and Roe, 2006, Mochel, et al., 2005). The effectiveness of combinations of these theoretically complementary substrates needs to be determined empirically.

5.2.2 Future research

The effect of additional propionate treatment requires further confirmation with larger animal numbers. The effectiveness of additional propionate during continuous 3OHB supplementation is unclear at present. For future studies of this effect a dosage regime needs to be established bearing in mind that propionate can have toxic side effects. To further characterize the mechanism involved, measurement of a broader range of metabolites, including high energy phosphates, citric acid intermediates and CoA-esters, is a first step. Further evaluations might include *in vitro* studies with labelled isotopes and flux measurements. The capacity of alternative substrates and their combinations to support function in white matter and grey matter may differ. It would be a challenging further project to investigate in vitro systems for both anatomic compartments in this regard.

A second aspect deserving further study is the exploration of other alternative substrate combinations, including 3OHB combined with lactate, mannose, or glycerol. Apart from a detailed characterization of effects of continuous or single dose treatment, the characterization of cerebral pathometabolism with these treatments should be diversified. A targeted metabolomic approach could be developed that could include characterization of glycolysis, citric acid cycle intermediates, pentose phosphate pathway, redox defences, amino acid metabolism, acetyl-CoA esters, high energy phosphates, and fatty acid metabolism.

5.3 Conclusion 2: Hypoglycemic white matter injury

The finding of white matter injury (chapter 3) is significant in the context of hypoglycemic white matter injury found in human infants. It is the first description of white matter injury in an *in vivo* model of hypoglycemia.

5.3.1 The spectrum of brain injury caused by hypoglycemia in humans

Evidence of neuropathological changes after hypoglycemia in infancy was scarce until recent advances in diffusion weighted MR imaging made more systematic investigations possible. Initial studies of neonatal brain injury after hypoglycemia suggested an injury pattern of cortical grey matter and subcortical white matter changes predominantly in parietal and occipital regions (Barkovich, et al., 1998). More recent studies showed that brain injury after neonatal hypoglycemia is more variable with around 94% of patients showing white matter abnormalities and 51% of patients grey matter abnormalities (Burns, et al., 2008). White matter injury includes signs of focal punctate lesions, hemorrhagic areas, and more widespread signs of infarction globally across the brain, with either posterior predominance or in periventricular localization. Cortical findings include cortical highlighting and loss of cortical markings. Other changes include abnormalities of the internal capsule or the basal ganglia. In adult brain, hypoglycemic injury of white matter has also been found upon MRI imaging (Aoki, et al., 2004, Kim, et al., 2007, Kim and Koh, 2007). In contrast to infants, the distribution between white and grey matter injury after hypoglycemia in adults appears to be equal with about 70% of patients showing signs of white matter injury and 70% showing signs of grey matter injury (Ma, et al., 2009).

The cellular correlate of irreversible grey matter injury is generally neuronal death, especially in cortex, hippocampus and basal ganglia. These findings are consistent in rat, piglet, and infant mouse models of insulin induced hypoglycemia as well as in adult and paediatric autopsy cases (Anderson, et al., 1967, Mori, et al., 2006). The cellular correlate of white matter injury, by contrast, is little understood. A single published autopsy case suggests loss of axons and myelin. This was described in a patient after hypoglycemia and prolonged persistence in a vegetative state. The diffusion weighted MRI showed hyperintense white matter signals in this patient (Mori, et al., 2006). Axonal injury is also suggested by Abeta-PP positive staining of axons from adult white matter after hypoglycemia (Dolinak, et al., 2000). In vitro studies show that oligodendrocytes are susceptible to hypoglycemic cell death (Yan and Rivkees, 2006, Zuppinger, et al., 1981). So white matter changes could be caused by axonal and/or oligodendroglial degeneration. Apparently vascular mechanisms of hypoglycemic injury including haemorrhage and infarction (Burns, et al., 2008, Mori, et al., 2006) are not well understood, but pathogenetic mechanisms could include hemodynamic effects of systemic hypoglycemia.

A possible correlation between MRI imaging data and neurological sequelae cannot be ascertained at present because of insufficient data. However, it appears that the degree of white matter injury in infants and involvement of the internal capsule are both associated with adverse long term consequences (Burns, et al., 2008). There is, however, no known relationship between duration and severity of hypoglycemia and MRI signal abnormalities. In adults, diffuse or extensive MRI signal abnormalities are associated with adverse outcome (Ma, et al., 2009).

5.3.2 Insights from this investigation

We found apoptosis of oligodendrocytes and possibly another cell population in white matter (corpus callosum, cingulum, external capsule) after prolonged ketotic hypoglycemia (chapter 3). Given the scarce pathologic evidence from humans it is not possible to say whether this injury corresponds pathologically to the injury observed upon MRI imaging in human infants. Any extrapolations of these findings to hypoglycemic injury in humans must therefore remain tentative.

White matter injury but not grey matter injury was apparent after prolonged ketotic hypoglycemia. This suggests that white matter injury and grey matter injury have different determinants and different pathogenetic pathways. 3OHB treatment may well have protected neurons from injury during the long phase of hypoglycemia, but it did not prevent white matter injury. Protective strategies should prevent both types of injury but will probably differ depending on the respective pathogenesis. Although animals did not survive after prolonged hypoglycemia and thus no studies of functional consequences of white matter injury is yet possible, our findings may contribute towards developing an in vivo model of hypoglycemic white matter injury for the analysis of its pathogenesis and protective strategies.

Hypothetical considerations suggest that oxidative injury may be a major factor contributing to oligodendroglial apoptosis after hypoglycemia. This is based on the susceptibility of oligodendrocytes to this type of injury in other disease models (Juurlink, 1997, McTigue and Tripathi, 2008, Todorich, et al., 2008) and the observation that the pentose phosphate pathway is depressed during ketotic hypoglycemia (chapter 4) and that therefore oxidative defences could be undermined. Anti-oxidative therapy or metabolic support for the pentose phosphate pathway may therefore be a promising future protective strategy against hypoglycemic white matter injury.

5.3.3 Future research

Results on white matter injury need to be replicated with a larger number of animals and a standardized experimental endpoint. A strategy to reduce mortality after 3OHB treated hypoglycemia needs to be sought for further investigations. It may be possible to resuscitate animals after 3.5 hrs of ketotic hypoglycemia, for instance, with improved survival and white matter injury. Once a standardized model of wm matter injury is available, systematic investigation of pathogenesis and protective strategies

can be conducted. In particular the dynamics of white matter injury and oligodendroglial apoptosis after hypoglycemia (including potential regenerative capacity), possible long term functional consequences, and the role of a reduced activity of the pentose phosphate pathway, and a possible synergistic effect of 3OHB availability, are important topics. For investigation of pathogenetic mechanisms a cell culture model of ketotic hypoglycemic oligodendrocyte injury would be useful.

For better comparison to human studies and as in vivo parameter of wm injury an MRI imaging including tensor diffusion imaging could yield valuable information, including development of injury during hypoglycemia. Protection studies should be carried out with this outcome parameter.

5.4 Conclusion 3: Hypoglycemic grey matter injury in developing rats

Hypoglycemic coma and EEG burst-suppression with subsequent glucose-resuscitation did not cause neuronal injury in PND 13 rats (chapter 3). The latency to burst suppression coma was prolonged in 3OHB treated animals by about 1.5 hrs. After prolonged hyperketotic hypoglycemia and resuscitation at a similar stage of the hypoglycemic encephalopathy as in untreated animals, there was neither any evidence for neuronal injury. This may suggest a protective effect during prolonged hypoglycemia. However, a direct investigation of a neuron-protective effect of 3OHB was not possible in this study because of the absence of neuronal injury.

Explanations of the absence of neuronal injury include the following: (a) the extent of neuronal death is too small to reach statistical significance with 5 animals per group, (b) the duration of EEG suppression was insufficient for injury to develop, (c) the ketogenic state of rat pups confers constitutively increased resistance to neuronal injury (discussion chapter 3), and (d) mildly elevated 3OHB plasma levels during hypoglycemia protect from neuronal injury (chapter 2.9). One experimental strategy to investigate these factors might be to create a setting for a prolonged period of EEG suppression in this model. This would require the use of a respirator because of imminent respiratory failure at the time of burst suppression coma. A respirator requires anaesthesia of the pups with potential effects of some anaesthetics on glucose metabolism (e.g. isoflurane causes increased plasma glucose levels, see method development). Such a strategy would therefore be technically challenging and of uncertain outcome. Alternatively, one could use nutritional manipulation of rat pups to alter the ketogenic state, reduce plasma ketone levels, and investigate the relationship between nutritional state, susceptibility to neuronal injury after hypoglycemia, and cerebral protein expression.

5.4.1 Future research

A ketogenic state is known to be neuroprotective in models of excitotoxic and hypoxic-ischemic brain injury (Bough and Rho, 2007, Puchowicz, et al., 2008, Sullivan, et al., 2003, Sullivan, et al., 2004).

Neuronal death during hypoglycemia is also partly mediated by excitotoxic mechanisms. Therefore, the role of the ketogenic state in determining the susceptibility to hypoglycemic neuronal injury of physiologically ketogenic rat pups is of particular interest. The ketogenic state modulates cerebral protein expression. The expression of anti-apoptotic proteins (Puchowicz, et al., 2008), the expression of uncoupling proteins and mitochondrial biogenesis are increased on a ketogenic diet (Sullivan, et al., 2004). These effects could result in an increased neuronal resistance to hypoglycemic cell death. Moreover, the mechanisms underlying these effects might be harnessed pharmacologically by targeted protein induction as the basis of a neuroprotective therapy in patients at risk of recurrent hypoglycemia.

Mechanisms to induce protein expression could involve direct effects of elevated concentrations of fatty acids in plasma, in particular of polyunsaturated fatty acids (Puchowicz, et al., 2008, Sampath and Ntambi, 2004). The effects of polyunsaturated fatty acids on gene expression have been more extensively analysed in liver, but effects on the brain might be interesting in this context. Nutritional manipulation of the ketogenic state of rat pups could provide an opportunity to map changes in protein expression in the brain together with susceptibility to hypoglycemic injury. Such a project could involve proteomic analysis of cerebral protein expression combined with a technique for artificially rearing rat pups (Auestad, et al., 1989, Hall, 1975, Vadlamudi, et al., 1995), so that the fat and carbohydrate content of their diet can be adjusted and non-ketogenic pups could be compared to ketogenic pups.

If a link between ketogenic diet, protein expression and protection from neuronal injury is found, this could be a basis for the pharmacological manipulation of cerebral protein expression and associated resistance to neuronal injury. For instance, PPAR agonists could serve to induce uncoupling proteins (Andrews, et al., 2005, Bordet, et al., 2006).

5.5 Conclusion 4: The role of cerebral glycolysis and glycolytic depression during hypoglycemia

Our results are compatible with a role for the depression of glycolysis in the pathobiochemistry of ketotic hypoglycemic coma (Conclusion 1). Glycolysis and its associated metabolic functions in the brain has recently received attention in other research fields. Inhibition of glycolysis with 2-deoxy-D-glucose or fructose-1,6-diphosphate increases seizure thresholds in some models of epilepsy (Ding, et al., Lian, et al., 2008, Stafstrom, et al., 2008). Inborn errors of the pentose phosphate pathway were recently described. Ribose 5 phosphate isomerase deficiency, for instance, causes leukencephalopathy as part of its phenotype (Wamelink, et al., 2008). Anaplerotic therapy with C5 ketone bodies in a clinical case study of a patient with pyruvate carboxylase deficiency led to an improved myelination status (Mochel, et al., 2005). Although these observations are diverse and are drawn from various fields, they highlight an increasing awareness that the metabolic role of cerebral glycolysis is complex and requires further

study. 3OHB treated hypoglycemia may provide an experimental setting for the study of glycolytic depression while oxidative metabolism remains active. Further biochemical studies of the hypoglycemic brain after continued 3OHB treatment are required for confirmation.

5.6 Conclusion 5: Other metabolic diseases

Our data on the limitation of 3OHB as substrate alternative for glucose in the brain have potential implications for the treatment of patients with cerebral glucose transporter deficiency (GLUT1-Deficiency). Glut-1 deficiency is a monogenic disease which results in chronic cerebral glucose deprivation despite systemic euglycemia because of a transporter insufficiency. It manifests with intractable seizures, developmental delay, and ataxia (Wang, et al., 2005). It is currently treated with a ketogenic diet, which controls seizures. Developmental delay, however, is not completely avoided with this treatment. The rationale for the ketogenic diet is to improve the energy deficit resulting from cerebral glucose deficiency by an increased availability of ketone bodies. The limitations of 3OHB to fully substitute for glucose as cerebral substrate we found in this project (glycolytic deficit associated with possibly anaplerotic and redox deficits) suggest that additional supplementation of these patients with alternative substrates supporting anaplerosis and/or glycolysis may be beneficial. Lactate or C5 ketone bodies are transported across the blood brain barrier by the MCT-1 transporter, as is 3OHB, and may be a useful adjunct. To test this hypothesis experiments, with a knock out mouse model of Glut-1 deficiency (Wang, et al., 2006) could be helpful.

Bibliography

Agardh, C. D., Chapman, A. G., Nilsson, B., and Siesjo, B. K., 1981. Endogenous substrates utilized by rat brain in severe insulin-induced hypoglycemia. J Neurochem 36**,** 490-500.

Akrawi, W. P., Drummond, J. C., Kalkman, C. J., and Patel, P. M., 1996. A comparison of the electrophysiologic characteristics of EEG burst-suppression as produced by isoflurane, thiopental, etomidate, and propofol. J Neurosurg Anesthesiol 8**,** 40-46.

Alton, G., Kjaergaard, S., Etchison, J. R., Skovby, F., and Freeze, H. H., 1997. Oral ingestion of mannose elevates blood mannose levels: a first step toward a potential therapy for carbohydrate-deficient glycoprotein syndrome type I. Biochem Mol Med 60**,** 127-133.

Anderson, J. M., Milner, R. D., and Strich, S. J., 1967. Effects of neonatal hypoglycaemia on the nervous system: a pathological study. J Neurol Neurosurg Psychiatry 30**,** 295-310.

Andrews, Z. B., Diano, S., and Horvath, T. L., 2005. Mitochondrial uncoupling proteins in the CNS: in support of function and survival. Nat Rev Neurosci 6**,** 829-840.

Aoki, T., Sato, T., Hasegawa, K., Ishizaki, R., and Saiki, M., 2004. Reversible hyperintensity lesion on diffusion-weighted MRI in hypoglycemic coma. Neurology 63**,** 392-393.

Arakawa, T., Goto, T., and Okada, Y., 1991. Effect of ketone body (D-3-hydroxybutyrate) on neural activity and energy metabolism in hippocampal slices of the adult guinea pig. Neurosci Lett 130**,** 53-56.

Arias, G., Asins, G., Hegardt, F. G., and Serra, D., 1997. The effect of fasting/refeeding and insulin treatment on the expression of the regulatory genes of ketogenesis in intestine and liver of suckling rats. Arch Biochem Biophys 340**,** 287-298.

Auer, R. N., Olsson, Y., and Siesjo, B. K., 1984a. Hypoglycemic brain injury in the rat. Correlation of density of brain damage with the EEG isoelectric time: a quantitative study. Diabetes 33**,** 1090-1098.

Auer, R. N., and Siesjo, B. K., 1993. Hypoglycaemia: brain neurochemistry and neuropathology. Baillieres Clin Endocrinol Metab 7**,** 611-625.

Auer, R. N., Wieloch, T., Olsson, Y., and Siesjo, B. K., 1984b. The distribution of hypoglycemic brain damage. Acta Neuropathol (Berl) 64**,** 177-191.

Auestad, N., Korsak, R. A., Bergstrom, J. D., and Edmond, J., 1989. Milk-substitutes comparable to rat's milk; their preparation, composition and impact on development and metabolism in the artificially reared rat. Br J Nutr 61**,** 495-518.

Back, S. A., Han, B. H., Luo, N. L., Chricton, C. A., Xanthoudakis, S., Tam, J., Arvin, K. L., and Holtzman, D. M., 2002. Selective vulnerability of late oligodendrocyte progenitors to hypoxia-ischemia. J Neurosci 22**,** 455-463.

Back, S. A., Luo, N. L., Borenstein, N. S., Levine, J. M., Volpe, J. J., and Kinney, H. C., 2001. Late oligodendrocyte progenitors coincide with the developmental window of vulnerability for human perinatal white matter injury. J Neurosci 21**,** 1302-1312.

Ballesteros, J. R., Mishra, O. P., and McGowan, J. E., 2003. Alterations in cerebral mitochondria during acute hypoglycemia. Biol Neonate 84**,** 159-163.

Banhegyi, G., Mandl, J., and Csala, M., 2008. Redox-based endoplasmic reticulum dysfunction in neurological diseases. J Neurochem 107**,** 20-34.

Barkovich, A. J., Ali, F. A., Rowley, H. A., and Bass, N., 1998. Imaging patterns of neonatal hypoglycemia. Am J Neuroradiol 19**,** 523-528.

Bartnik, B. L., Hovda, D. A., and Lee, P. W., 2007. Glucose metabolism after traumatic brain injury: estimation of pyruvate carboxylase and pyruvate dehydrogenase flux by mass isotopomer analysis. J Neurotrauma 24**,** 181-194.

Behar, K. L., den Hollander, J. A., Petroff, O. A., Hetherington, H. P., Prichard, J. W., and Shulman, R. G., 1985. Effect of hypoglycemic encephalopathy upon amino acids, high-energy phosphates, and pHi in the rat brain in vivo: detection by sequential 1H and 31P NMR spectroscopy. J Neurochem 44**,** 1045-1055.

Bellin, M. F., Jakobsen, J. A., Tomassin, I., Thomsen, H. S., Morcos, S. K., Almen, T., Aspelin, P., Clauss, W., Flaten, H., Grenier, N., Idee, J. M., Krestin, G. P., Stacul, F., and Webb, J. A., 2002. Contrast medium extravasation injury: guidelines for prevention and management. Eur Radiol 12**,** 2807-2812.

Bengtsson, G., Gentz, J., Hakkarainen, J., Hellstrom, R., and Persson, B., 1969. Plasma levels of FFA, glycerol, beta-hydroxybutyrate and blood glucose during the postnatal development of the pig. J Nutr 97**,** 311-315.

Beskow, A. P., Fernandes, C. G., Leipnitz, G., da Silva Lde, B., Seminotti, B., Amaral, A. U., Wyse, A. T., Wannmacher, C. M., Vargas, C. R., Dutra-Filho, C. S., and Wajner, M., 2008. Influence of ketone bodies on oxidative stress parameters in brain of developing rats in vitro. Metab Brain Dis 23**,** 411-425.

Bhat, R. V., Axt, K. J., Fosnaugh, J. S., Smith, K. J., Johnson, K. A., Hill, D. E., Kinzler, K. W., and Baraban, J. M., 1996. Expression of the APC tumor suppressor protein in oligodendroglia. Glia 17**,** 169-174.

Bonnefont, J. P., Specola, N. B., Vassault, A., Lombes, A., Ogier, H., de Klerk, J. B., Munnich, A., Coude, M., Paturneau-Jouas, M., and Saudubray, J. M., 1990. The fasting test in paediatrics: application to the diagnosis of pathological hypo- and hyperketotic states. Eur J Pediatr 150**,** 80-85.

Bordet, R., Ouk, T., Petrault, O., Gele, P., Gautier, S., Laprais, M., Deplanque, D., Duriez, P., Staels, B., Fruchart, J. C., and Bastide, M., 2006. PPAR: a new pharmacological target for neuroprotection in stroke and neurodegenerative diseases. Biochem Soc Trans 34**,** 1341-1346.

Bough, K. J., and Rho, J. M., 2007. Anticonvulsant mechanisms of the ketogenic diet. Epilepsia 48**,** 43-58.

Brandorff, N. P., 1980. The effect of dietary fat on the fatty acid composition of lipids secreted in rats' milk. Lipids 15**,** 276-278.

Brown, A. M., and Ransom, B. R., 2007. Astrocyte glycogen and brain energy metabolism. Glia 55**,** 1263-1271.

Brown, A. M., Wender, R., and Ransom, B. R., 2001. Metabolic substrates other than glucose support axon function in central white matter. J Neurosci Res 66**,** 839-843.

Brunengraber, H., and Roe, C. R., 2006. Anaplerotic molecules: Current and future. J Inherit Metab Dis 29**,** 327-331.

Burns, C. M., Rutherford, M. A., Boardman, J. P., and Cowan, F. M., 2008. Patterns of cerebral injury and neurodevelopmental outcomes after symptomatic neonatal hypoglycemia. Pediatrics 122**,** 65-74.

Byrne, H. A., Tieszen, K. L., Hollis, S., Dornan, T. L., and New, J. P., 2000. Evaluation of an electrochemical sensor for measuring blood ketones. Diabetes Care 23**,** 500-503.

Carli, F., Ronzoni, G., Webster, J., Khan, K., and Elia, M., 1993. The independent metabolic effects of halothane and isoflurane anaesthesia. Acta Anaesthesiol Scand 37**,** 672-678.

Choi, I. Y., Seaquist, E. R., and Gruetter, R., 2003. Effect of hypoglycemia on brain glycogen metabolism in vivo. J Neurosci Res 72**,** 25-32.

Clancy, R. R., Bergqvist, A. G. C., and Dlugos, D. J., 2003. Neonatal Electroencephalography. In: Ebersole, J. S., and Pedley, T. A., (Eds.), Current practice of clinical electroencephalography. Lippincott Williams and Wilkins, Philadelphia, pp. 160-134.

Conklin, P., and Heggeness, F. W., 1971. Maturation of temperature homeostasis in the rat. Am J Physiol 220**,** 333-336.

Cooper, A. J., and Plum, F., 1987. Biochemistry and physiology of brain ammonia. Physiol Rev 67**,** 440-519.

Craig, A., Ling Luo, N., Beardsley, D. J., Wingate-Pearse, N., Walker, D. W., Hohimer, A. R., and Back, S. A., 2003. Quantitative analysis of perinatal rodent oligodendrocyte lineage progression and its correlation with human. Exp Neurol 181**,** 231-240.

Cremer, J. E., 1982. Substrate utilization and brain development. J Cereb Blood Flow Metab 2**,** 394-407.

Cremer, J. E., and Heath, D. F., 1974. The estimation of rates of utilization of glucose and ketone bodies in the brain of the suckling rat using compartmental analysis of isotopic data. Biochem J 142**,** 527-544.

Dahlquist, G., and Persson, B., 1976. The rate of cerebral utilization of glucose, ketone bodies, and oxygen: a comparative in vivo study of infant and adult rats. Pediatr Res 10**,** 910-917.

de Graaf, R. A., Mason, G. F., Patel, A. B., Rothman, D. L., and Behar, K. L., 2004. Regional glucose metabolism and glutamatergic neurotransmission in rat brain in vivo. Proc Natl Acad Sci U S A 101**,** 12700-12705.

Dell, C. A., Likhodii, S. S., Musa, K., Ryan, M. A., Burnham, W. M., and Cunnane, S. C., 2001. Lipid and fatty acid profiles in rats consuming different high-fat ketogenic diets. Lipids 36**,** 373-378.

Dhalla, A. K., Santikul, M., Smith, M., Wong, M. Y., Shryock, J. C., and Belardinelli, L., 2007. Antilipolytic activity of a novel partial A1 adenosine receptor agonist devoid of cardiovascular effects: comparison with nicotinic acid. J Pharmacol Exp Ther 321**,** 327-333.

Diltoer, M., and Camu, F., 1988. Glucose homeostasis and insulin secretion during isoflurane anesthesia in humans. Anesthesiology 68**,** 880-886.

Ding, L., Liang, X., Zhu, D., and Lou, Y., 2007. Peroxisome proliferator-activated receptor alpha is involved in cardiomyocyte differentiation of murine embryonic stem cells in vitro. Cell Biol Int.

Ding, Y., Wang, S., Zhang, M. M., Guo, Y., Yang, Y., Weng, S. Q., Wu, J. M., Qiu, X., and Ding, M. P., Fructose-1,6-diphosphate inhibits seizure acquisition in fast hippocampal kindling. Neurosci Lett 477**,** 33-36.

Dolinak, D., Smith, C., and Graham, D. I., 2000. Hypoglycaemia is a cause of axonal injury. Neuropathol Appl Neurobiol 26**,** 448-453.

Dombrowski, G. J., Jr., Swiatek, K. R., and Chao, K. L., 1989. Lactate, 3-hydroxybutyrate, and glucose as substrates for the early postnatal rat brain. Neurochem Res 14**,** 667-675.

Edmond, J., Robbins, R. A., Bergstrom, J. D., Cole, R. A., and de Vellis, J., 1987. Capacity for substrate utilization in oxidative metabolism by neurons, astrocytes, and oligodendrocytes from developing brain in primary culture. J Neurosci Res 18**,** 551-561.

Elam, E. A., Dorr, R. T., Lagel, K. E., and Pond, G. D., 1991. Cutaneous ulceration due to contrast extravasation. Experimental assessment of injury and potential antidotes. Invest Radiol 26**,** 13-16.

Erecinska, M., Cherian, S., and Silver, I. A., 2004. Energy metabolism in mammalian brain during development. Prog Neurobiol 73**,** 397-445.

Farooqui, A. A., Ong, W. Y., and Horrocks, L. A., 2006. Inhibitors of brain phospholipase A2 activity: their neuropharmacological effects and therapeutic importance for the treatment of neurologic disorders. Pharmacol Rev 58**,** 591-620.

Fern, R., Davis, P., Waxman, S. G., and Ransom, B. R., 1998. Axon conduction and survival in CNS white matter during energy deprivation: a developmental study. J Neurophysiol 79**,** 95-105.

Fernandes, J., Berger, R., and Smit, G. P., 1984. Lactate as a cerebral metabolic fuel for glucose-6-phosphatase deficient children. Pediatr Res 18**,** 335-339.

Fernandez, E., and Medina, J. M., 1986. Lactate utilization by the neonatal rat brain in vitro. Competition with glucose and 3-hydroxybutyrate. Biochem J 234**,** 489-492.

Fernando-Warnakulasuriya, G. J., Staggers, J. E., Frost, S. C., and Wells, M. A., 1981. Studies on fat digestion, absorption, and transport in the suckling rat. I. Fatty acid composition and concentrations of major lipid components. J Lipid Res 22**,** 668-674.

Ferrand-Drake, M., Zhu, C., Gido, G., Hansen, A. J., Karlsson, J. O., Bahr, B. A., Zamzami, N., Kroemer, G., Chan, P. H., Wieloch, T., and Blomgren, K., 2003. Cyclosporin A prevents calpain

activation despite increased intracellular calcium concentrations, as well as translocation of apoptosis-inducing factor, cytochrome c and caspase-3 activation in neurons exposed to transient hypoglycemia. J Neurochem 85**,** 1431-1442.

Ferre, P., Pegorier, J. P., Williamson, D. H., and Girard, J. R., 1978. The development of ketogenesis at birth in the rat. Biochem J 176**,** 759-765.

Follett, P. L., Rosenberg, P. A., Volpe, J. J., and Jensen, F. E., 2000. NBQX attenuates excitotoxic injury in developing white matter. J Neurosci 20**,** 9235-9241.

Frank, M. G., and Heller, H. C., 1997. Development of REM and slow wave sleep in the rat. Am J Physiol 272**,** R1792-1799.

Friberg, H., Ferrand-Drake, M., Bengtsson, F., Halestrap, A. P., and Wieloch, T., 1998. Cyclosporin A, but not FK 506, protects mitochondria and neurons against hypoglycemic damage and implicates the mitochondrial permeability transition in cell death. J Neurosci 18**,** 5151-5159.

Frost, S. C., and Wells, M. A., 1981. A comparison of the utilization of medium and long-chain fatty acids for oxidation and ketogenesis in the suckling rat: in vivo and in vitro studies. Arch Biochem Biophys 211**,** 537-546.

Fukao, T., Lopaschuk, G. D., and Mitchell, G. A., 2004. Pathways and control of ketone body metabolism: on the fringe of lipid biochemistry. Prostaglandins Leukot Essent Fatty Acids 70**,** 243-251.

Fuss, B., Mallon, B., Phan, T., Ohlemeyer, C., Kirchhoff, F., Nishiyama, A., and Macklin, W. B., 2000. Purification and analysis of in vivo-differentiated oligodendrocytes expressing the green fluorescent protein. Dev Biol 218**,** 259-274.

Gentz, J., Bengtsson, G., Hakkarainen, J., Hellstrom, R., and Persson, B., 1970. Metabolic effects of starvation during neonatal period in the piglet. Am J Physiol 218**,** 662-668.

Ghajar, J. B., Plum, F., and Duffy, T. E., 1982. Cerebral oxidative metabolism and blood flow during acute hypoglycemia and recovery in unanesthetized rats. J Neurochem 38**,** 397-409.

Ghosh, A. K., Mukherji, B., and Sloviter, H. A., 1972. Metabolism of isolated rat brain perfused with glucose or mannose as substrate. J Neurochem 19**,** 1279-1285.

Gille, A., Bodor, E. T., Ahmed, K., and Offermanns, S., 2008. Nicotinic acid: pharmacological effects and mechanisms of action. Annu Rev Pharmacol Toxicol 48**,** 79-106.

Gorell, J. M., Dolkart, P. H., and Ferrendelli, J. A., 1976. Regional levels of glucose, amino acids, high energy phosphates, and cyclic nucleotides in the central nervous system during hypoglycemic stupor and behavioral recovery. J Neurochem 27**,** 1043-1049.

Gramsbergen, A., 1976. The development of the EEG in the rat. Dev Psychobiol 9**,** 501-515.

Gramsbergen, A., Schwartze, P., and Prechtl, H. F., 1970. The postnatal development of behavioral states in the rat. Dev Psychobiol 3**,** 267-280.

Grigor, M. R., and Warren, S. M., 1980. Dietary regulation of mammary lipogenesis in lactating rats. Biochem J 188**,** 61-65.

Grimaldi, L. M., Babic, B., Brunelli, S., Moore, H., and Vannucci, S. J., 2005. Hypoglycemia in Immature Brain Has Long-Lasting Neuropathologic And Behavioral Consequences [Abstract]. Pediatric Critical Care Medicine 6**,** 105.

Gruetter, R., 2003. Glycogen: the forgotten cerebral energy store. J Neurosci Res 74**,** 179-183.

Haces, M. L., Hernandez-Fonseca, K., Medina-Campos, O. N., Montiel, T., Pedraza-Chaverri, J., and Massieu, L., 2008. Antioxidant capacity contributes to protection of ketone bodies against oxidative damage induced during hypoglycemic conditions. Exp Neurol 211**,** 85-96.

Haces, M. L., Montiel, T., and Massieu, L., 2009. Selective vulnerability of brain regions to oxidative stress in a non-coma model of insulin-induced hypoglycemia. Neuroscience 165**,** 28-38.

Hack, A., Busch, V., Pascher, B., Busch, R., Bieger, I., Gempel, K., and Baumeister, F. A., 2006. Monitoring of ketogenic diet for carnitine metabolites by subcutaneous microdialysis. Pediatr Res 60**,** 93-96.

Hagberg, H., Bona, E., Gilland, E., and Puka-Sundvall, M., 1997. Hypoxia-ischaemia model in the 7-day-old rat: possibilities and shortcomings. Acta Paediatr Suppl 422**,** 85-88.

Hahn, P., and Taller, M., 1987. Ketone formation in the intestinal mucosa of infant rats. Life Sci 41**,** 1525-1528.

Hall, W. G., 1975. Weaning and growth of artificially reared rats. Science 190**,** 1313-1315.

Ham, M. R., Okada, P., and White, P. C., 2004. Bedside ketone determination in diabetic children with hyperglycemia and ketosis in the acute care setting. Pediatr Diabetes 5**,** 39-43.

Hawdon, J. M., and Ward Platt, M. P., 1993. Metabolic adaptation in small for gestational age infants. Arch Dis Child 68**,** 262-268.

Hawdon, J. M., Ward Platt, M. P., and Aynsley-Green, A., 1992. Patterns of metabolic adaptation for preterm and term infants in the first neonatal week. Arch Dis Child 67**,** 357-365.

Hawkins, R. A., Williamson, D. H., and Krebs, H. A., 1971. Ketone-body utilization by adult and suckling rat brain in vivo. Biochem J 122**,** 13-18.

Hayashi, K., Okumura, K., Matsui, H., Murase, K., Kamiya, H., Saburi, Y., Numaguchi, Y., Toki, Y., and Hayakawa, T., 2001. Involvement of 1,2-diacylglycerol in improvement of heart function by etomoxir in diabetic rats. Life Sci 68**,** 1515-1526.

Hellmann, J., Vannucci, R. C., and Nardis, E. E., 1982. Blood-brain barrier permeability to lactic acid in the newborn dog: lactate as a cerebral metabolic fuel. Pediatr Res 16**,** 40-44.

Hertz, L., and Hertz, E., 2003. Cataplerotic TCA cycle flux determined as glutamate-sustained oxygen consumption in primary cultures of astrocytes. Neurochem Int 43**,** 355-361.

Ho, H. T., Yeung, W. K., and Young, B. W., 2004. Evaluation of "point of care" devices in the measurement of low blood glucose in neonatal practice. Arch Dis Child Fetal Neonatal Ed 89**,** F356-359.

Honegger, P., Braissant, O., Henry, H., Boulat, O., Bachmann, C., Zurich, M. G., and Pardo, B., 2002. Alteration of amino acid metabolism in neuronal aggregate cultures exposed to hypoglycaemic conditions. J Neurochem 81**,** 1141-1151.

Horber, F. F., Krayer, S., Miles, J., Cryer, P., Rehder, K., and Haymond, M. W., 1990. Isoflurane and whole body leucine, glucose, and fatty acid metabolism in dogs. Anesthesiology 73**,** 82-92.

Hue, L., and Taegtmeyer, H., 2009. The Randle cycle revisited: a new head for an old hat. Am J Physiol Endocrinol Metab 297**,** E578-591.

Innis, S. M., and Dyer, R. A., 1999. Dietary canola oil alters hematological indices and blood lipids in neonatal piglets fed formula. J Nutr 129**,** 1261-1268.

Itoh, T., and Quastel, J. H., 1970. Acetoacetate metabolism in infant and adult rat brain in vitro. Biochem J 116**,** 641-655.

Izumi, Y., Ishii, K., Katsuki, H., Benz, A. M., and Zorumski, C. F., 1998. beta-Hydroxybutyrate fuels synaptic function during development. Histological and physiological evidence in rat hippocampal slices. J Clin Invest 101**,** 1121-1132.

Johnson, W. A., and Weiner, M. W., 1978. Protective effects of ketogenic diets on signs of hypoglycemia. Diabetes 27**,** 1087-1091.

Jones, E. L., and Thomas Smith, W., 1971. Hypoglycaemic Brain Damage in the Neonatal Rat. In: Brierly, J. B., and Meldrum, B. S., (Eds.), Brain Hypoxia. Lippincott, Philadelphia, pp. 231-241.

Jouvet-Mounier, D., Astic, L., and Lacote, D., 1970. Ontogenesis of the states of sleep in rat, cat, and guinea pig during the first postnatal month. Dev Psychobiol 2**,** 216-239.

Juurlink, B. H., 1997. Response of glial cells to ischemia: roles of reactive oxygen species and glutathione. Neurosci Biobehav Rev 21**,** 151-166.

Kashiwaya, Y., Sato, K., Tsuchiya, N., Thomas, S., Fell, D. A., Veech, R. L., and Passonneau, J. V., 1994. Control of glucose utilization in working perfused rat heart. J Biol Chem 269**,** 25502-25514.

Kashiwaya, Y., Takeshima, T., Mori, N., Nakashima, K., Clarke, K., and Veech, R. L., 2000. D-beta-hydroxybutyrate protects neurons in models of Alzheimer's and Parkinson's disease. Proc Natl Acad Sci U S A 97**,** 5440-5444.

Kawaguchi, M., Furuya, H., and Patel, P. M., 2005. Neuroprotective effects of anesthetic agents. J Anesth 19**,** 150-156.

Kim do, Y., Davis, L. M., Sullivan, P. G., Maalouf, M., Simeone, T. A., van Brederode, J., and Rho, J. M., 2007. Ketone bodies are protective against oxidative stress in neocortical neurons. J Neurochem 101**,** 1316-1326.

Kim, J. H., Choi, J. Y., Koh, S. B., and Lee, Y., 2007. Reversible splenial abnormality in hypoglycemic encephalopathy. Neuroradiology 49**,** 217-222.

Kim, J. H., and Koh, S. B., 2007. Extensive white matter injury in hypoglycemic coma. Neurology 68**,** 1074.

Kim, M., Yu, Z. X., Fredholm, B. B., and Rivkees, S. A., 2005. Susceptibility of the developing brain to acute hypoglycemia involving A1 adenosine receptor activation. Am J Physiol Endocrinol Metab 289**,** E562-569.

Kinnala, A., Suhonen-Polvi, H., Aarimaa, T., Kero, P., Korvenranta, H., Ruotsalainen, U., Bergman, J., Haaparanta, M., Solin, O., Nuutila, P., and Wegelius, U., 1996. Cerebral metabolic rate for glucose during the first six months of life: an FDG positron emission tomography study. Arch Dis Child Fetal Neonatal Ed 74**,** F153-157.

Kiorpes, T. C., Hoerr, D., Ho, W., Weaner, L. E., Inman, M. G., and Tutwiler, G. F., 1984. Identification of 2-tetradecylglycidyl coenzyme A as the active form of methyl 2-tetradecylglycidate (methyl palmoxirate) and its characterization as an irreversible, active site-directed inhibitor of carnitine palmitoyltransferase A in isolated rat liver mitochondria. J Biol Chem 259**,** 9750-9755.

Kraus, H., Schlenker, S., and Schwedesky, D., 1974. Developmental changes of cerebral ketone body utilization in human infants. Hoppe Seylers Z Physiol Chem 355**,** 164-170.

Kristensen, G. B., Christensen, N. G., Thue, G., and Sandberg, S., 2005. Between-lot variation in external quality assessment of glucose: clinical importance and effect on participant performance evaluation. Clin Chem 51**,** 1632-1636.

Kruszynska, Y. T., and Sherratt, H. S., 1987. Glucose kinetics during acute and chronic treatment of rats with 2[6(4-chloro-phenoxy)hexyl]oxirane-2-carboxylate, etomoxir. Biochem Pharmacol 36**,** 3917-3921.

Kuwa, K., Nakayama, T., Hoshino, T., and Tominaga, M., 2001. Relationships of glucose concentrations in capillary whole blood, venous whole blood and venous plasma. Clin Chim Acta 307**,** 187-192.

Laber-Laird, K., Smith, A., Swindle, M. M., and Colwell, J., 1992. Effects of isoflurane anesthesia on glucose tolerance and insulin secretion in Yucatan minipigs. Lab Anim Sci 42**,** 579-581.

LaManna, J. C., Salem, N., Puchowicz, M., Erokwu, B., Koppaka, S., Flask, C., and Lee, Z., 2009. Ketones suppress brain glucose consumption. Adv Exp Med Biol 645**,** 301-306.

Langhans, W., Pantel, K., and Scharrer, E., 1985. Ketone kinetics and D-(-)-3-hydroxybutyrate-induced inhibition of feeding in rats. Physiol Behav 34**,** 579-582.

Lewis, L. D., Ljunggren, B., Norberg, K., and Siesjo, B. K., 1974a. Changes in carbohydrate substrates, amino acids and ammonia in the brain during insulin-induced hypoglycemia. J Neurochem 23**,** 659-671.

Lewis, L. D., Ljunggren, B., Ratcheson, R. A., and Siesjo, B. K., 1974b. Cerebral energy state in insulin-induced hypoglycemia, related to blood glucose and to EEG. J Neurochem 23**,** 673-679.

Lian, X. Y., Xu, K., and Stringer, J. L., 2008. Oral administration of fructose-1,6-diphosphate has anticonvulsant activity. Neurosci Lett 446**,** 75-77.

Lu, Q. R., Yuk, D., Alberta, J. A., Zhu, Z., Pawlitzky, I., Chan, J., McMahon, A. P., Stiles, C. D., and Rowitch, D. H., 2000. Sonic hedgehog--regulated oligodendrocyte lineage genes encoding bHLH proteins in the mammalian central nervous system. Neuron 25**,** 317-329.

Ma, J. H., Kim, Y. J., Yoo, W. J., Ihn, Y. K., Kim, J. Y., Song, H. H., and Kim, B. S., 2009. MR imaging of hypoglycemic encephalopathy: lesion distribution and prognosis prediction by diffusion-weighted imaging. Neuroradiology 51**,** 641-649.

Maalouf, M., Rho, J. M., and Mattson, M. P., 2009. The neuroprotective properties of calorie restriction, the ketogenic diet, and ketone bodies. Brain Res Rev 59**,** 293-315.

Maalouf, M., Sullivan, P. G., Davis, L., Kim, D. Y., and Rho, J. M., 2007. Ketones inhibit mitochondrial production of reactive oxygen species production following glutamate excitotoxicity by increasing NADH oxidation. Neuroscience 145**,** 256-264.

Mandard, S., Muller, M., and Kersten, S., 2004. Peroxisome proliferator-activated receptor alpha target genes. Cell Mol Life Sci 61**,** 393-416.

Martini, W. Z., Stanley, W. C., Huang, H., Rosiers, C. D., Hoppel, C. L., and Brunengraber, H., 2003. Quantitative assessment of anaplerosis from propionate in pig heart in vivo. Am J Physiol Endocrinol Metab 284**,** E351-356.

Massieu, L., Haces, M. L., Montiel, T., and Hernandez-Fonseca, K., 2003. Acetoacetate protects hippocampal neurons against glutamate-mediated neuronal damage during glycolysis inhibition. Neuroscience 120**,** 365-378.

Mattiasson, G., Shamloo, M., Gido, G., Mathi, K., Tomasevic, G., Yi, S., Warden, C. H., Castilho, R. F., Melcher, T., Gonzalez-Zulueta, M., Nikolich, K., and Wieloch, T., 2003. Uncoupling protein-2 prevents neuronal death and diminishes brain dysfunction after stroke and brain trauma. Nat Med 9**,** 1062-1068.

Mayor, F., Veloso, D., and Williamson, D. H., 1967. Effects of nicotinic acid on the acetoacetate and 3-hydroxybutyrate concentrations of rat blood and liver. Biochem J 104**,** 57P.

McGowan, J. E., Cai, W., Gabrielson, K. R., and Mishra, O. P., 2005. Hypoglycemic brain injury in an awake newborn piglet model. Dev Neurosci 27**,** 263.

McGowan, J. E., Chen, L., Gao, D., Trush, M., and Wei, C., 2006. Increased mitochondrial reactive oxygen species production in newborn brain during hypoglycemia. Neurosci Lett 399**,** 111-114.

McTigue, D. M., and Tripathi, R. B., 2008. The life, death, and replacement of oligodendrocytes in the adult CNS. J Neurochem 107**,** 1-19.

Medina, J. M., 1985. The role of lactate as an energy substrate for the brain during the early neonatal period. Biol Neonate 48**,** 237-244.

Medina, J. M., and Tabernero, A., 2005. Lactate utilization by brain cells and its role in CNS development. J Neurosci Res 79**,** 2-10.

Meissner, T., Wendel, U., Burgard, P., Schaetzle, S., and Mayatepek, E., 2003. Long-term follow-up of 114 patients with congenital hyperinsulinism. Eur J Endocrinol 149**,** 43-51.

Mejia-Toiber, J., Montiel, T., and Massieu, L., 2006. D-beta-hydroxybutyrate prevents glutamate-mediated lipoperoxidation and neuronal damage elicited during glycolysis inhibition in vivo. Neurochem Res 31**,** 1399-1408.

Menni, F., de Lonlay, P., Sevin, C., Touati, G., Peigne, C., Barbier, V., Nihoul-Fekete, C., Saudubray, J. M., and Robert, J. J., 2001. Neurologic outcomes of 90 neonates and infants with persistent hyperinsulinemic hypoglycemia. Pediatrics 107**,** 476-479.

Mills, P. B., Struys, E., Jakobs, C., Plecko, B., Baxter, P., Baumgartner, M., Willemsen, M. A., Omran, H., Tacke, U., Uhlenberg, B., Weschke, B., and Clayton, P. T., 2006. Mutations in antiquitin in individuals with pyridoxine-dependent seizures. Nat Med 12**,** 307-309.

Mirmiran, M., and Corner, M., 1982. Neuronal discharge patterns in the occipital cortex of developing rats during active and quiet sleep. Brain Res 255**,** 37-48.

Mochel, F., DeLonlay, P., Touati, G., Brunengraber, H., Kinman, R. P., Rabier, D., Roe, C. R., and Saudubray, J. M., 2005. Pyruvate carboxylase deficiency: clinical and biochemical response to anaplerotic diet therapy. Mol Genet Metab 84**,** 305-312.

Mori, F., Nishie, M., Houzen, H., Yamaguchi, J., and Wakabayashi, K., 2006. Hypoglycemic encephalopathy with extensive lesions in the cerebral white matter. Neuropathology 26**,** 147-152.

Morris, A. A., 2005. Cerebral ketone body metabolism. J Inherit Metab Dis 28**,** 109-121.

Mutomba, M. C., Yuan, H., Konyavko, M., Adachi, S., Yokoyama, C. B., Esser, V., McGarry, J. D., Babior, B. M., and Gottlieb, R. A., 2000. Regulation of the activity of caspases by L-carnitine and palmitoylcarnitine. FEBS Lett 478**,** 19-25.

Nadal, A., Marrero, P. F., and Haro, D., 2002. Down-regulation of the mitochondrial 3-hydroxy-3-methylglutaryl-CoA synthase gene by insulin: the role of the forkhead transcription factor FKHRL1. Biochem J 366**,** 289-297.

Nehlig, A., 2004. Brain uptake and metabolism of ketone bodies in animal models. Prostaglandins Leukot Essent Fatty Acids 70**,** 265-275.

Nehlig, A., de Vasconcelos, A. P., and Boyet, S., 1988. Quantitative autoradiographic measurement of local cerebral glucose utilization in freely moving rats during postnatal development. J Neurosci 8**,** 2321-2333.

Nehlig, A., and Pereira de Vasconcelos, A., 1993. Glucose and ketone body utilization by the brain of neonatal rats. Prog Neurobiol 40**,** 163-221.

Nguyen, N. H., Morland, C., Gonzalez, S. V., Rise, F., Storm-Mathisen, J., Gundersen, V., and Hassel, B., 2007. Propionate increases neuronal histone acetylation, but is metabolized oxidatively by glia. Relevance for propionic acidemia. J Neurochem 101**,** 806-814.

Nicolay, D. J., Doucette, J. R., and Nazarali, A. J., 2007. Transcriptional control of oligodendrogenesis. Glia 55**,** 1287-1299.

Noyan-Ashraf, M. H., Brandizzi, F., and Juurlink, B. H., 2005. Constitutive nuclear localization of activated caspase 3 in subpopulations of the astroglial family of cells. Glia 49**,** 588-593.

Olpin, S. E., 2004. Implications of impaired ketogenesis in fatty acid oxidation disorders. Prostaglandins Leukot Essent Fatty Acids 70**,** 293-308.

Oomman, S., Finckbone, V., Dertien, J., Attridge, J., Henne, W., Medina, M., Mansouri, B., Singh, H., Strahlendorf, H., and Strahlendorf, J., 2004. Active caspase-3 expression during postnatal development of rat cerebellum is not systematically or consistently associated with apoptosis. J Comp Neurol 476**,** 154-173.

Ortega, E., Wagner, A., Caixas, A., Barcons, M., and Corcoy, R., 2000. Hypoglycemia and pulmonary edema: a forgotten association. Diabetes Care 23**,** 1023-1024.

Owen, O. E., Kalhan, S. C., and Hanson, R. W., 2002. The key role of anaplerosis and cataplerosis for citric acid cycle function. J Biol Chem 277**,** 30409-30412.

Oz, G., Berkich, D. A., Henry, P. G., Xu, Y., LaNoue, K., Hutson, S. M., and Gruetter, R., 2004. Neuroglial metabolism in the awake rat brain: CO2 fixation increases with brain activity. J Neurosci 24**,** 11273-11279.

Oz, G., Kumar, A., Rao, J. P., Kodl, C. T., Chow, L., Eberly, L. E., and Seaquist, E. R., 2009. Human brain glycogen metabolism during and after hypoglycemia. Diabetes 58**,** 1978-1985.

Patel, A. B., Chowdhury, G. M., de Graaf, R. A., Rothman, D. L., Shulman, R. G., and Behar, K. L., 2005. Cerebral pyruvate carboxylase flux is unaltered during bicuculline-seizures. J Neurosci Res 79**,** 128-138.

Patel, A. B., De Graaf, R. A., Mason, G. F., Rothman, D. L., Shulman, R. G., and Behar, K. L., 2003. Coupling of glutamatergic neurotransmission and neuronal glucose oxidation over the entire range of cerebral cortex activity. Ann N Y Acad Sci 1003**,** 452-453.

Patsouris, D., Reddy, J. K., Muller, M., and Kersten, S., 2006. Peroxisome proliferator-activated receptor alpha mediates the effects of high-fat diet on hepatic gene expression. Endocrinology 147**,** 1508-1516.

Paxinos, G., Watson, C., 1997. The Rat Brain in Stereotaxic Coordinates. Academic Press, San Diego, London.

Penna, C., Mancardi, D., Gattullo, D., and Pagliaro, P., 2005. Myocardial protection from ischemic preconditioning is not blocked by sub-chronic inhibition of carnitine palmitoyltransferase I. Life Sci 77**,** 2004-2017.

Persson, B., Settergren, G., and Dahlquist, G., 1972. Cerebral arterio-venous difference of acetoacetate and D- -hydroxybutyrate in children. Acta Paediatr Scand 61**,** 273-278.

Phillis, J. W., and O'Regan, M. H., 2004. A potentially critical role of phospholipases in central nervous system ischemic, traumatic, and neurodegenerative disorders. Brain Res Brain Res Rev 44**,** 13-47.

Plecko, B., Stoeckler-Ipsiroglu, S., Schober, E., Harrer, G., Mlynarik, V., Gruber, S., Moser, E., Moeslinger, D., Silgoner, H., and Ipsiroglu, O., 2002. Oral beta-hydroxybutyrate supplementation in two patients with hyperinsulinemic hypoglycemia: monitoring of beta-hydroxybutyrate levels in blood and cerebrospinal fluid, and in the brain by in vivo magnetic resonance spectroscopy. Pediatr Res 52**,** 301-306.

Poleni, P. E., Bianchi, A., Etienne, S., Koufany, M., Sebillaud, S., Netter, P., Terlain, B., and Jouzeau, J. Y., 2007. Agonists of peroxisome proliferators-activated receptors (PPAR) alpha, beta/delta or gamma reduce transforming growth factor (TGF)-beta-induced proteoglycans' production in chondrocytes. Osteoarthritis Cartilage 15**,** 493-505.

Popken, G. J., Hodge, R. D., Ye, P., Zhang, J., Ng, W., O'Kusky, J. R., and D'Ercole, A. J., 2004. In vivo effects of insulin-like growth factor-I (IGF-I) on prenatal and early postnatal development of the central nervous system. Eur J Neurosci 19**,** 2056-2068.

Puchowicz, M. A., Zechel, J. L., Valerio, J., Emancipator, D. S., Xu, K., Pundik, S., LaManna, J. C., and Lust, W. D., 2008. Neuroprotection in diet-induced ketotic rat brain after focal ischemia. J Cereb Blood Flow Metab 28**,** 1907-1916.

Ralser, M., Wamelink, M. M., Kowald, A., Gerisch, B., Heeren, G., Struys, E. A., Klipp, E., Jakobs, C., Breitenbach, M., Lehrach, H., and Krobitsch, S., 2007. Dynamic rerouting of the carbohydrate flux is key to counteracting oxidative stress. J Biol 6**,** 10.

Reaven, G. M., Chang, H., Ho, H., Jeng, C. Y., and Hoffman, B. B., 1988a. Lowering of plasma glucose in diabetic rats by antilipolytic agents. Am J Physiol 254**,** E23-30.

Reaven, G. M., Chang, H., and Hoffman, B. B., 1988b. Additive hypoglycemic effects of drugs that modify free-fatty acid metabolism by different mechanisms in rats with streptozocin-induced diabetes. Diabetes 37**,** 28-32.

Reszko, A. E., Kasumov, T., Pierce, B. A., David, F., Hoppel, C. L., Stanley, W. C., Des Rosiers, C., and Brunengraber, H., 2003. Assessing the reversibility of the anaplerotic reactions of the propionyl-CoA pathway in heart and liver. J Biol Chem 278**,** 34959-34965.

Roeder, L. M., Tildon, J. T., and Holman, D. C., 1984a. Competition among oxidizable substrates in brains of young and adult rats. Dissociated cells. Biochem J 219**,** 131-135.

Roeder, L. M., Tildon, J. T., and Stevenson, J. H., Jr., 1984b. Competition among oxidizable substrates in brains of young and adult rats. Whole homogenates. Biochem J 219**,** 125-130.

Romijn, H. J., Hofman, M. A., and Gramsbergen, A., 1991. At what age is the developing cerebral cortex of the rat comparable to that of the full-term newborn human baby? Early Hum Dev 26**,** 61-67.

Sampath, H., and Ntambi, J. M., 2004. Polyunsaturated fatty acid regulation of gene expression. Nutr Rev 62**,** 333-339.

Sato, K., Kashiwaya, Y., Keon, C. A., Tsuchiya, N., King, M. T., Radda, G. K., Chance, B., Clarke, K., and Veech, R. L., 1995. Insulin, ketone bodies, and mitochondrial energy transduction. Faseb J 9**,** 651-658.

Saunders, A. C., Feldman, H. A., Correia, C. E., and Weinstein, D. A., 2005. Clinical evaluation of a portable lactate meter in type I glycogen storage disease. J Inherit Metab Dis 28**,** 695-701.

Schmitz, F. J., Rosen, P., and Reinauer, H., 1995. Improvement of myocardial function and metabolism in diabetic rats by the carnitine palmitoyl transferase inhibitor Etomoxir. Horm Metab Res 27**,** 515-522.

Schmued, L. C., Stowers, C. C., Scallet, A. C., and Xu, L., 2005. Fluoro-Jade C results in ultra high resolution and contrast labeling of degenerating neurons. Brain Res 1035**,** 24-31.

Schutz, P. W., Struys, E. A., Sinclair, G., and Stockler, S., 2011a. Protective effects of d-3-hydroxybutyrate and propionate during hypoglycemic coma: Clinical and biochemical insights from infant rats. Mol Genet Metab in press.

Schutz, P. W., Wong, P. K., O'Kusky, J., Innis, S. M., and Stockler, S., 2011b. Effects of d-3-hydroxybutyrate treatment on hypoglycemic coma in rat pups. Exp Neurol 227**,** 180-187.

Schwartz, R. M., Boyes, S., and Aynsley-Green, A., 1989. Metabolic effects of three ketogenic diets in the treatment of severe epilepsy. Dev Med Child Neurol 31**,** 152-160.

Sibson, N. R., Dhankhar, A., Mason, G. F., Rothman, D. L., Behar, K. L., and Shulman, R. G., 1998. Stoichiometric coupling of brain glucose metabolism and glutamatergic neuronal activity. Proc Natl Acad Sci U S A 95**,** 316-321.

Sibson, N. R., Mason, G. F., Shen, J., Cline, G. W., Herskovits, A. Z., Wall, J. E., Behar, K. L., Rothman, D. L., and Shulman, R. G., 2001. In vivo (13)C NMR measurement of

neurotransmitter glutamate cycling, anaplerosis and TCA cycle flux in rat brain during [2-13C]glucose infusion. J Neurochem 76**,** 975-989.

Sloviter, H. A., and Kamimoto, T., 1970. The isolated, persed rat brain preparation metabolizes mannose but not maltose. J Neurochem 17**,** 1109-1111.

Sloviter, H. A., Shimkin, P., and Suhara, K., 1966. Glycerol as a substrate for brain metabolism. Nature 210**,** 1334-1336.

Sloviter, H. A., and Suhara, K., 1967. A brain-infusion method for demonstrating utilization of glycerol by rabbit brain in vivo. J Appl Physiol 23**,** 792-797.

Soupart, A., Penninckx, R., Namias, B., Stenuit, A., Perier, O., and Decaux, G., 1996. Brain myelinolysis following hypernatremia in rats. J Neuropathol Exp Neurol 55**,** 106-113.

Stafstrom, C. E., Roopra, A., and Sutula, T. P., 2008. Seizure suppression via glycolysis inhibition with 2-deoxy-D-glucose (2DG). Epilepsia 49 Suppl 8**,** 97-100.

Strosznajder, J., 1984. Effect of hypoglycemia on the brain free fatty acid level and the uptake of fatty acids by phospholipids. Neurochem Res 9**,** 465-476.

Suh, S. W., Aoyama, K., Chen, Y., Garnier, P., Matsumori, Y., Gum, E., Liu, J., and Swanson, R. A., 2003. Hypoglycemic neuronal death and cognitive impairment are prevented by poly(ADP-ribose) polymerase inhibitors administered after hypoglycemia. J Neurosci 23**,** 10681-10690.

Suh, S. W., Bergher, J. P., Anderson, C. M., Treadway, J. L., Fosgerau, K., and Swanson, R. A., 2007a. Astrocyte glycogen sustains neuronal activity during hypoglycemia:studies with the glycogen phosphorylase inhibitor CP-316,819. J Pharmacol Exp Ther.

Suh, S. W., Bergher, J. P., Anderson, C. M., Treadway, J. L., Fosgerau, K., and Swanson, R. A., 2007b. Astrocyte glycogen sustains neuronal activity during hypoglycemia:studies with the glycogen phosphorylase inhibitor CP-316,819. J Pharmacol Exp Ther 321**,** 45-50.

Suh, S. W., Gum, E. T., Hamby, A. M., Chan, P. H., and Swanson, R. A., 2007c. Hypoglycemic neuronal death is triggered by glucose reperfusion and activation of neuronal NADPH oxidase. J Clin Invest 117**,** 910-918.

Suh, S. W., Hamby, A. M., and Swanson, R. A., 2007d. Hypoglycemia, brain energetics, and hypoglycemic neuronal death. Glia 55**,** 1280-1286.

Sullivan, P. G., Dube, C., Dorenbos, K., Steward, O., and Baram, T. Z., 2003. Mitochondrial uncoupling protein-2 protects the immature brain from excitotoxic neuronal death. Ann Neurol 53**,** 711-717.

Sullivan, P. G., Rippy, N. A., Dorenbos, K., Concepcion, R. C., Agarwal, A. K., and Rho, J. M., 2004. The ketogenic diet increases mitochondrial uncoupling protein levels and activity. Ann Neurol 55**,** 576-580.

Sutherland, G. R., Tyson, R. L., and Auer, R. N., 2008. Truncation of the krebs cycle during hypoglycemic coma. Med Chem 4**,** 379-385.

Suzuki, M., Kitamura, Y., Mori, S., Sato, K., Dohi, S., Sato, T., Matsuura, A., and Hiraide, A., 2002. Beta-hydroxybutyrate, a cerebral function improving agent, protects rat brain against ischemic damage caused by permanent and transient focal cerebral ischemia. Jpn J Pharmacol 89**,** 36-43.

Suzuki, M., Sato, K., Dohi, S., Sato, T., Matsuura, A., and Hiraide, A., 2001. Effect of beta-hydroxybutyrate, a cerebral function improving agent, on cerebral hypoxia, anoxia and ischemia in mice and rats. Jpn J Pharmacol 87**,** 143-150.

Swithers, S. E., Melendez, R. I., Watkins, B. A., and Davis, R. J., 2001. Metabolic and behavioral responses in pre-weanling rats following alteration of maternal diet. Physiol Behav 72**,** 147-157.

Tabernero, A., Vicario, C., and Medina, J. M., 1996. Lactate spares glucose as a metabolic fuel in neurons and astrocytes from primary culture. Neurosci Res 26**,** 369-376.

Tanaka, T., Nabatame, H., and Tanifuji, Y., 2005. Insulin secretion and glucose utilization are impaired under general anesthesia with sevoflurane as well as isoflurane in a concentration-independent manner. J Anesth 19**,** 277-281.

Thurston, J. H., Hauhart, R. E., and Schiro, J. A., 1983. Lactate reverses insulin-induced hypoglycemic stupor in suckling-weanling mice: biochemical correlates in blood, liver, and brain. J Cereb Blood Flow Metab 3**,** 498-506.

Thurston, J. H., Hauhart, R. E., and Schiro, J. A., 1986. Beta-hydroxybutyrate reverses insulin-induced hypoglycemic coma in suckling-weanling mice despite low blood and brain glucose levels. Metab Brain Dis 1**,** 63-82.

Tieu, K., Perier, C., Caspersen, C., Teismann, P., Wu, D. C., Yan, S. D., Naini, A., Vila, M., Jackson-Lewis, V., Ramasamy, R., and Przedborski, S., 2003. D-beta-hydroxybutyrate rescues mitochondrial respiration and mitigates features of Parkinson disease. J Clin Invest 112**,** 892-901.

Todorich, B., Pasquini, J. M., Garcia, C. I., Paez, P. M., and Connor, J. R., 2008. Oligodendrocytes and myelination: The role of iron. Glia.

Trachtman, H., Yancey, P. H., and Gullans, S. R., 1995. Cerebral cell volume regulation during hypernatremia in developing rats. Brain Res 693**,** 155-162.

Tucker, A. M., Aquilina, K., Chakkarapani, E., Hobbs, C. E., and Thoresen, M., 2009. Development of amplitude-integrated electroencephalography and interburst interval in the rat. Pediatr Res 65**,** 62-66.

Vadlamudi, S., Kalhan, S. C., and Patel, M. S., 1995. Persistence of metabolic consequences in the progeny of rats fed a HC formula in their early postnatal life. Am J Physiol 269**,** E731-738.

Van Hove, J. L., Grunewald, S., Jaeken, J., Demaerel, P., Declercq, P. E., Bourdoux, P., Niezen-Koning, K., Deanfeld, J. E., and Leonard, J. V., 2003. D,L-3-hydroxybutyrate treatment of multiple acyl-CoA dehydrogenase deficiency (MADD). Lancet 361**,** 1433-1435.

van Vlies, N., Tian, L., Overmars, H., Bootsma, A. H., Kulik, W., Wanders, R. J., Wood, P. A., and Vaz, F. M., 2005. Characterization of carnitine and fatty acid metabolism in the long-chain acyl-CoA dehydrogenase-deficient mouse. Biochem J 387**,** 185-193.

Vannucci, S. J., and Simpson, I. A., 2003. Developmental switch in brain nutrient transporter expression in the rat. Am J Physiol Endocrinol Metab 285**,** E1127-1134.

Vicario, C., and Medina, J. M., 1992. Metabolism of lactate in the rat brain during the early neonatal period. J Neurochem 59**,** 32-40.

Vijn, P. C., and Sneyd, J. R., 1998. I.v. anaesthesia and EEG burst suppression in rats: bolus injections and closed-loop infusions. Br J Anaesth 81**,** 415-421.

Volpe, J. J., 2001. Neurology of the Newborn. Saunders, Philadelphia.

Wada, H., Okada, Y., Nabetani, M., and Nakamura, H., 1997. The effects of lactate and beta-hydroxybutyrate on the energy metabolism and neural activity of hippocampal slices from adult and immature rat. Brain Res Dev Brain Res 101**,** 1-7.

Wamelink, M. M., Struys, E. A., Huck, J. H., Roos, B., van der Knaap, M. S., Jakobs, C., and Verhoeven, N. M., 2005. Quantification of sugar phosphate intermediates of the pentose phosphate pathway by LC-MS/MS: application to two new inherited defects of metabolism. J Chromatogr B Analyt Technol Biomed Life Sci 823**,** 18-25.

Wamelink, M. M., Struys, E. A., and Jakobs, C., 2008. The biochemistry, metabolism and inherited defects of the pentose phosphate pathway: a review. J Inherit Metab Dis 31**,** 703-717.

Wang, D., Pascual, J. M., Yang, H., Engelstad, K., Jhung, S., Sun, R. P., and De Vivo, D. C., 2005. Glut-1 deficiency syndrome: clinical, genetic, and therapeutic aspects. Ann Neurol 57**,** 111-118.

Wang, D., Pascual, J. M., Yang, H., Engelstad, K., Mao, X., Cheng, J., Yoo, J., Noebels, J. L., and De Vivo, D. C., 2006. A mouse model for Glut-1 haploinsufficiency. Hum Mol Genet 15**,** 1169-1179.

Watanabe, K., Iwase, K., and Hara, K., 1974. Development of slow-wave sleep in low-birthweight infants. Dev Med Child Neurol 16**,** 23-31.

Wells, M. A., 1985. Fatty acid metabolism and ketone formation in the suckling rat. Fed Proc 44**,** 2365-2368.

Xu, H. E., Stanley, T. B., Montana, V. G., Lambert, M. H., Shearer, B. G., Cobb, J. E., McKee, D. D., Galardi, C. M., Plunket, K. D., Nolte, R. T., Parks, D. J., Moore, J. T., Kliewer, S. A., Willson, T. M., and Stimmel, J. B., 2002. Structural basis for antagonist-mediated recruitment of nuclear co-repressors by PPARalpha. Nature 415**,** 813-817.

Xu, Y., Oz, G., LaNoue, K. F., Keiger, C. J., Berkich, D. A., Gruetter, R., and Hutson, S. H., 2004. Whole-brain glutamate metabolism evaluated by steady-state kinetics using a double-isotope procedure: effects of gabapentin. J Neurochem 90**,** 1104-1116.

Yamada, K. A., Rensing, N., Izumi, Y., De Erausquin, G. A., Gazit, V., Dorsey, D. A., and Herrera, D. G., 2004. Repetitive hypoglycemia in young rats impairs hippocampal long-term potentiation. Pediatr Res 55**,** 372-379.

Yamada, K. A., Rensing, N., and Thio, L. L., 2005. Ketogenic diet reduces hypoglycemia-induced neuronal death in young rats. Neurosci Lett 385**,** 210-214.

Yan, H., and Rivkees, S. A., 2006. Hypoglycemia influences oligodendrocyte development and myelin formation. Neuroreport 17**,** 55-59.

Yeh, Y. Y., and Zee, P., 1976. Insulin, a possible regulator of ketosis in newborn and suckling rats. Pediatr Res 10**,** 192-197.

Zarain-Herzberg, A., and Rupp, H., 2002. Therapeutic potential of CPT I inhibitors: cardiac gene transcription as a target. Expert Opin Investig Drugs 11**,** 345-356.

Zuppinger, K., Wiesmann, U., Siegrist, H. P., Schafer, T., Sandru, L., Schwarz, H. P., and Herschkowitz, N., 1981. Effect of glucose deprivation on sulfatide synthesis and oligodendrocytes in cultured brain cells of newborn mice. Pediatr Res 15**,** 319-325.

Appendix

Appendix A: Monitoring sheets

A.1 Welfare assessment sheet for neonatal rats and dam

(adapted from P. Hawkins, Lab Anim 2002, 36(4), pp378-95),

Neonatal scores 0-4 = Good, 5-8 = Fair, 9-13 = Poor; Maternal score: 5-6 = suvival of litter questionable

Parameter (neonates) summary observation or individual examinations as required	Date/Time Summary (S) evaluation or individual (I)					
	Age (days)					
Appearance/colour	Normal (pink)	0				
	Pink/blue abdomen	1				
	Pink/pale extremities	2				
	Blue/pale	3				
Surface temperature	Warm	0				
	Intermediate	1				
	Cold	2				
Natural activity	Wriggling ++	0				
	Wriggling +	1				
	Wriggling +/-	2				
	Still	3				
Reflexes/respond to touch	+++ righting reflex + to touch	0				
	++ righting reflex +/- to touch	1				
	+	2				
	- no response	3				
Milk in stomach (milk band?)	++	0				
	+	1				
	-	2				
TOTAL SCORE (Neonates)	0-13					
Parameter (mother)	Date					
Milk score	Most pups fed	0				
	Some pups fed	1				
	Hardly any fed	2				
Nest building	Good nest making	0				
	Some nest making	1				
	No nest	2				
Retrieval of young	Always	0				
	Sometimes	1				
	Never	2				
TOTAL SCORE (Mother)	0-6					

A.2 Monitoring sheet for post hypoglycemic rat pups – recovery phase

Study: Date:

Litter No.: Animal:

	Time post return to dam (Minutes)						
General Appearance							
Activity	mobile/alert						
	quiet						
	still/lethargic						
Retrieval	with littermates						
	on fringe						
	clearly isolated						
Suckling	yes						
	no						
Posture	unremarkable						
	abnormal (hunched, head pressing)						
Coat/Skin	unremarkable						
	soiled or rough						
	signs of inflammation						
Maternal grooming behavior	unremarkable						
	excessive						
Neurological Signs							
Response to touch	+ +						
	+ -						
	- -						
Righting reflex	+ +						
	+ -						
	- -						
Gait	unremarkable						
	ataxic						
	paretic/paralytic limb(s)						
Seizures	none						
	short clonic movements < 30 seconds						
	seizure activity > 30 seconds						
Head tilt	yes						
	no						
Clinical Signs							
Temperature	warm to touch						
	cool to touch						
Hydration Status	unremarkable						
	dry eyes						
	sunken eyes						
	listlessnes/skin tenting						
Respiration	unremarkable						
	laboured						
	shallow						
	irregular/gasping						
Stool	formed						
	soft						
Skin over infusion/injection site	unremarkable						
	red, no swelling						
	red and swollen						
	ulcerating/blisters						

A.3 Monitoring sheet for rat mother during posthypoglycemic reacceptance

Study: Date:

Litter:

	Time post return to mother (Minutes)														
Behavioral state	actively caring														
	agitated/nervous														
	aggressive														
	fearful/decreased activity														
	hyperactive														
Retrieval of young	systematic														
	occasional														
	never														
Grooming of young	sensible														
	excessive														
	generally reduced														

A.4 Monitoring for posthypoglycemic rat pups during survival period

Study: Date:

Litter: Animal:

Body weight before procedure in g:

	Date						
	Time						
General Appearance							
Activity	mobile/alert						
	quiet						
	still/lethargic						
Retrieval	with littermates						
	on fringe						
	clearly isolated						
Suckling	yes						
	no						
Posture	unremarkable						
	abnormal (hunched, head pressing)						
Coat/Skin	unremarkable						
	soiled or rough						
	signs of inflammation including pruritus or ulceration						
	alopecia or minor abrasion						
Face	unremarkable						
	nasal/ocular discharge or crusts						
Maternal grooming behavior	unremarkable						
	excessive						
Body Weight							
Weight	weight /g						
Weight change	< 5% loss						
	5-10% loss						
	10-15% loss						
	15-20% loss						
	> 20% loss						
Hydration Status							
	unremarkable						
	dry eyes						
	sunken eyes						
	listlessnes/skin tenting						

Posthypoglycemic Monitoring Page 2

Study: Date:

Litter: Animal:

	Date						
	Time						
Neurological Signs							
Response to touch	+ +						
	+ -						
	- -						
Righting reflex	+ +						
	+ -						
	- -						
Gait	unremarkable						
	ataxic						
	paretic/paralytic limb(s)						
Seizures	none						
	short clonic movements < 30 seconds						
	seizure activity > 30 seconds						
Head tilt	yes						
	no						
Clinical Signs							
Temperature	warm to touch						
	cool to touch						
Respiration	unremarkable						
	laboured						
	shallow						
	irregular/gasping						
Stool	formed						
	soft						
	severe diarrhea						
Skin over infusion/injection site	unremarkable						
	red, no swelling						
	red and swollen						
	ulcerating/blisters						

Appendix B: Standard operating procedures (SOPs)

B.1 Non-invasive EEG electrode attachment

UBC Animal Care Guidelines.

SOP: Stockler-Ipsiroglu – 001

Attachment of cutaneous EEG electrodes in developing rats

Submitted by: Peter W. Schutz

Last date revised: January 8, 2007

Date approved: January 26, 2007

Attachment of cutaneous EEG electrodes in developing rats

PURPOSE:

Short term recordings of interhemispheric EEG from developing rats with one pair of differential electrodes and one reference electrode.

POLICY:

This is a non-invasive method designed for short term monitoring of electroencephalographic activity from rat pups with subsequent return of the pup to the dam. Anaesthetic restraint is necessary for precise electrode placement. Procedure has been validated for 13-17 day old rats.

RESPONSIBILITY:

Investigator, technical personnel, veterinarian

MATERIALS:

- Isoflurane with anaesthetic machine, anaesthesia chamber, face mask
- Warming mat
- 3 Small silver-silver chloride cutaneous electrodes (total diameter less than 5 mm)
- Clippers, depilatory agent
- Mildly abrasive electrode skin prep gel
- Conductive electrode paste
- Collodion glue for electrodes
- 22G needle
- Acetone for removal

- Powder-free, latex examination glove for cap
- Cotton swabs, forceps, small scissors
- Fine-tip, permanent marker pen

PROCEDURE:

1. Anaesthetize rat pup with isoflurane. Place in sternal recumbency on warming mat and maintain light anaesthesia with face mask.
2. Shave head in area of electrode attachment anterior to, and between the ears (see figure 1), depilate (eg Nair cream for 2-3 minutes), wash with warm water several times, and dab dry. Eyes and ears must not get in contact with depilatory agent. This is achieved by applying the agent with small cotton swabs and washing the skin always in a direction away from eyes and ears.
3. Draw topographic landmark lines with marker pen: A) interauricular line: joins anterior margins of base of ears, B) midline perpendicular and anterior to interauricular line (see figure 2). Note also mentally the lines joining the anterior margin of the bases of the ears with posterior ocular margins (auricular-ocular line).
4. Locate positions for electrode placement: Differential electrodes are in symmetrical position about 3-5 mm anterior to interauricular line and medial of auricular-ocular line to avoid jaw muscles. The interelectrode distance is 5-10 mm. The reference electrode is posterior to interauricular line on the midline. See figure 1.
5. Abrade skin for electrode placement by applying abrasive prep gel and rubbing with cotton tips in circular motion for 5-15 seconds.
6. Apply conductive electrode paste to electrodes, hold in place on skin with forceps so that electrode leads point caudally. Apply collodion glue through a 22G needle around the electrode margin sealing it to the skin. Blow collodion dry (eg through a straw). Repeat for all electrodes. Attached electrodes are shown in figure 3.
7. Cut rubber glove finger of correct size to a length of 2-3 cm to slide over head of the animal, so that it fits comfortably covering all electrodes and the ears. With forceps and small scissors cut holes for ears and trim anterior margin so that eyes and mouth remain free. Check that cap does not impair respiration.
8. Optionally cut several holes in top of rubber cap to reduce sweating, and bundle electrode leads with a thread.
9. Terminate anaesthesia and observe recovery of the animal.
10. For EEG recording, rat pups are kept individually in a medium sized cage (e.g. as used for mice) with bedding as in home cage. It is placed on a warming mat. Healthy animals are observed

at least every 15 minutes. Maximum time for electrode attachment is 4 hours provided the animal remains without major distress given the other circumstances of the EEG recording (e.g. removal from dam). Monitoring frequency and maximum time for electrode attachment must be adjusted according to model specific requirements for any given disease model under investigation.

11. To remove electrodes, apply acetone with cotton tips for removal collodion.

SOP 001 Illustration 1: Geometry of electrode attachment and anatomic landmarks

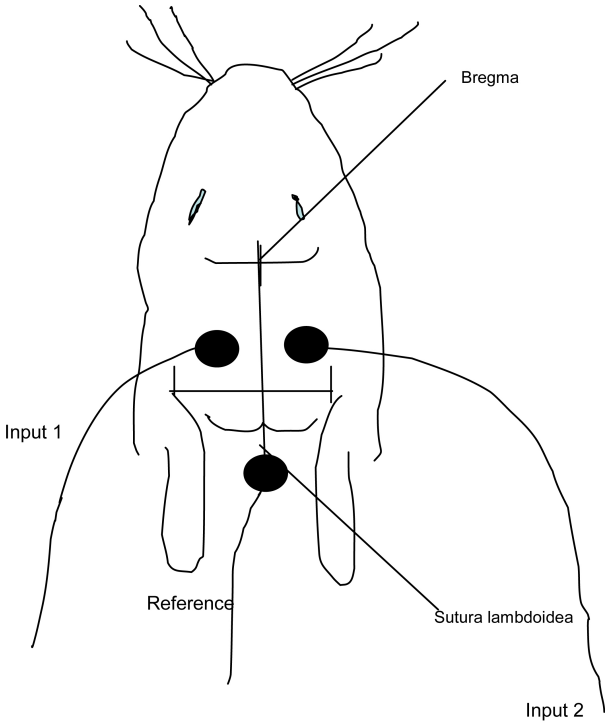

SOP 001 Illustration 2: Marking lines on shaved heads (A) and electrodes glued in place (B).

A)

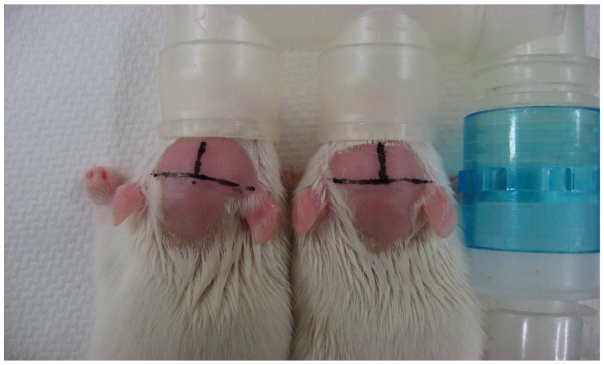

B)

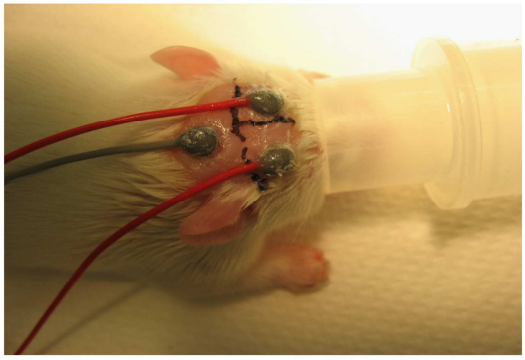

B.2 Perfusion fixation of rat brain for ages 10 to 20 days

UBC Animal Care Guidelines.

SOP: Stockler-Ipsiroglu – 002

Perfusion-fixation of infant rat brain

Submitted by: Peter W. Schutz

Last date revised: January 8, 2007

Date approved: January 26, 2007

Perfusion-fixation of rat brain for rats aged 10 to 20 days

PURPOSE:

This procedure is used to fixate the brain of infantile rats for histological analysis while keeping the distress for the animal during the procedure to a minimum.

POLICY:

This is a terminal procedure and conducted under anaesthesia.

RESPONSIBILITY:

Veterinarian, technical personnel, investigator.

MATERIALS:

- Anaesthetic, e.g. isoflurane or ketamine-xylazine, with respective equipment in correct dosage
- small scissors, curved and straight forceps, optionally curette
- 20-25 G needles
- 0.9% saline, sterile
- fixative: e.g. 10% formaldehyde in 0.1M phosphate buffer, or similar
- infusion bags for 0.9% saline and fixative, or large syringes
- fumehood or similar protection from fixative fumes

PROCEDURE:

1. Anaesthetize the rat pup.
2. Place anaesthetized animal in dorsal recumbency on a bench under fumehood or similar protection, with a drain or sufficient cloth underneath to soak up overflowing fixative.

3. Monitor depth of anaesthesia by checking the absence of a pedal withdrawal reflex and reaction to toe pinch. If responsive, increase depth of anaesthesia by augmenting injectible anaesthetic dose or increasing concentration of inhalant anaesthetic until reflexes subside. Re-examine reflexes every 10 minutes during procedure and adjust anaesthetic depth accordingly. If at any point the animal is responsive to surgical manipulation, stop and augment anaesthesia.
4. With small scissors, open the abdomen along a line across the upper abdomen of the animal, close to the lower margin of the ribcage. Lift abdominal wall with forceps taking care not to injure any intraabdominal organs.
5. Make skin incisions with scissors on either side of the ribcage starting from the lateral ends of the abdominal opening and leading anteriorily to the axilla. Dissect the skin off the breast cage and fold skin flap back over the head.
6. Thoracotomize on both sides up to the axilla and dissect the ribcage off the frontal margin of the diaphragm. Fold ribcage open.
7. Inspect thoracic cavity an localize right and left ventricles of the beating heart.
8. Introduce 25 G needle (or possibly larger in older animals) into left ventricle. If needed, collect blood sample.
9. Open right ventricle by means of a small cut made with scissors.
10. Connect infusion line from bag with 0.9% saline to needle in right ventricle, or use syringe. Suspend bag about 75 cm above the animal and start to perfuse it. To check for proper perfusion, observe for clear fluid coming out of the right ventricle after a couple of minutes. As soon as this happens, most of the blood has drained from circulation and the animal will be brain dead at this point. If inhalant anaesthesia is used, it is now discontinued. Total time of saline perfusion is around 5 minutes or according to volume specified in individual protocols individual protocol.
11. Stop saline perfusion and connect infusion bag with fixative. Perfuse for around 45 minutes, or volume specified according to individual protocol.
12. Terminate perfusion. Carefully dissect brain out: Cut spine just caudal to skull, open skull by means of a midline incision with scissors, dissect both flanks of the skull away and carefully scoop the brain out with curved forceps or a curette. Place brain in fixative.
13. Dispose of animal remains according to animal care facility procedures.

Appendix C: Implementation of online calculation of EEG suppression ratio

Vijin's algorithm (Vijn and Sneyd, 1998) was implemented on Chart 5 data recording software, version 5.5 (AD Instruments, USA). Chart 5 data analysis is channel (Ch) based and allows online display of processed data from one channel in another channel. EEG suppression calculation was organised as consecutive transformations from Channel 1 to Channel 8. Some of these steps may be condensed into single steps for efficiency. The following table shows technical details of channel programming:

Channel and Calculation	**Comment**
Channel 1: Raw EEG data	
Channel 2: Band pass 1-50 Hz	Band pass filter raw data
Channel 3: Window(Differentiate(Ch2),-0.0004,0.0004)	detects trace with absolute derivative below threshold, assigned 1, or above threshold, assigned 0
Channel 4: Threshold(-Abs(Differentiate(Ch3)),0)	marks cahnges in window function with a spike
Channel 5: Cyclic Measurements: Measurement: Integral; Source Ch. 5; Cycle detection: Spikes (Arithmetic); Threshold:0.52 V; Output: Set scale: -0.125 to 1.38 V.s	integrates time between spikes
Channel 5: Threshold(Ch3*Ch5,0.2)	assigns 1 to suppressed periods if longer than 0.2 s
Channel 6: Integral: Source: Ch5; Standard integral; Timed reset 10 s	integrates duration of suppressed period in 10s interval
Channel 7: Cyclic Measurements:Measurement: Maximum; Source: Ch 6; Threshold 0.01 Vs	takes maximum integral value for each episode
Channel 8: Ch9/10	divides suppression time in every 10 s interval by total time span to obtain suppression ratio